Journal of Hazardous Materials Advances 13 (2024) 100401

Contents lists available at ScienceDirect

Journal of Hazardous Materials Advances

journal homepage: www.elsevier.com/locate/hazadv

Green synthesis of metal oxide nanoparticles, and their various applications

Uyiosa Osagie Aigbe *, Otolorin Adelaja Osibote

Department of Mathematics and Physics, Cape Peninsula University of Technology, Cape Town, South Africa

ARTICLE INFO

Keywords:
Nanoparticles
Green synthesis
Microorganism
Nanotechnology
Plant extracts

ABSTRACT

Bio-synthesized metal oxide (MeO) nanoparticles (NPs) have triggered a huge global research interest owing to their advancement and various environmental remediation, personal care products, medical, energy, sensing, and water treatment applications. They demonstrate developing assets in various industries, remarkably with their heightened physicochemical, optical, mechanical, and electronic attributes. The physical and chemical routes have been a sticking point in the production of MeO NPs, owing to the natural and environmental risks linked with utilizing these approaches. The growth of MeO NPs production via the biologic method employing plants and microorganisms as a precursor material for metal-ions (MIs) reduction and stabilization has been the focus of research scientists in recent years. Hence, in this review, a comprehensive brief of the bio-synthesis approaches using plant extracts (PEs) and microorganism components for MeO NPs production as well as the various factors affecting the bio-production of MeO NPs, their various applications and their toxicity were considered.

1. Introduction

The phrase "nano" was taken from the ancient Greek word "nanos" implying 'dwarf' (Boholm, 2016). Nanotechnology (NT) idea came from the Nobel-Laureate (Richard Feynman-1959) talk titled "There's Plenty of Room at the Bottom" at the California Institute of Technology, United States of America. NT concept became completely operational in 1974 and the term was introduced 25 years later through Eric Drexler. Currently, NT and nanoscience (NS) are two peculiar words that are generally employed for a distinct array of research discoveries globally (Adeola, 2023; Alhalili, 2023). According to the Royal Society/Royal Academy of Engineering Working Group, NS is defined as the research of molecules and structures at the microscopic, molecular, and macromolecular scales, with their properties substantially discrete from those ensuing on a larger scale, NT is described as the technology that utilizes NS in real applications like the multiplicity of devices or systems, by controlling shape and size at the nanometer (nm) scale (Szczyglewska et al., 2023).

NT is a multifaceted area of science that focuses on the research of nano-range materials of 1–100 nm. This area has shown massive development with the opening of new basic and applied frontiers in engineering and materials science (Aziz et al., 2019). NT has made noteworthy advances in water purification, healthcare, transportation, energy, agriculture, electronic and environmental bioremediation (Taha et al., 2022). The fundamental concepts in the discipline of NT are the nanoscale, nanoparticle (NP), nanomaterial (NM), nanocomposite (NC) and nanostructured materials (Szczyglewska et al., 2023). The obvious and overwhelming differences in features between the nanoscale and macroscale are the quantum confinement dominance and the extraordinary surface phenomena at the nanoscale. This has resulted in the intensification of the surface area to the volume ratio. This increased surface area to volume ratio modifies the reaction of materials and the mechanical, thermal and catalytic properties of materials (Taha et al., 2022).

NPs have received a huge deal of attention among the already used NMs owing to their miniature size and huge surface area features (Negrescu et al., 2022). Their exclusive physical and chemical properties give NPs superior features in comparison to their mass composition. At the nanoscale, particles are created with different distinct features such as magnetic, optical, electrical, etc. owing to their extraordinary surface energy and specific considerable surface area and quantum confinement (Annu and Ahmed, 2018; Pal et al., 2019). NPs can be achieved in nature from volcanic eruptions, dust, and existing organisms like fungi, bacteria, algae, plants, etc., and by synthetically using biotic, physical, and chemical production routes (Smita et al., 2012; Tarrahi et al., 2021).

NPs are grouped into inorganic, organic, and semi-organic forms according to their chemical nature. They can also be grouped according to their shape (flower, spherical, cubic, rob, triangular, octahedral, star,

* Corresponding author.
E-mail addresses: uyi4we@gmail.com (U.O. Aigbe), osibotea@cput.ac.za (O.A. Osibote).

https://doi.org/10.1016/j.hazadv.2024.100401
Received 26 September 2023; Received in revised form 30 December 2023; Accepted 8 January 2024
Available online 12 January 2024

etc.) and the number of their dimension in the nanoscale (zero-quantum dots, one-nanorods and nanowires, two-nanolayers and nanoplates and three-nanoflowers and nano coils dimensions) (Hamida et al., 2021). Metal-NPs, polymer-based-NMs, lipid-based-NMs, semi-conductor-based-NMs, and carbon-based-NMs are the various classes of nanomaterials (NMs) identified based on their morphological shape, size, and other attributes. NMs are applied in the various fields of photonics, catalysis, fuel-cells, energy storage, drug delivery, environmental remediation, nanomedicine etc. (Annu and Ahmed, 2018).

MeO is an interesting class and distinct form of NMs, with general uses in physical, chemical and material sciences. They are designed as meaningful coordination inclinations of metal ions (MIs) such that the oxide ions form a sphere of coordination around MIs and give rise to the close-packed structure. MeO NPs are of huge significance owing to their exceptional features and prospective utilization in NS and NT. Physical features of nanoscopic materials such as shape, size, and surface morphology control their chemical, electronic, optical, and physical features. They are used in essential applications like fluorescence and optical sensors, photovoltaic, environmental applications, catalysts, biomedicine, supercapacitors, anode materials for fuel cells, energy storage, electrode material for lithium (Li) batteries, gas sensors etc. when their size is in the nanoscale range (Alhalili, 2023; Kumar et al., 2022; Khan et al., 2022; Khayoon et al., 2023). The various types of MeO NPs include titanium oxide-NPs (TiO_2 NPs), iron oxide-NPs (FeO NPs), zinc oxide-NPs (ZnO NPs), silver oxide-NPs (AgO NPs), magnesium oxide-NPs (MgO NPs), cerium oxide-NPs (CeO_2 NPs), and other MeO (chromium dioxide (CrO_2), molybdenum trioxide (MoO_3), bismuth trioxide (Bi_2O_3) and binary oxides (Li-cobalt dioxide ($LiCoO_2$) or indium-tin-oxide (InSnO)) (Alhalili, 2023; Naseem and Durrani, 2021; Farré and Barceló, 2012; Negrescu et al., 2022).

A task that has been a long source of attraction to materials scientists is nanosized functional materials creation and assembly started by nature. Remarkably, the well-recognized chemical production of an array of NMs with outstanding manipulation of their size and shape, chemical synthesis paths generally use harsh reaction conditions (unsafe pH and temperature), lethal chemicals, are not energy effective, scale-up issues and mostly result in harmful by-products. These problems are hence tremendous sources of motivation for the creation of functional materials in a natural way. To tackle these problems, ideas and concepts from different science fields are teaming up to make exceptional techniques for the green production of bio-mineral materials with desirable properties (Bansal et al., 2011).

The various physicochemical and organic routes for the creation of MeO NPs fall under two definite groups, which are the top-down (TDM) and bottom-up (BUM) methods. The TDM comprises of procedures in which NPs are created through the decrease of the size of bulk materials to fine particles via the application of suitable lithographic methods like chemical etching, photo-reduction, thermal evaporation, grinding, sputtering, and milling (Pal et al., 2019). TDM approach provides a consistent particle shape, size and geometry and a monodisperse population with enhanced yields, permitting the scale-up of production. These methods are excellent for creating structures with long-range order and for making macroscopic connections (Pandit et al., 2022). Also, synthesized materials through this technique generally preserve high-crystallinity, which is achieved from the host-material. A key disadvantage of this technique is surface imperfection and particle destruction, poor quality distribution of the obtained product, wide-ranging size distribution, diverse sizes and shapes of product, internal stress creation, structural defects and wear, and the prerequisite of suitable host materials (Poolakkandy and Menamparambath, 2020). Noxious solvents, excessive temperature and pressure requirements, laborious downstream handling, excessive cost, instability, low yield, and reduced biocompatibility make TDM routes further uneconomical. Hence, to overcome the drawbacks associated with MeO NPs produced via the standard classical approaches, there is an increasing requirement to synthesize nanostructures employing the green technique to overcome all challenges by scientists currently (Nadeem et al., 2020; Negrescu et al., 2022).

The BUM (self-assembly) deals with the creation of NPs from the assembly of miniature matter such as atoms and molecules into novel nuclei, which further develop into a particle having nanoscopic sizes using different chemical and biological techniques (Pal et al., 2019; Michael et al., 2022; Pandit et al., 2022). The exploitation of the biological synthesis route is considered an advanced substitute for the physicochemical synthesis routes. This technique utilizes natural biomass sources like micro and macro-organisms (fungi, algae, bacteria, and selected viruses), biomolecules (lipids, pigments, proteins, polysaccharides, etc.), and plants as biologic-reducing and stabilizing agents for the green production of NPs with minimum contamination (Hamida et al., 2021; Andra et al., 2019; Jeevanandam et al., 2022).

The clear expansion of NPs synthesis options and green methods that make use of various biological sources is quite breathtaking. Wet, dry, and computational engineering procedures can all be categorized under NT. Wet NT deals with processes resulting from marine settings, typically using existing systems and mechanisms found in living organisms' cells, tissue, and organs. In contrast to computational NT, which deals with the development and usage of modelling, computer-based-quantum and molecular design, and simulation of the behavior or attributes of systems pertinent to NT, dry engineering deals with the production of inorganic inflexible structures and parts using physicochemical approaches (Chavali and Nikolova, 2019). Fig. 1 shows the various methods engaged for NPs production.

Various noteworthy features of the green (bio-synthesis) technique are the nonexistence of noxious chemical compounds being employed as stabilizing or reducing agents resulting in biocompatibility, no noxious yield being created from this procedure using low energy consumption at a reasonable cost and being highly scalable (Hamida et al., 2021). The applicability of bio-NPs facilitated by the green route is more analogous to MeO NPs owing to their advanced properties such as quantum size, miniature size, quantum tunnelling, and surface effects (Berta et al., 2021; Ali et al., 2023). Furthermore, attributes such as enhanced morphologies, high yield, and permanent stability in MeO are achieved by employing a greener method (Nadeem et al., 2020).

The morphological characteristics of NMs put forward to different applications can be varied by altering the reactant composition/concentrations and condition of the reaction. Their applications are constrained by the lack of knowledge of the controlling mechanisms and other modelling factors, relentless stability in the existing environment, analysis requisite, bioaccumulation, noxiousness impacts, skilled technicians requirement, obstacles created during the design of devices and structures assembling and the recycling/regeneration approach. These drawbacks can be overcome by employing the green synthesis approach, where NMs created via these routes are governed by the right regulation, organised control, clean-up action, and bioremediation procedure will assist in uplifting environmental suitability and stability (Kumar et al., 2021).

From the analysis of papers published in SCOPUS for the last ten years as shown in Fig. 2, it is obvious that there has been a keen interest in the utilization of green synthesis techniques for the creation of MeO employed for various applications. Hence, this review article aims to provide a comprehensive brief of the various bio-synthesis routes via plants and microbes extracts as reducing and stabilizing agents in the green production of MeO NPs as well as their various current applications.

2. MeO properties

Metals, non-metals, and semiconducting materials make up the bulk of the most well-known and extensively researched inorganic NMs (Alshammari et al., 2023). Inorganic NMs, specifically MeO, have drawn more attention lately than organic NMs. In contrast to bulk-materials, their high-surface-area-to-volume proportion offers several benefits,

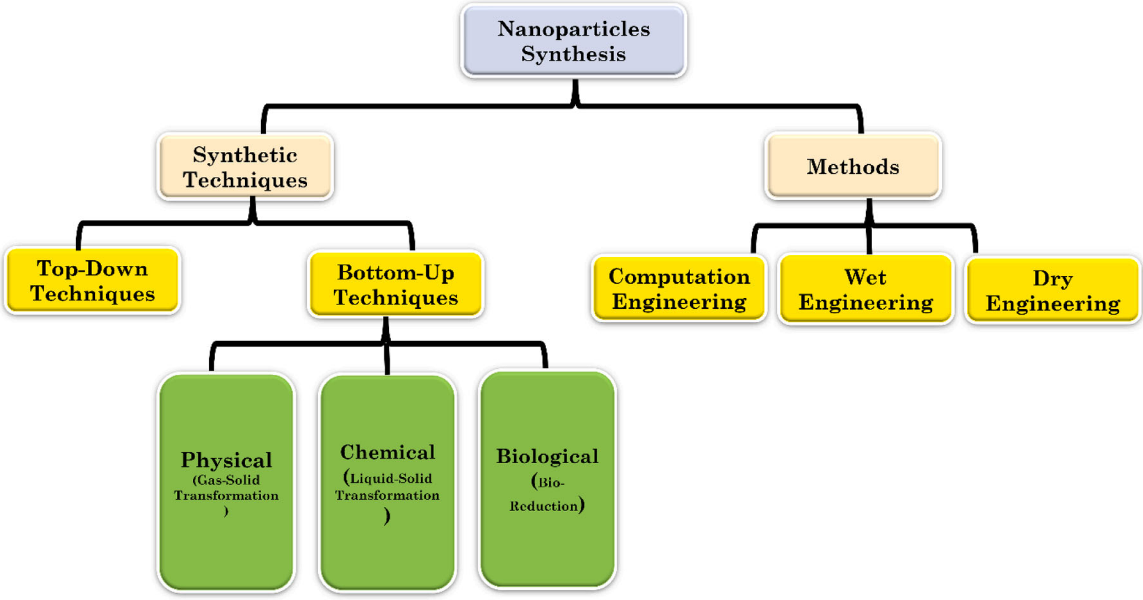

Fig. 1. Approaches devoted to the NPs production.

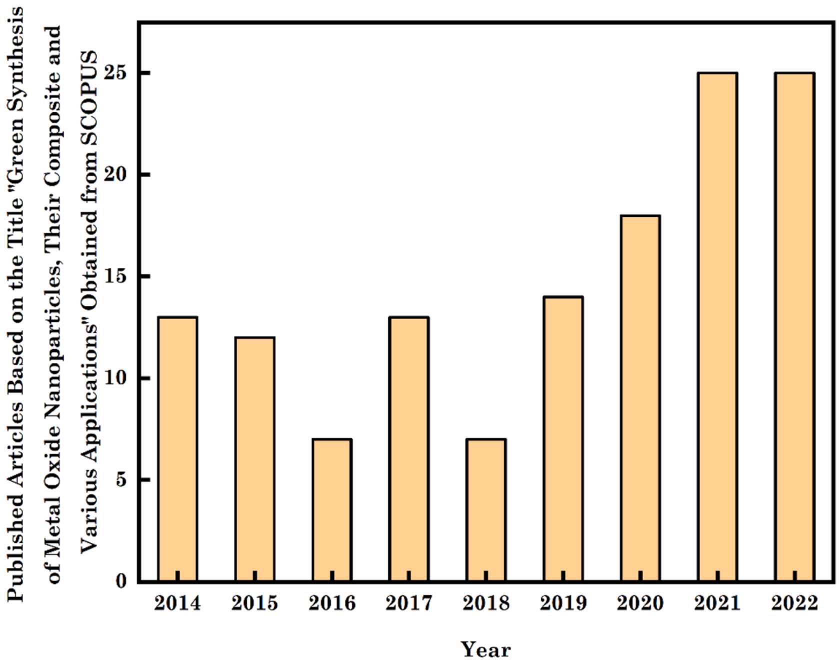

Fig. 2. The number of published articles with the title “Green synthesis of metal oxides nanoparticles, their composite and various applications” obtained from SCOPUS.

including sturdy catalytic performance, extraordinary loading, surface functionalization practicability, drug administration, biomedical applications, and flexible mechanical features. MeO is more intriguing and commonly applied in a range of applications among the many inorganic NMs. This is due to the well-established simple synthesis methods, the effortlessness with which the physicochemical properties can be controlled, and the intriguing and tunable characteristics (Kumar et al., 2022).

The phrase “oxide” is precisely associated with chemical compounds that have a minimum of one oxygen (O_2) atom alongside an alternative element present in chemical or molecular formula. It can also be deemed as a di-anion of O^{2-}. Thus, MeO generally comprises of an anion of O_2 with an oxidation state of -2. MeO compounds can be classified based on the number included with or taking the exact oxidation state of the metal. They mostly have several arrays of different structures, which start from the distinct molecules to polymeric and crystalline structures (Montemore et al., 2017).

They can extend from solids to gases at the quality level and they adopt polymeric structures when studied specifically. Taking MeO distinct occurrence, they take on primarily polymeric forms. When they are combined with three and at least six metal atoms, they give a rutile form and rock-salt or carborundum, which is due to the metal-O_2 bonds that are generally sturdy and creäting cross-connected polymeric structures that are extremely insoluble in solvent and may be attached by bases or acids. They exist in the soil in mineral form as hydroxides, oxyhydroxides with hydrated oxides of aluminum (Al), manganese

(Mn), Ti, Fe, silicon (Si), and simple oxides (Masroor, 2022).

MeO NPs show a comprehensive structural diversity owing to their ability to yield phase of various metals to O_2 ratio owing to the existence of multiple stable oxidations on their MIs. They are classified into various orbitals like oxides of 3-d transition elements (Nwachukwu et al., 2023). TMeO naturally has unfilled D-shells, which authorize reactive electronic transitions, wide bandgaps (E_g), outstanding electrical properties, and high dielectric constants. Furthermore, they have remarkable and flexible catalytic, optoelectronic, thermal, optical, electrical, magnetic, mechanical and photochemical characteristics. They have been utilized as sensors, batteries, actuators, supercapacitors, fuel cells, optical devices, pyroelectric, piezoelectric, ferroelectric and random access memory owing to their extraordinary size and shape, which display characteristic physicochemical properties (Yoon et al., 2021). MeO NPs' diverse structure and features, particularly those related to their size, shape as well as their pore size, and stability, have a meaningful influence on their functional performance in the context of their specific applications. Size together with shape is crucial for effectiveness or desirability in applications (Lane and Zimmerman, 2019; Khan et al., 2022).

Beyond obtaining tunable features, the controlled adaptation of nanostructures to MeO designing has attracted significant interest in exploring the increased action spectrum in the nanoscale size range, the major applications of MeO include fluorescence and optical sensors, photo-voltaic, catalysts, wastewater purification, biomedicine, etc. This has sparked a study into morphologically controlled NMs with consistent pore sizes to achieve desired qualities. In addition to all these uses, NPs have also been employed as fuel cell anode materials as well as gas sensors. The size and form of the nanostructured MeO mostly influences the surface-dependent NMs' properties, including those relating to optics, mechanics, electricity, magnetism, and catalysis (Alhalili, 2023; Lane and Zimmerman, 2019; Aigbe and Osibote, 2020).

The orientation and the number of electron spins determine the magnetic properties. In transition MeO (TMeO), single electrons are sturdy associated with their motion and the ion spin, which is described by the single universal atomic-spin. The atomic-spins of neighbouring ions may be also sturdily associated to form a spin sub-lattice. Supporting the magnitude, the number of spin sub-lattices, and the orientation, TMeO possesses various magnetic fields and responses (dia-, para-, antiferro-, ferri-, and superparamagnetism) with the purpose of a peripheral magnetic field. They show intriguing magnetic (ferro-, ferri-, or antiferromagnetic behavior) and electronic properties. Specific oxides hold switchable orientation states as in ferroelectrics (titanates, niobates, or tantalates). Their magnetic properties are assessed by the number and orientation of electron spins. For MeO, their electrons are sturdy linked with their motion and the individual total atomic spin characterizes the spin of an ion. The formation of spin sublattice is sturdy associated with the atomic spins of neighbouring ions. Owing to the orientation, magnitude, and number of spin sublattices, MeO acquire various magnetic fields and responses when external magnetic fields are employed (Laurent et al., 2018). The low-dimensional structures of MeO NPs have a unique physical characteristic, which accounts for both the scientific and technological relevance of NPs. The creation of MeO nanostructures with exceptional explicit features in comparison to those of bulk particle species is the aim of this new branch of advanced NT (Arunadevi and Kirubavathy, 2022).

3. Green approaches for the creation of MeO NPs

Today's core science gets its full expression in the words of the artist-scientist Leonardo da Vinci "Where nature finishes creating its own species, man begins, utilizing natural things and with the help of nature" to produce an infinitude of species (Bansal et al., 2011). With Richard Carson's launch of Silent Spring in 1962, the environmental protection program began and led to the establishment of the United States Environmental Protection Agency (USEPA) and the beginning of green chemistry (Das and Chatterjee, 2019). The 12 green chemistry principles were formulated in 1998, based on the book titled "Green Chemistry: Theory and Practice" by Paul Anastas and John Warner. It is advocated in the book that industrialists, government, and scientists should direct their actions to decrease or remove hazardous materials and chemical procedures utilization. A major contribution to the development and founding of new philosophy has been made by these principles owing to their relevance, specificity, and usefulness. Fig. 3(a and b) shows the "12 Green Chemistry Principles" and their acronym description using "Productivity" (Soltys et al., 2021).

The green NPs synthesis route is founded on the '12 green chemistry ethics", which are the advancement and design of NPs employing non-noxious chemicals, renewable energy, biologically benign solvents, and reduced waste products. The three key steps in NPs creation from green-chemistry insight involve the use of a reliable solvent medium, non-noxious reducing agents, and biologically benign stabilization-agents. Another critical component is the choice of capping agent employed to passivate the NPs surface. NPs size, morphologies and target applications are extensively impacted by the capping agent (Annu and Ahmed, 2018).

Regulations relating to health and safety are crucial in prioritizing risks related to NPs. The use of a set of fundamentals reduces or eliminates the usage of harmful substances in the design, production, and application of chemical products while creating new chemical processes that prioritize minimal hazard as an execution criterion. This is the key factor in the evolving green chemistry industry (Shafey, 2020).

3.1. MeO NPs production utilizing plants

Plants belong to unique family trees in a taxonomic group like Lamiaceae, Fabaceae, Rutaceae, Euphorbiaceae and others (Sunny et al., 2022). There are 452 plant groups, with the individual plants being pools of principal and resulting metabolites/phytochemicals. Plants in desert-like environments or at elevated elevations always store exclusive kinds of phytochemicals. Plant parts such as roots, stems, leaves, and seeds have been utilized to create NPs. Plant extract composition is a critical factor in NPs creation and is responsible for NPs bioreduction. Extracts of plants are cocktails of metabolites (flavonoids, alkaloids, terpenoids, polyphenols, and low/high-molecular-weight proteins) that decrease bulk metal salts (MSs) to nano-sized particles. Most plants produce these chemicals for defence against abiotic and biotic stresses. Regular PEs are utilized in efficient, eco-friendly ways to fabricate NPs without utilizing intermediate base groups. NPs produced are very pure and of enhanced quantity that is free from contaminations (Khan et al., 2022; El Messaoudi et al., 2023; Singh et al., 2018).

PEs can be utilized in either fresh or dried plant parts. Owing to water content, dried plant parts are preferred. The dried plant parts are subjected to milling, while the fresh plant parts are sliced into fragments. The plant parts reduction will assist in enhancing the surface area. Hence, extraction is executed through non-polar or polar solvents. Plant part drying is executed through sun or shade. Owing to this technique being timewasting, people have shifted to oven aeration and freezing drying approaches. Oven aeration decreases the time spent to a few hours while freezing drying is recounted to be the most appropriate approach for drying and retaining the reducing agents. Bio-molecules like terpenoids and flavonoids are temperature sensitive, hence, extraction of desired compounds is achieved by employing appropriate solvents that have the matching polarity as the bio-molecules. This involves plant parts' dispersion in water under mixing. Also, green solvents like methanol or ethanol can be employed for extraction, and cell-wall degradation is more efficient in green solvents compared to water (Varghese et al., 2020).

To produce NPs facilitated from the extract of various plant leaves, the extract is combined with the precursor (MIs) solutions at various reaction conditions. The factors defining plant leaf extract specifications like the phytochemical types, the concentration of phytochemicals,

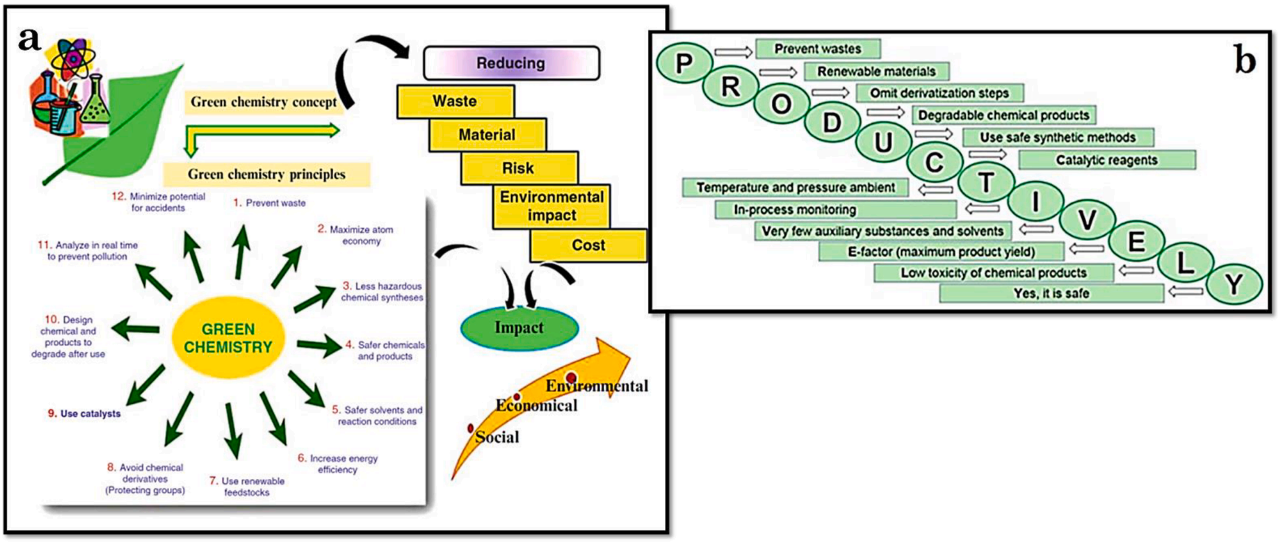

Fig. 3. (a) "12 Green Chemistry Principles" and (b) their abbreviation using "Productivity" (de Marco et al., 2019; Soltys et al., 2021).

concentrations of metal salt, temperature, and pH are acknowledged to manipulate NPs formation rate, yield, and stability (Miu and Dinischiotu, 2022).

The mechanisms involved in the bio-production of MeO NPs applying plant parts are grouped into three stages, which include the activation stage, which involves the conversion of MIs from a mono or divalent oxidation state to a zero-valent state. Reduced MI occurs because of nucleation at the stage. In the growth stage, small NPs form aggregates, which form large NPs with varied shapes like pentagonal, hexagonal, spherical, cubical, triangular, etc. Extract from plants also acts as a stabilizing and capping agent to get a stable morphology in the phase. In the termination stage, NPs aggregates produce a variety of other irregularly shaped NPs (Sunny et al., 2022).

Proteins with functionalized amino groups (-NH_2) available in the extracts of plants partake in MIs reduction. While functional groups like –C–O–C–, –C–O–, –C=C–, and –C=O– existing in alkaloids, phenols, anthracenes and flavones assist in creating MeO NPs (Singh et al., 2018). Flavonoids for instance contain different functional groups, which have an improved potential to reduce MIs. Owing to the tautomeric transformation in flavonoids, the hydrogen atom is released, by which the enol form is transformed into keto form. The reduction of MIs into MeO NPs completes this procedure (Singh et al., 2018). In most cases, phytochemicals such as polyphenols act as electron donors (reduction agents) and their interaction with the MIs leads to the creation of NPs via the reduction of target MIs. Plant phytoremediation properties have been used to phytosynthesize metal NPs. Frequently, such chemical components function as reducing, capping and stabilising agents in MeO NPs assembly. The key functional groups of various plant parts, which allow plant-based parts to function as reducing and stabilizing agents are the hydroxyl (OH^-) and carbonyl groups (Bagheri et al., 2023).

The phytochemicals existing in extracts of plant leaves have a mysterious capability to reduce MIs in a much fleeting instance as related to fungi and bacteria, which requires an extended incubation pace. Hence, extracts from plant leaves are considered superb and benign sources for MeO NPs production (Singh et al., 2018).

The benefits of plants in the production of NPs are due to their cost-effectiveness, non-noxiousness, ease, safety, and time-saving (Rasheed et al., 2022). The utilization of new plant resources for extract preparation is better and health-conscious owing to the plant body having various unstable chemicals, hormones, proteins, vitamins, enzymes, and micro and macro trace elements that are non-existent in plants resulting biologic products. In the green production of NPs, their surface is encapsulated by functional groups present in the extract of the plant converting them into less noxious, biodegradable, and biocompatible products (Khan et al., 2022; Akintelu et al., 2021). Plants are resources of numerous biochemical components that act as stabilizing and reducing agents in producing green NPs (Vijayaram et al., 2023). Fig. 4 shows the process involved in the production of MeO NPs using extracts from plants.

Reaction settings, as well as plant extract chemical conditions (concentration metal precursor, use of reaction temperature, plant extract amount, and reaction time coupled with plant extract variation-preparation time, concentration, pH and phytochemical molecules), considerably impact the synthesized NPs' physicochemical properties. A visual confirmation of the NPs' formation is the color change of the mixture of plant extract and the metal precursor. However, different physiochemical and surface study methods are also needed to confirm NPs formation and to study their impacts on the natural environment, human health or other anticipated applications. More essentially, a thorough recognition of the synthesized NPs' properties and characteristics enables laboratory discoveries to be transformed into everyday use (Tan et al., 2023). Aqueous extract of Zea mays lea plant was employed as a reducing, stabilizing and chelating agent in the synthesis of TMeO (CuO, ZnO, Fe_2O_3, Cu_2O, NiO, Cr_2O_3 and CdO NPs) NPs (Nwanya et al., 2021). Psidium guajava and Trigonella foenum-graecum leaf extracts were employed in the bio-synthesis of TiO_2, which was explored for the antibacterial activity against Staphylococcus aureus (S. aureus) and Escherichia coli (E. coli) and antimicrobial activity against microorganisms (S. aureus, Enterococcus faecalis, Klebsiella pneumoniae, Streptococcus faecalis, Pseudomonas aeruginosa, E. coli, Proteus vulgaris, Bacillus subtilis, Yersinia enterocolitica and fungus Candida albicans). The bio-synthesized was found to have phenolic compounds, which were responsible for the reduction of the MSs to TiO_2 NPs (Santhoshkumar et al., 2014; Subhapriya and Gomathipriya, 2018). Kniphofia foliosa root and Lippia adoensis leaf extracts were used in the bioreduction of titanium tetrabutoxide and zinc acetate dihydrate to produce TiO_2 and ZnO NPs in a ratio of 1:2, 1:1 and 2:1 and 3:2. Both biosynthesized NPs were used for antibacterial activity (Bekele et al., 2020; Demissie et al., 2020). While ZnO, TiO_2, and CuO NPs were bio-synthesized using extracts of Cassia fistula and Melia azedarach plant, leaves of Raphanus sativus var. Longipinnatus, Passiflora caerulea fresh leaf, Syzygium cumini leaf, Eucalyptus Globoulus leaf and Catha edulis leaves. They were employed for antibacterial activity, anticancer agent, inhibition against urinary tract infection pathogens, photocatalytic degradation of Pb^{2+} ions, sorption of methyl orange dye and antimicrobial activity (Naseer et al., 2020; Umamaheswari et al., 2021;

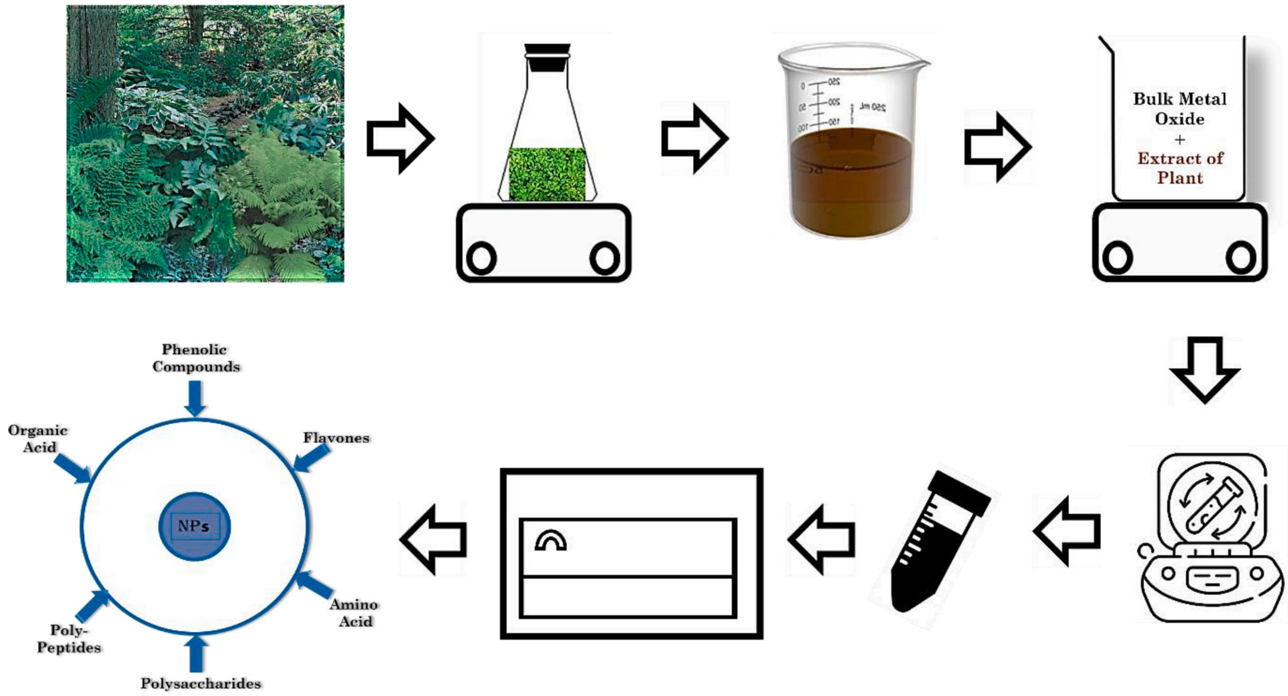

Fig. 4. Schematic of the process of MeO synthesis using extracts of plants.

Santhoshkumar et al., 2017; Sethy et al., 2020; Alhalili, 2022; Andualem et al., 2020).

3.1.1. MeO production utilizing bacteria

Bacteria species are generally used for commercial bio-technology applications like genetic engineering, bio-leaching, and bio-remediation. They have the capacity to decrease MIs and are important applicants in the preparation of NPs. Prokaryotic bacteria and actinomycetes have generally been applied in creating MeO NPs. This approach for NPs creation is embraced owing to the comparative ease of bacteria manipulation (Singh et al., 2018). Prokaryotic and eukaryotic organisms bio-mineralize substances within or exterior of their cell to create metal NPs (El Messaoudi et al., 2023). These synthesis paths are considered in terms of extracellular (synthesis procedure happens outside living cells. This process is achieved via cell biomass filtrate, cell-free, culture medium and biomolecule-mediated production of NPs) and intracellular synthesis methods (involves the use of cellular enzymes and synthesis of NPs take place inside living-cells with biotic procedures like respiration, metabolic action, and growth stage, playing critical parts in the bio-synthesis procedure. NPs can be regained by destroying the cell wall of the plant cell). The bacterial system is employed by the extracellular mode of bio-synthesizing metal NPs owing to their genetic transfer and economical use (Hamida et al., 2021; Jassal et al., 2022).

NPs bio-synthesis using various bacteria that have been isolated, intracellularly by the MIs encapsulation in the microbial-cells and extracellularly through the MIs reduction on the microbial cells' surface inhabiting different pH, temperature, and oxygenation incubation time situations, hence, presenting extraordinary catalytic activity and surface area for enzymes interactions with MSs. The exact degree of buildup accomplished by both forms of microorganisms depends on the pH, temperature, preliminary MI concentration, and homogeneousness of the experimental medium. Enzymes play a critical part in NPs synthesis and thus, optimized factors are crucial for the optimum activity and interactions of enzymes (El-Seedi et al., 2019).

By acting as a normal capping during the NPs production procedure, they provide additional stability by stopping the aggregation of NPs and supporting their extensive stability. However, the overwhelming limitations of using this microbial in NPs synthesis include the time spent on the process to monitor the broth containing the bacteria cultures, stopping contaminations and microbial species screening (El Messaoudi et al., 2023). The mechanism of MeO NPs bio-synthesis using bacteria is given in Fig. 5a–c. The MIs are reduced by the electron transferred intracellularly to NPs within the cell and it grows on it before it is moved to the exterior membranes (Fig. 5a) and the inorganic MIs are reduced to NPs through the extracellular bio-synthesis of the NPs employing produced enzymes and enzymes situated on the exterior membrane (Fig. 5b) (Jassal et al., 2022).

3.1.2. MeO synthesis using algae

These are photo-produced marine filamentous organisms that belong to the domain Plantae. They are either multi-cellular or unicellular organisms, which are pervasive and live in damp rock surfaces, freshwater, and seawater. They are valuable in pharmaceuticals, aquaculture, cosmetics, medicine, and agriculture (Michael et al., 2022). Algae are eukaryotic marine oxygenic photo-synthetic organisms that extend from uni-cellular forms such as chlorella to multi-cellular forms such as brown algae, which lack basic plant structures such as leaves and roots

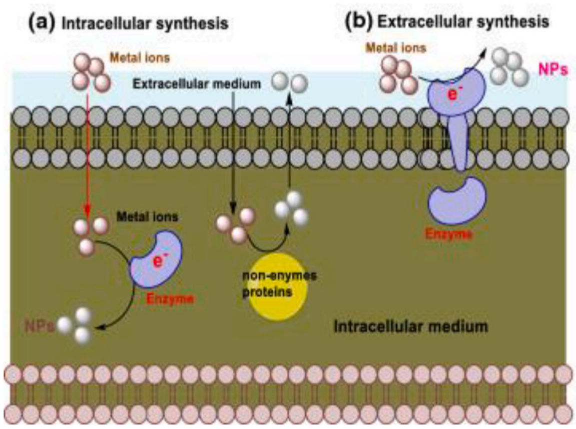

Fig. 5. (a) Intracellular and (b) extracellular bio-synthesis of MeO NPs in bacterial-cells (Jassal et al., 2022).

(Gebre and Sendeku, 2019). These eukaryotic organisms are progressively and sustainably showing the application in the NT field for economic development and reduction of metals, owing to their minimal noxiousness and biological value. Their extracts comprise of a collection of bioactive constituents such as carotenoids, enzymes, minerals, chlorophylls, phycobilin, lipids, carbs, polyphenols, and polyunsaturated fatty acids (El Messaoudi et al., 2023).

They are utilized as stabilizing and reducing agents for NPs production as their cell walls have functional groups and biomolecules. They are also referred to as bio-nano factors, as NPs can be created from both live and dead biomass. The major forms of algae are macroalgae and microalgae. NPs synthesis via algae is relatively faster than employing other bioagents. In comparison to most biomass, they can be collected anytime in a year and do not require any outside chemicals or fertilizers for their growth (Michael et al., 2022). Microalgae can bio-remediate noxious metals, and then alter them to other adaptable forms. For NPs synthesis, macro algae have various active metabolites such as cyclic peptides, alkaloids, proteins, polyketides, polysaccharides, stereos, lipids, glycerol, quinones, etc. for their production. The extracellular and intracellular methods are the two fabrication routes. In the intracellular route, nitrogen fixation and photosynthesis are used in the metabolic processes for NPs production. The extracellular procedure takes place outside the cell and with the attachment of the MIs to the algae cell surface. The MIs are subsequently reduced at the surface via cell metabolism exudates like pigments, various enzymes, and non-protein molecules like lipids, antioxidants, and metabolites. Overall, the whole process is energy-effective. Fig. 6 displays the steps involved in the bio-production of NPs using algae, which involves the process of washing collected seaweeds to remove dirt, salt and other foreign materials, drying of seaweeds, powdering of the dried seaweeds, extraction of seaweed extracts using deionized water or solvent, filtering of the seaweed extracts, and the addition of seaweed extracts for the bio-reduction and capping of MIs to bio-produce MeO (El Messaoudi et al., 2023; Gebre and Sendeku, 2019; Michael et al., 2022).

Extract of Padina pavonica algae was employed as a reducing and capping agent in the green synthesis of Fe_3O_4 NPs, which was employed and found to be effective for the photodegradation of congo red (CR), and antioxidant and neurotoxicity activity for Human neuroblastoma (Caf, 2022). In the study by El-Kassas et al. (2016), the green synthesis approach was employed for the bio-production of Fe_3O_4 NPs using Padina pavonia (Linnaeus) Thivy and Sargassum acinarium (Linnaeus) Setchell 1933 seaweeds. The biosynthesized Fe_3O_4 NPs were assessed for the bioremediation of lead ($Pb^{2+)}$ ions and were found to be effective NPs for the bioremediation of Pb^{2+} ions (El-Kassas et al., 2016). Ulva Lactuca seaweed extract was used as a reducing and capping agent in the bio-synthesis of ZnO, which was assessed for the photocatalytic degradation of methylene blue (MB) dye as well as antibiofilm activity on Gram-positive (Gram+ve) and Gram-negative (Gram-ve) bacteria and insecticidal activity on Aedes aegypti fourth instar larvae (Ishwarya et al., 2018; Fouda et al., 2022). Employing Ulva Lactuca seaweed extract, Fe_3O_4 NPs were biosynthesized and used for the anti-bactericidal activity against enteropathogens (Bensy et al., 2022).

3.1.3. *MeO synthesis using fungi*

They are acknowledged as eukaryotic creatures that stay in different regular sheltering and from naturally decomposed creatures. From an estimated aggregate of 1.5 million global fungi species, approximately 70,000 species have been documented. More recent data highlight that around 5.1 million fungal species were discovered according to high-output sequencing (Boroumand Moghaddam et al., 2015). Fungi have gained heightened consideration for the biologic creation of MeO NPs due to their tolerance and ability to bio-amass metals. Acquiring a considerable magnitude of synthesized NPs with fungi assistance is straightforward, as they are remarkably effective extracellular enzyme secretors, reasonably feasible and effortless utilization of this biomass, and easy to cultivate resulting in the swift rate of fungi growth (Boroumand Moghaddam et al., 2015).

MeO NPs are produced using fungi through the enzyme reduction intracellularly or extracellularly and the biomimetic mineralization process (Boroumand Moghaddam et al., 2015). Enzymes inside and exterior of the fungi cells are recognized to facilitate the creation of NPs as a reducing agent. However, a critical issue of utilizing fungi in NPs creation is that the deoxyribonucleic acid (DNA) evidence of eukaryotic organisms in specific distinct enzymes is akin to much more complicated than that in prokaryotes. The main challenge in the intracellular route is low yields resulting from the extraction procedure in the downstream processing and on the contrary, NPs created on the cells' surface or at the edge of the cells are the result of extracellular creation, hence, making it easy for downstream processing to recover them (El Messaoudi et al., 2023).

In the extracellular production of NPs employing fungal species is useful owing to ease of scaling up, usage of inexpensive raw materials for growth, extraordinary biomass establishing capacity, straightforward downstreaming stages, minimal noxiousness of residue and economic viability. Furthermore, fungal species show more tolerance and bioaccumulation properties, which assist in the creation of MeO NPs. Fungi are also known to excrete huge sums of extracellular enzymes which are proficient for hydrolyzing metals. MeO NPs created using fungi are judged based on the biological material utilized (strain of microorganism employed, the growth parameters and sample preparation technique) and the applied reaction conditions (metal precursor used, concentration of metal precursor, pH, and reaction temperature). The different techniques employed in the NPs synthesis include the use of fungal biomass as well as the use of cell-free filtrate of the fungal culture or biomass homogenate and fungal cell filtrate. Another merit of employing the green technique mediated by fungal to bio-synthesize MeO NPs is the economic livability and the resource. Additionally, several fungal species grow quickly and hence culturing and keeping them in the laboratory are very straightforward. Most fungi's capabilities are high wall binding and intracellular metal uptake. MeO NPs are produced by fungi through enzyme reduction intracellularly or extracellularly and the biomimetic mineralization process (Priya and Sidhu, 2021; Boroumand Moghaddam et al., 2015).

Fungi facilitated the bio-production of MeO NPs for the creation of mono-dispersed NPs with well-described morphologies (Michael et al., 2022). They act as a better biologic agent for MeO NPs preparation owing to the diversity of intracellular enzyme presence. Large quantities of NPs can be produced by fungi in comparison to bacteria (Singh et al., 2018). Substantial attempts have been made to grasp NPs bio-synthesis mechanisms in bacteria and fungi. Per unit of bio-mass, fungi mostly

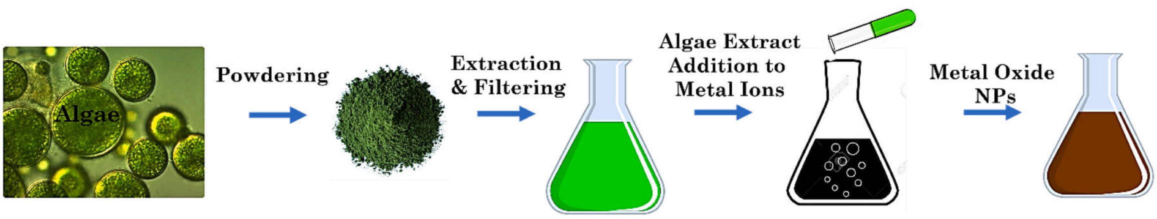

Fig. 6. Schematic of the green process for the production of NPs using algae.

have a superior capacity for the bio-buildup of MIs than bacteria owing to their remarkable cations' bio-sorption. But the specific stage of buildup accomplished by both forms of microorganisms relies on the experimental medium homogeneity, initial MIs concentrations, pH, and temperature. In heavy metals (HMs) presence, enormous quantities of redox-active-extracellular proteins are secreted to bio-reduce MIs, leading to the creation of insoluble metal-protein nano-conjugates, which ultimately create nano-crystals. Fungi sustain sizable biologic diverse hotspots, which may contain unique fungal proteins and enzymes capable of bio-decrease and purification (El-Seedi et al., 2019; Bhati, 2023; Jha et al., 2023). Owing to enzymes, peptides and reductive elements on their cell surface, fungi have a substantial advantage over other species. The most probable approach for the synthesis of MeO NPs is the enzymatic reduction (reductase) in the cell wall or inside infectious cells. Infectious enzymes enhance the magnitude of NPs synthesized and accelerate the reductive abilities for stable NPs synthesis (Pandit et al., 2022).

In the bio-synthesis of NPs, fungi are desirable owing to their mycelia having a larger surface area of interaction and can create more protein than bacteria allowing for the swift change of metal salts to MeO NPs (Zakariya et al., 2022). Cell-free filtrate of 5 isolated fungi isolated and cultured using pure culture methods and in Potato Dextrose Broth, was utilized in the bio-synthesis of FeO NPs through the mycoreduction of metal salts. The formation of FeO NPs was confirmed by the visual color change in the reaction mixture (Mahanty et al., 2019). While cell-free filtrate of endophytic fungus Xylaria arbuscula isolated from Blumea axillaris was employed in the bio-synthesis of ZnO NPs. 100 mL of the mycelium-free filtrate was mixed with 1 mM zinc acetate as a precursor salt solution and further inoculated in a rotary shaker at 150 rpm for 72 h. Observed creamy white precipitate formation from the reaction mixture was a confirmation of ZnO NPs creation (Nehru et al., 2023). Endophytic fungal strain Aspergillus terreus was isolated from Allium sativum L root and employed in the bio-synthesis of CuO NPs. This involved the mixture of 100 ug of $Cu(CH_3COO)_2\ H_2O$ with 95 mL of the fungal biomass filtrate in 5 mL distilled water. The color change of the reaction mixture from colorless to greenish confirmed the creation of CuO NPs (Nassar et al., 2023). Fungi-free cell filtrate isolated from soil samples was used as a reducing or stabilizing agent for the mycoreduction of precursor salts to produce ZnO—CuO NPs. An observed solution change to a faint brown color confirmed the formation of the NPs (Gaber et al., 2023). Fig. 7 shows the bio-process of producing MeO NPs using fungi modified from Periakaruppan et al. (2023).

3.1.4. MeO synthesis using yeast

Yeast is a uni-cellular micro-creature that exists in eukaryotic-cells (Soltys et al., 2021). Yeast are distinct-celled microorganisms existing in the eukaryotic cells, with 1500 yeast varieties recognized (Singh et al., 2018). They are excellent protein and vitamin sources, especially vitamin B complexes, and are utilized in brewing and baking manufacturing. They can also be employed in bio-remedy processes to degrade fatty acids, oils, combined arsenic, and other noxious contaminants and hydrocarbons. The advantages of employing yeast for bio-remediation processes include modest scaling of the procedure, non-noxious growth settings, storage ease, and modest cultivation (Patel et al., 2021).

Most of them are widely utilized in the creation of metal NPs. Their strains are ideal in the production of NPs as they have added benefits over bacteria owing to the NPs' mass creation and the modesty in managing yeast in laboratory settings, different enzyme creation, and swift growth employing essential nutrients. Oxidoreductases and quinones are membrane-bounded and play a critical part in NPs synthesis using yeast. The oxidoreductases function contrarily and are pH-sensitive. Oxidase is initiated at reduced pH values, while reductase is initiated at elevated values of pH. Furthermore, two classes of metal-binding ligands (phytochelatins and metallothioneins) and a key tripeptide (glutathione-GSH) with a part in various metabolic routes in yeasts are the key molecules that contribute to the mechanisms of yeast cells purification (El Messaoudi et al., 2023). For microorganisms, the mechanism involved in the formation of NPs involves the capture of MIs on microbial cells' surface or interior and the subsequent capture and reduction of MIs into NPs via enzyme action (Singh et al., 2018).

3.2. Factors impacting MeO synthesis

NPs morphology classification is adapted based on various specifications like temperature, reaction time, reactant concentration, and pH (Fig. 8). These factors mostly recognized the effects of green parameters on NPs synthesis and their imperative functions during MeO NPs fabrication (Vijayaram et al., 2023). The whole process of MeO NPs production is influenced by several factors such as the type of species of plant used, the kind and extent of biomolecules existing in it, and reaction parameters like pH, reactant concentration, temperature, and reaction time. Changes in any of these factors can alter the size, shape, and pace of synthesis of NPs, as well as their morphology and yield (Guleria et al., 2022).

The shape of developed NPs is motivated by a variety of factors. In NPs structure, pH plays a substantial purpose, with pH and temperature also controlling nucleation center formation. The reaction solution pH has been shown to significantly influence the creation of the resulting NPs. Reaction pH variations may affect the produced NPs' shape and size. The acidified media, on the other hand, form a range of diverse-sized particles when compared to lower acidic pH values (Chopra et al., 2022; Vijayaram et al., 2023). The size and form of MeO NPs created may modified in the reaction pH. NPs sizes and shapes are controlled by the pH (buzzer strength) and must remain stable throughout the NPs creation process (Ashour et al., 2023).

Phytochemical deprotonation and activation are triggered in the alkaline pH environment. Lower pH values inhibit the phytochemicals, causing them to remain protonated, leading to a decreased reduction or capping activity of metal salts. Overall, NPs created in an alkaline reaction mixture have a reduced size and are more stable over time. NPs created at acidic pH are generally less unstable owing to the ineffective capping process (Miu and Dinischiotu, 2022). Bigger particles are produced by matching lower acidic pH values to extreme acidic pH values. In distinction, an elevated pH environment favors spherical NPs growth and synthesis is exceptional for small-sized MeO NPs production. The surface plasmon resonance (SPR) peak developed is thick and draws away towards a longer wavelength region, resulting in a wide range of

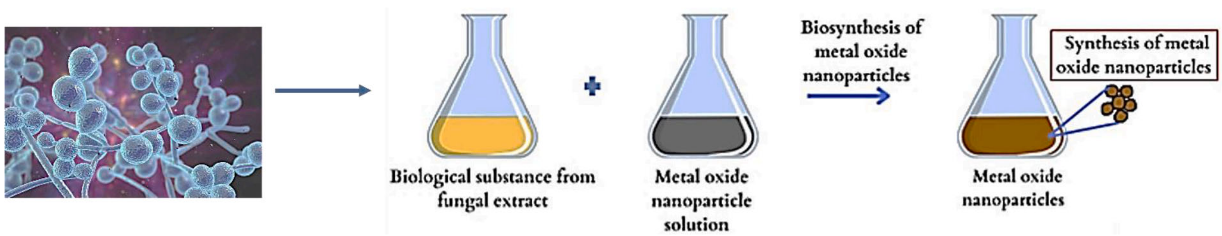

Fig. 7. Schematic of the bio-production of MeO NPs using fungi.

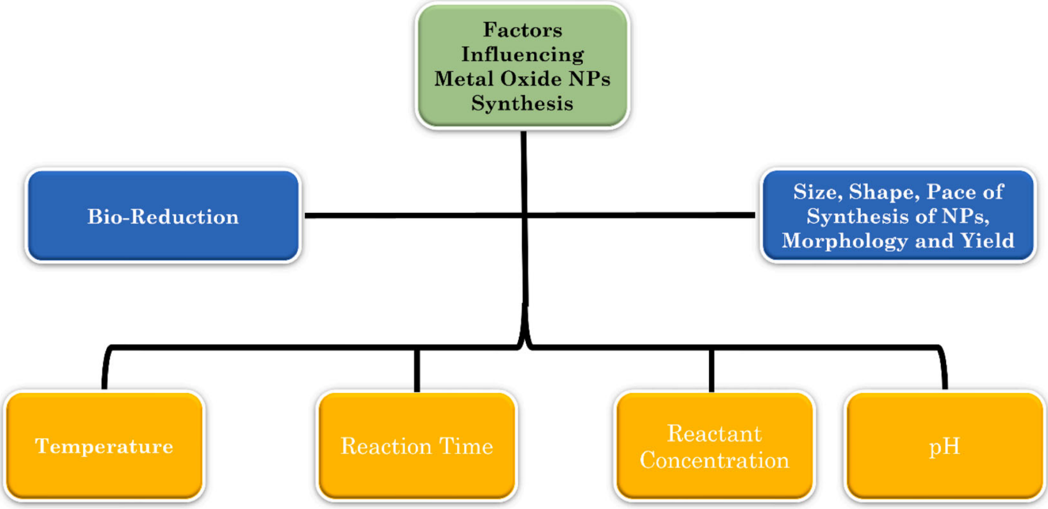

Fig. 8. Factors influencing the bio-synthesis of MeO NPs.

NPs (cylindrical and triangular shaped) compared with small-sized NPs produced when pH is low (Ashour et al., 2023).

Green synthesized NPs' physicochemical properties are impacted by the reaction and the drying of the particle with the application of temperature (Miu and Dinischiotu, 2022). For any synthesis, the temperature must also be taken into consideration. Temperature is a critical factor that changes the dimension and shape of NPs as well as their synthesis phases. The nucleation center's formation is strengthened by the reaction response rate as a result of the increase in temperature level. The production of NPs can be fitted as a function of temperature, resulting in different shape types and dimensions (Miu and Dinischiotu, 2022; Vijayaram et al., 2023). While utilizing biologic entities to formulate NPs, temperature intensification has shown catalytic behavior by accelerating the reaction rate and increasing the efficiency of NPs formation as well as impacting the NPs structures. Overall, temperatures of about 100 °C are needed for the production of NPs employing green approaches. While chemical synthesis approaches need mild temperatures and physical reactions need temperatures exceeding 350 °C (Ashour et al., 2023). The increase in reaction time is directly related to the particle size and the quantity of generated nuclei. If the comprehensive reduction time is surpassed, larger structures are created as a result of NPs aggregating. While the reaction time influences synthesized NPs size, shape, and yield. It also controls the NPs' structural morphology (Vijayaram et al., 2023; Miu and Dinischiotu, 2022).

The amount of bio-reducing agents affects the attributes of NPs by controlling the size and shape of particles (Ashour et al., 2023). Improving the reducing agent concentration speeds up particle growth. Extremely concentrated biological extracts lead to the creation of massive NPs. The enlarged size of the NPs can be attributed to the secondary reduction process that takes place on the metal nuclei owing to the redundant reducing phytochemicals. Biologic extracts reducing power is associated with their composition and quantity of biochemical. Hence, the solvent employed for acquiring the extract can influence the bio-synthesis of NPs. The decreased average size of NPs is relative to the increase in the precursor concentration. High extract content fast-tracked the production of smaller NPs by improving NPs nucleation and they are swiftly stabilised by the capping agents. But with a relatively high concentration of precursor, a sizable amount of the nuclei are unstabilized owing to the inadequate level of phytochemicals (Miu and Dinischiotu, 2022; Ashour et al., 2023).

3.3. MeO stability

The extraordinary chemical action with an enhanced surface of engineered NPs is mostly owing to the critically severe and largely irremediable action like aggregation. Exclusive surface area reductions and the interfacial spontaneous energy can be realized by aggregation, hence, reducing particle reactivity (Shafey, 2020). MeO NPs production can be generally grouped into hydrophobic environments and direct formulation in a water-soluble medium creating hydrophobic and hydrophilic NPs. Most of the NPs production procedures create hydrophobic NPs owing to the process conditions and surfactants' existence. This restricts NPs solubility in water or biologic medium. Advanced functionalization of the hydrophobic NPs surface is thought-provoking compared to hydrophobic NPs. Thus, improving the solubility of water and functionalization are the two key tasks that require to be overwhelmed to employing NPs for different purposes. NPs functionalization is a major phase towards enhancing colloidal stability, and water-solubility and pioneering a flexible surface (Wang et al., 2023).

Although they are stable and reasonable to produce, NPs aggregation can cause their instability and size expansion owing to the extreme surface-energy, hence capping them with agents or surfactants is required, resulting in a substantial size decrease which contributes to their stability (Alabdallah et al., 2021). To improve stability and speed up the dispersion of NPs, a capping agent is included in their production process. These capping agents may unswervingly affect the NPs' noxiousness owing to their capacity to lessen NP agglomeration (Slavin et al., 2017). It is important to increase the NP's stability improvement during storage, transportation, and its complete life cycle. The mainstream of the stabilization route is dispersant molecules like polyelectrolytes or surfactants, which not only adapt the chemistry and the surface physics of NPs as well as produce a massive stream waste owing to that they take up a worthy (more than 50 %) of the mass function system of NPs (Shafey, 2020).

Thus, there is a requirement to find biologically benign stabilization and functionalization routes and bio-appropriate to prevent contamination and the subsequent corrective impacts on the ecosystem such as non-immunogenic, non-noxious, and hydrophilic stabilizing agents. Various stabilizing agents are utilized to avoid NPs aggregations and to functionalize the particles for the preferred application at the same pace (Shafey, 2020). These biologic extracts are a valuable supply of phyto-chemicals like amines, enzymes, phenols, biodegradable polymers, silica, citric acid, vitamins, and ketones, which are credited to be accountable for the stabilization and reduction of mass salts into individual NPs without the unfavorable impacts on the ecosystem and bio-synthesis (Nadeem et al., 2020; Shafey, 2020).

The approaches involved in the functionalization of MeO NPs include surface encapsulation, in-situ production, coating, conjugation approaches, self-assembly, and producing core-shell NPs. The most applied materials for the functionalization of MeO NPs are synthetic polymers, silica, dendrimers, bio-polymers, and small molecules (Wang et al., 2023). As shown in Fig. 9(a and b), functionalization creates a buffer layer on the surface of the NPs, which improves the gap between the NPs, hence decreasing the intra-molecular forces (Van der Waals forces) and hindering aggregation. This process also creates a protective layer on the NPs surface and keeps the peripheral polarity of the additives unswerving over the complete surface (Wang et al., 2023; Borah et al., 2021).

4. Application of MeO

MeO NPs constitute a class of inert solids that have fascinated the interest of materials researchers and engineers. They are made technically valuable owing to their optical, electrical, magnetic, catalytic, and mechanical properties. These TMeO NPs are composed of O_2 compounds that are connected to the transition metals and applied for various electronic purposes owing to their superior semiconducting properties. They also demonstrate extraordinary physical characteristics among which spinal oxides (ferrites) display equivalent useful and fascinating electrical and magnetic properties. In current years, TMeO NPs have also emerged as prospective applicants for biomedical applications, photovoltaic, resistive switching, etc. (Patel and Munjal, 2021). NPs' electronic structures can show whether they are insulators, semiconductors, or metals. The extraordinary density and small-size of corners and edges on the surfaces of the MNPs' are responsible for their unusual chemical and physical features. Researchers from the fields of information technology, electronics, bio-medicine, optical, catalysis, environment, energy, and senses have expressed a great deal of interest in the potential technological usage of MeO NPs (Chavali and Nikolova, 2019).

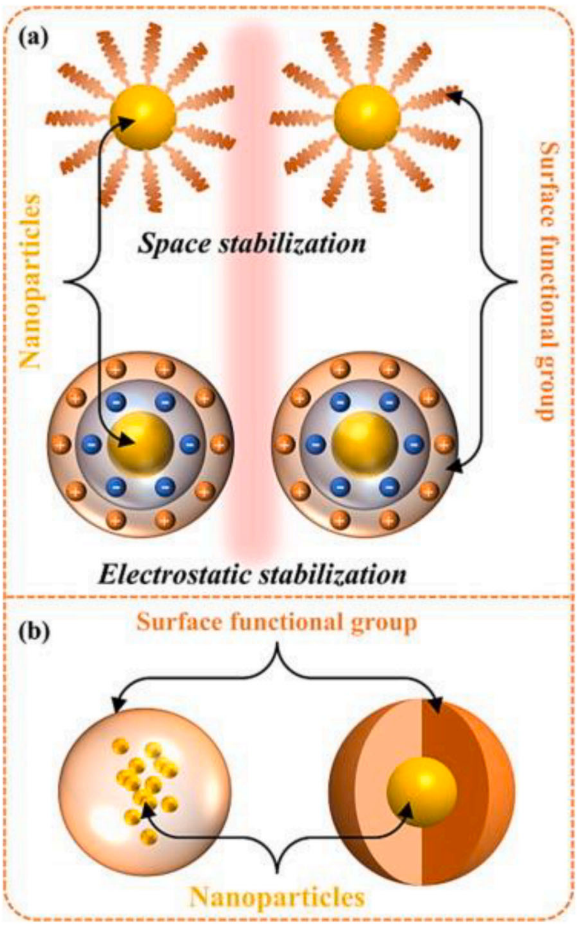

Fig. 9. (a) Schematics showing the distribution stabilization mechanism of functionalized NPs surfaces and (b) the influence of surface functionalization on NPs (Wang et al., 2023).

A growing number of surface and interface atoms produce strain or stress, as well as adjacent structural disturbances, as the size of the NPs decreases. The magnetic, conductive, chemical, and electrical characteristics of an NPs can change depending on its size. Because the properties of magnetic MeO NPs may be tailored based on their shape and size, they have attracted considerable interest. A particular size of the NPs material can affect the magnetic, electrical, and chemical properties of the particles (Chavali and Nikolova, 2019).

Most MeO NPs are used based on their surface features which will induce various structural assemblies. MeO NPs' atomic surface configurations are fundamentally transformed by the crystalline phases with the same shape and size. The lattice O_2 species and the surface vacancies may be instantaneously concerned in the sensing working and the reaction temperature may modify the crystalline structure (Gangwar et al., 2016). MeO NPs give superb optical features such as UV-absorption, photoluminescence, detailed coloring absorption in the dichroism, and visible-region (Chouke et al., 2022). MeO NPs have distinctive structures, extraordinary surface area, bio-compatibility, fascinating redox and catalytic features, and excellent mechanical stability. Owing to these attributes and distinctive plasmonic properties, MeO NPs have substantial attention, in bio-medical field applications such as bio-medical therapeutic, biosensing, implant devices, bio-imaging, neurochemical observation, and diagnostics (Annu and Ahmed, 2018). Other potential applications of MeO NPs owing to their high density of surface sites and nanostructures are microelectronics, energy, environmental decontaminations, gas sensing, ceramic fabrication, catalysis, storage devices, personal care products etc. (Laurent et al., 2018; Cañas-Carrell et al., 2014). A brief conversation on the various applications of MeO NPs is given in the subsections below.

4.1. *MeO NPs application in wastewater treatment*

The survival of species is dependent on the suitable consumption of vital elements of water (Aigbe and Osibote, 2020; Aigbe et al., 2018). An existing critical issue facing the world is water contamination, which has been amplified owing to rapid industrialization and the immense population increase. On a sizable scale, the demand for clean water for agricultural purposes has increased, with a high array of contaminants in industrial, domestic, and other forms of intake of fresh and clean water is about 70 %, 22 %, and 8 %, respectively. The key classes of contaminants are heavy metals (HMs) ions and dye molecules. In most affected regions of progressing nations, wastewater administration is generally non-present, hence imperative action is needed. Yet, existent effluent administration and technologies are increasing their capability to offer suitable clean water to meet human and other environmental requirements (Naseem and Durrani, 2021).

HMs and organic molecules are the most universal contaminants making their way into different water resources due to human caused events. Low concentration levels of these contaminants (ng/L-mg/L) are the principal cause of various tumours and skin and respiratory disorders. Fig. 10 shows the various sources of water resource contamination (Pratt, 2014; El-Nemr et al., 2022).

Contaminants move from one place to another and bio-accumulate into the food chain with many harmful effects on the environment and human physical condition. Natural contaminants are continually being consumed by humans, animals, and marine life and their existence in water supplies is a serious problem. Also, exposure to these contaminants raises the chance of general health problems (El Messaoudi et al., 2023). Water contamination harmfully impacts the environment, health, and socio-economic advancement. To curtail this challenge, advances in technology enable non-viable and commercial solutions. NT has also been shown to be one of the most superior and top approaches for the treatment of wastewater. NPs have high adsorption, reactivity,

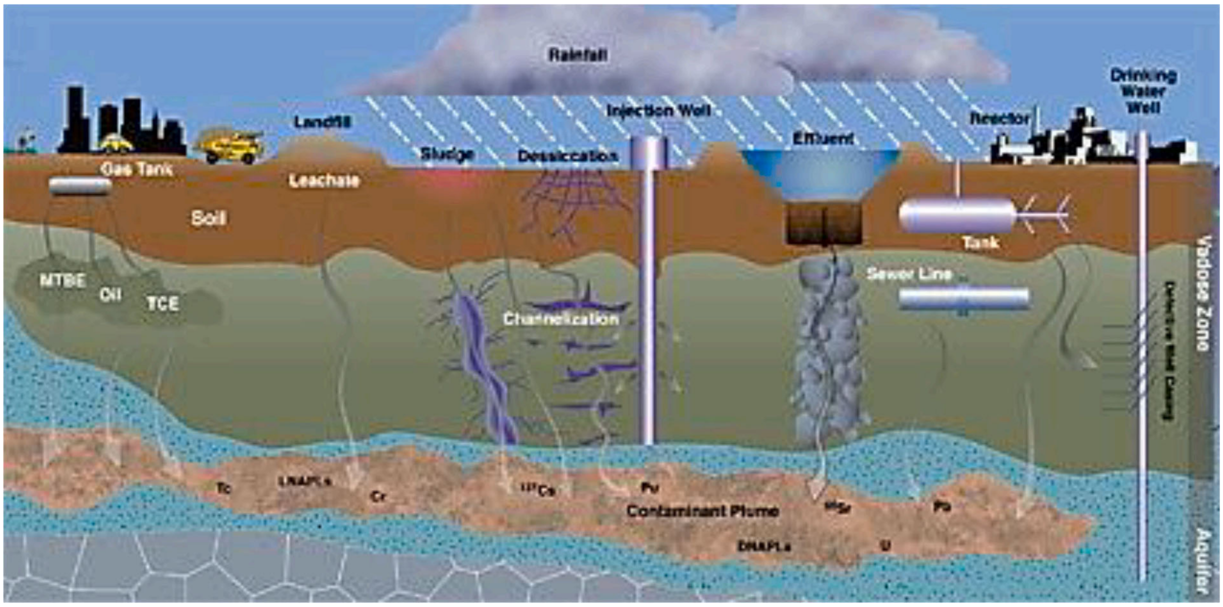

Fig. 10. Schematic of various sources of water contamination resulting from man-made activities (Pratt, 2014).

and interaction owing to their miniature size and extraordinary surface-atom proportion. NPs have an outstanding vantage in water treatment at great distances and in any site that has not been cleaned by traditional accessible approaches (Alhalili, 2023).

It is indisputable that the different NMs and their properties are useful in wastewater treatment. For the development of progressive water reserves and arrangements, existing developments and advances in NS and NT show prospects. The exceptionally useful, integrated, and multi-functional advancements accelerated by NT and NS are expected to offer superior rates of performance and realistic effluent treatment solutions compared to substantial setups. Hence, contaminant sequestration via naturally responsive and effective techniques is critical (Naseem and Durrani, 2021).

Various techniques are employed to treat wastewater. However, most of these procedures are not adequate for the sequestration of wastewater owing to the individual constraints of respective methods. The most employed method among these methods is the adsorption method, owing to the availability of various adsorbents, economical and easy execution, and utilized in both small and large operations. To tackle the shortcomings resulting from the use of other typical techniques, researchers are now engaging in the use of biological systems and thereby favoring the green approach (El Messaoudi et al., 2023). Green fabricated NPs have been shown to have considerable importance in the decontamination of HMs and dyes from the ecosystem (Vijayaram et al., 2023). This is an affordable approach for creating nano-structured materials with various morphologies, topologies, and particle size distribution (El Messaoudi et al., 2023). It is significant to note that the operation cost, initial concentration of contaminants, impact on the ecosystem, value of pH, added chemicals removal effectiveness, and financial feasibility all play a key part in assessing the ideal technique for contaminant confiscation (Onyancha et al., 2022).

4.1.1. Photocatalytic application of wastewater treatment using MeO NPs

Another interesting approach that has been employed currently by researchers in the treatment of organic contaminants in wastewater is the advanced oxidation process (AOP). These technologies are exceptionally effective methods for several types of wastewater treatment (Pattnaik et al., 2023). This approach is an alternative to conventional methods like adsorption and coagulation owing to the mineralizing of organic contaminants by this process. Hence, a promising AOP is photocatalysis, which is a non-selectivity green technique for the degradation of unsafe and noxious contaminants swiftly from wastewater employing semiconductor MeO as photocatalyst materials. Hence, the catalyst initiates and improves the chemical reaction rate, without the material being unchanged at the halt of the reaction (Geldasa et al., 2023).

AOP depend on OH^- radicals production, which presents a remarkable electrochemical oxidant power and oxidizing potential. For wastewater degradation, the most established AOPs exploited are ozonation, Fenton and photo-Fenton reactions, photocatalytic oxidation, and electrochemical oxidation. Photocatalysis mechanisms result in a cycle of oxidative and reductive reactions on the surface of the photocatalyst. The lower and upper vacant energy bands are distinguished by the semiconductor E_g. Photocatalysis can be either heterogeneous or homogeneous. The homogeneous photo-reaction procedure enables the breakdown of contaminants in saline conditions. While in heterogeneous photocatalysis, photoreactions happen in the existence of the catalysis. The catalytic variants phase is distinct from the reactant, hence it is significant for the treatment of wastewater (Pattnaik et al., 2023).

The photocatalytic contaminants degradation approach involves light sorption (sorbing and converting light into energy) and the redox reaction (simultaneous oxidation and reaction reduction). Contaminants are catalyzed by MeO NPs in direct and indirect processes. The steps involved in direct contaminant degradation are the photoexcitation of electrons from the materials using light from the occupied valence band (VB) of the MeO to the vacant conduction band (CB). The energy of the sorbed photon should be equal to or greater than the catalyst E_g. A hole is left behind in the VB and an electron in the CB as a result of the excitation as shown by Eq. (1).

$$\text{MeO} + hv\ (UV) \rightarrow MeO(e^-(CB)) + h^+\ (VB) \tag{1}$$

The interaction of water molecules with the holes in the VB leads to the creation of OH^- radicals. The generated OH^- acts as a powerful oxidizing agent, which oxidizes organic contaminants sorbed on the catalyst surface (Eq. (2)).

$$H_2O\ (ads) + h^+(VB) \rightarrow OH^-(ads) + H^+(ads) \tag{2}$$

The photogenerated electrons in the CB of the catalyst are taken up by the O_2 molecules, thereby creating a superoxide radical anion as well as terminating electron-hole recombination. Hydroperoxy radicals are formed by the protonated superoxide ion. H_2O_2 are created from the hydroperoxy radicals, which separate to create reactive OH^{-}radicals (Eqs. (3) and (6).

$$O_2 + e^{-}(\mathrm{CB}) \rightarrow O_2^{-}\ (ads) \tag{3}$$

$$O_2^{-}(\mathrm{ads}) + H^{+} \rightleftarrows HOO\ (ads) \tag{4}$$

$$2HOO\ (ads) \rightarrow H_2O_2(ads) + O_2 \tag{5}$$

$$H_2O_2(ads) \rightarrow 2OH\ (ads) \tag{6}$$

OH^{-}radicals created react with the contaminants and separate them into non-hazardous products (Eq. (7)).

$$Contaminant + OH \rightarrow CO_2 + H_2O \tag{7}$$

The entire photocatalytic reaction is denoted by Eqs. (8) and (9).

$$Contaminant + H^{+}(VB) \rightarrow Oxidation\ products \tag{8}$$

$$Contaminant + e^{-} \rightarrow Reduction\ products \tag{9}$$

The indirect degradation of various contaminants involves the excitation of ions or molecules of contaminants into a triplet-excited state (contaminant*) in the light region (400 nm $\leq \lambda \leq$ 800 nm). Hence, the excited contaminants ions or molecules are transformed into a semi-oxidized radial cation with the admission of electrons into the CB of MeO NPs. Superoxide radical anions are created due to the interaction between stuck electrons and the dissolved O_2 in the system, creating OH^{-} radicals (Eqs. (10) and (11).

$$Contaminant + hv \rightarrow Contaminant* \tag{10}$$

$$Contaminant * + MeO \rightarrow Contaminant^{+} + MeO^{-} \tag{11}$$

(Krishnan et al., 2023).

For a catalyst to be photoactive these important requirements must be met, which are high surface area (higher active sites), lower E_g and stability to photo-corrosion. Photocatalyst reaction rates are not projected precisely in relationship to the surface area, the number of active sites of the catalyst and weight. The rate of photocatalysis is expressed in terms of the selected contaminant and the catalyst. The photocatalyst's performance is expressed in terms of the quantum yield (ϕ)- a mathematical assessment of the effectiveness of a photocatalyst for contaminant degradation after sorbing radiation of a certain frequency (Eq. (12))

$$\phi = \frac{Number\ of\ molecules\ that\ undergoes\ degradation}{Number\ of\ photons\ sorbed} \tag{12}$$

The equation holds for homogeneous catalysis but for heterogeneous catalysis, it is difficult to assess the number of photons sorbed owing to the scattering and reflection of incident photons. However, the number of incident photons is considered for this case. The efficacy thus evaluated is not the actual quantum yield, which is less than the assessed value and is known as the apparent quantum yield (AQY) (Eq. (13))

$$\mathrm{AQY} = \frac{Number\ of\ molecules\ that\ undergoes\ degradation}{Number\ of\ incident\ photons} \tag{13}$$

The number of incident photons is determined by employing a photodiode or actinometer. In the figure of merit (FOM), factors such as catalysis mass, light source, energy consumed, pollutant concentration, final products and other factors that impact the efficiency of the catalysis are considered (Eq. (14)). The maximum value of FOM is set at 100 and the specific system is assessed proportionally.

$$FOM = \frac{Product\ obtained\ (L)}{Catalyst\ dosage\ \left(\frac{g}{L}\right) \times Time\ (hr) \times Energy\ consumption\left(\frac{Wh}{mol}\right)} \tag{14}$$

The industrial appropriateness of the catalytic system should be at least five reusable cycles (Krishnan et al., 2023; Bathla et al., 2022). The frequently used MeO semiconductors for photocatalysts are ZnO, TiO_2, SiO_2, and CeO_2 NPs (Pattnaik et al., 2023; Danish et al., 2021). Factors that influence the photocatalytic degradation process are the quantity of catalyst (increased catalyst dosage leads to an increased quantity of photo-mineralization of water contaminants due to the increased OH^{-} radicals and +ve holes generated when the active sites of the photocatalyst are exposed to light), the quantity of contaminant, pH effect (impacts surface charge, aggregation, ionization, photocatalyst valence band potential and the sorption of contaminants) and temperature (Ashour et al., 2023).

4.2. MeO NPs application in medical science and cancer treatment

Cancer is utilized to define malignant cells in which irregular cells develop uncontrollably and can overrun the adjoining healthy tissues. These irregular cells come from any tissue in the human body and can take place wherever in the body. Bio-NPs act as chemo-therapeutic agents in handling tumour cells and show a collaborative impact with drug chemo-treatment (Berta et al., 2021).

Cancer causes early death in almost all territories of the world and holds its leading spot even though it is occasionally superseded by cardiac disorders. Owing to the statistical influences and cancer incidence impacts trends in various places, it is anticipated that the occurrences of cancer will almost double in the next 50 years worldwide. Nevertheless, the rate of the population of all nations being affected by cancer is not similar and it is projected that there will be a higher increase in developing nations (low-middle income nations) (Sanko and Kuralay, 2023; Aigbe et al., 2023).

According to the "Global Cancer Statistics" report in 2020, it was reported that prostate cancer is the recorded widespread cancer in men followed by lung, colorectal, and liver cancers. In women, breast and cervical cancers were the most prevalent. Furthermore, according to the same report in 2020, a predictable 19.3 million new cases of cancer were discovered globally and about 10.0 million deaths were considered owing to cancer, which was outstanding. Regardless of the cancer type, cancer identification and therapy at the early point is very critical to decrease the occurrence of cancer and the death rate due to cancer. One of the main issues restricting the beforehand identification of cancer is the non-presence of recognizable indicators in the early stages of cancer and the non-detection of appropriate biomarkers. Hence, there is a critical requirement to create sensitive, non-invasive (bio)sensors for the detection of cancer at the early stages (Sanko and Kuralay, 2023).

In most developing nations, cancer is a known cause of human death owing to the ineffectiveness of traditional chemo-treatment. The inefficiency of this traditional chemo-treatment is because of the non-specific distribution of the drug, the resistance of the drug at the tumour spot, swift anticancer agent clearance, and the minimal effectiveness of existing anticancer agents. Hence, to offset such issues like side impacts and to consider the influenced benefit of drug targeting, the delivery of drugs plays a very intriguing part in bio-medical disciplines (Annu and Ahmed, 2018).

NT has pinched fantastic attention in the medical field. Specifically, MeO NPs play a critical responsibility in cancer detection and the delivery of drugs in specific areas of the human body. To decrease the sum of drug applications in the body and their bordering effect, drugs must be absorbed in ideal doses in the affected area. This approach reduces the price and causes side impacts. NT also assists in repairing and restoring injured tissue in certain areas (Chouke et al., 2022). NPs synthesis via the green approach is considered an excellent alternative to overcome cytotoxicity and genotoxicity challenges (Khan et al., 2022).

MeO NPs have shown potential in various biomedical uses from targeted drug delivery to magnetic hyperthermia uses. For such uses, NPs must be biocompatible as well as water dispersibility for primary biomedical uses such as magnetic hyperthermia applications. By the careful decrease of the NPs sizes, they can be converted into superparamagnetic NPs and explored in magnetic hyperthermia (Patel and Munjal, 2021). The miniaturized delivery systems of NP-based drug delivery systems and vaccines were introduced by researchers during the later years of the 1960s. There has been great advancement in the diagnosis and treatment of various diseases using NMs (Nyoka et al., 2020).

Owing to the antitumour properties of MeO NPs, the mechanisms of action involved in cancer treatment include active or passive targeting of tumours, tumour targeting through gene silencing, drug delivery through NPs, NPs-based hyperthermia, and radiotherapy treatment through NPs (Xu et al., 2022). For the treatment of cancer, abnormal branching and leaky sites with pore sizes extending from 100 nm to respective hundred nm are mostly found in tumour vasculatures. Due to this reason, there is swift development of endothelial cells, which decreases the amount of pericytes. Medicinal agent collection can be improved by MeO NPs treatment via passive and active targeting of tumours. Under the passive targeting mechanism, MeO NPs are concentrated in the tumour by the body (increase permeability and retention effect (EPR)). In active targeting, the medicinal delivery system is enhanced by functionally altering the MeO NPs surface using tumour-targeting ligands like antibodies, folic acids and peptides, resulting in selective tissue targeting (Xu et al., 2022).

Gene silencing involves the control of gene expression in a cell to exclude the specific gene expression. This is achieved generally via the use of antisense DNA and short-intrusive Ribonucleic acid (RNA). In clinical practice, drugs for cancer are low molecular weight chemicals that can disperse directly into healthy tissues and tumour tissues. This results in an equal supply to the body, a brief half-life and a swift clearance percentage. MeO NPs can act as vectors for the targeted delivery of drugs and the amount of medicine that reaches the target sites is extremely small, with lower treatment effectiveness and the enhanced threat of side effects as well as the likelihood of drug resistance. In radiation treatment (RT), elevated energy radiations are utilized to slow the multiplication of cancerous cells. These are electromagnetic radiations with ample energy to ionize electrons from molecules or atoms, thereby resulting in the realization of ions. A sizable amount of energy is deposited in the cells as ions with elevated kinetic energy collide numerous times and travel through the cells. The transferred energy is sufficient to halt tumour cells from replicating DNA or transcribing RNA resulting in the death of cells. MeO NPs are generally used in radiotherapy to enhance the unique radiations to the target spot, decreasing radiation dose and preventing noxiousness and harm to normal tissues. The radiolysis of water molecules is caused by ionization radiations, resulting in ROS production (Xu et al., 2022).

Tumour cells can be directly destroyed by non-noxious wavelength radiation like near-infrared (NIR) or oscillating magnetic fields that can sorb and transform into noxious stimuli of reactive oxygen species (ROS) manufactured or hyperthermic by NPs of MeO. The plus of this method originates from the fact that NPs owing to their particulate nature can be straightforwardly targeted at the tumour site by covalently connecting tissue explicit molecular determinants or, with the assistance of a peripheral applied local magnetic field in the case of magnetic NPs. Hence, they can be utilized to selectively destroy cancer cells, and convert radiant energy into heat or ROS. This assists in decreasing healthy tissue damage, which is the highest-threatening side of cancer treatment. Anticancer hyperthermia treatment comprises of the application of heat at a temperature above 40 °C aim of destroying tumour cells. To prevent magnetisation-NP-induced aggregation during hyperthermia treatment of tumours (a phenomenon that is appropriate during treatment), and which is very unsafe to the patient after treatment. Hence, *in vivo* hyperthermia treatments are utilized and this involves the use of MeO NPs of sizes below 30–40 nm (Vinardell and Mitjans, 2015).

Fluid metal NPs heat efficiency is calculated by the specific sorption rate (SAR) or specific loss power (SLP). SAR is outlined by the heat amount released by a specific amount of active materials per unit time during exposure to an AC magnetic, which is described by the frequency and field strength (Eq. (15)).

$$SAR = C(\Delta t/\Delta t)_{t\to 0} \tag{15}$$

C is the specific heat capacity assessed as a mass of magnetic carriers per equivalent of medium and it defines the rate of temperature increase, expressed as an average sorbed power per mass unit (W/g). $\Delta t/\Delta t$ is the increased temperature per unit time. The SAR or SLP of a sample can be assessed experimentally by the calorimeter techniques. SLP is described as electromagnetic power lost per magnetic material mass unit (watt/kilogram (W/kg)). In hyperthermia applications, SLP or SAR should be as large as possible and can be stated to be proportional to the rate of increased temperature. For *in-vivo* experiments, it is obligatory to study the biologic limits (Atkinson's principles) like the main probable SLP within the biologic limit (Brezovich criterion-product of field amplitude (H) and frequency (f) of maximum heat dose $< 4.85 \times 10^8$ 1 /Ams) and the improvisation of nano-objects in terms of the heating efficiency is given by Eq. (16).

$$SLP = \frac{C}{m}\left(\frac{dT}{dt}\right)_{t\to 0} \tag{16}$$

m, C and dT/dt is the mass of heat-generating material, the sample as a whole thermal capacity and the rate of temperature increased as a function of time. The dosage utilized for a tumour to accomplish a dependable deactivation of target cells can be assessed using SAR. The dose used for a patient can be possibly decreased for materials with elevated SAR to the lowest level. For metal NPs, shape, size and microstructure can impact SAR values and NPs with elevated surface anisotropy can create superior SAR values than in their bulk form. For a direct comparison of the superparamagnetic NPs heating effectiveness, the intrinsic loss power (ILP) is used. The ILP is not completely fundamental and the following assumptions must be followed by the system, crystallite size should have a polydispersity index > 0.1, frequency utilized in the experiment should be of several MHz, the value of sample H should be > the saturation of the NPs and the system thermal losses should be reproducible, The ILP is defined by Eq. (17) (Sharma et al., 2019).

$$ILP = \frac{SAR}{H^2 f} \tag{17}$$

Another area of biomedicine that the application of magnetic MeO NPs has benefited from is magnetic resonance imaging (MRI). It is a powerful non-invasive instrument employed in medicine but experiences low signal sensitivity. Contrast agents assist with this problem, and the most common contrast agents employed are paramagnetic materials that use spin-lattice relaxation time ((T_1)-the mechanism by which the constituent of the magnetization vector along the static magnetic field direction reaches thermodynamic equilibrium with its surroundings). Superparamagnetic MeO like Fe_3O_4 influences the spin-spin (T_2) relaxation time (associated with the time of relaxation of protons interfering with each other) by changing the confined magnetic field surrounding the protons. The effectiveness of an MRI contrast agent is defined by the longitudinal (r_1) and the transversal (r_2) relaxivities. These proton relaxivities give the efficiency of magnetic NPs to enhance the longitudinal (R_1) or transversal (R_2) relaxation rate of water protons induced by one millimolar of Fe (Eq. (18)).

$$R_i^{obs} = \frac{1}{T_i^{obs}} = \frac{1}{T_i^{dia}} + r_i C \ (i = 1 \ or \ 2) \tag{18}$$

R_i^{obs}, T_i^{obs}, T_i^{dia}, C and r_i represent the global system relaxation rate (s^{-1}), the global system relaxation time and the system relaxation time before the addition of the contrast agent (s), Fe concentration of the superparamagnetic compound (mmol/L) and the relaxivity (Laurent et al., 2018; Abdal Dayem et al., 2017). MeO NPs have an enormous surface area, which supports the integration of elevated drug doses. However, in most situations, the functionalization of the surface would be needed to fix, control, and target the release of the drug. Superparamagnetic FeO NPs are one of the most generally employed NPs in drug target delivery owing to their magnetic behavior (Annu and Ahmed, 2018).

4.3. Antimicrobial and antibacterial application of MeO NPs

Among the bio-medical applications, the antimicrobial ability of NPs is believed to be the most used (Nadeem et al., 2020). NPs can be considered as potential antimicrobial agents owing to their outstanding action against surface pollution, adhesion and colonization which are detrimental to the health of humans. MeO NPs CuO, FeO, TiO_2, ZnO etc. have demonstrated antimicrobial properties at extremely subtle concentrations owing to their distinctive physicochemical properties. These metal-based NPs have also demonstrated a biocompatible nature against human cells as well as acting as key micronutrients for vital performance of the human body (Gharpure et al., 2022).

Phytochemicals, specifically polyphenols (flavonoids and phenolic acids) exist in plants. Flavonoids for instance shield the body from free radicals, assist in strengthening the immune system, and decrease inflammation. These green compounds are comprised of one or more OH^- groups associated with carbon molecules of the aromatic ring. These phytochemicals together with NPs decrease the risk of breast or colon cancer, and lung cancer. This is owing to the antioxidants that combat the destructive impacts that free radicals exhibit. The two processes involved in the antioxidant activity are grouped as the hydrogen atom transfer (HAT) technique that contributes hydrogen ions from stable molecules, hence permitting the elimination of ROS by the antioxidant and individual electron transfer (SET) which changes with the potential of the antioxidant to decrease certain molecules and compounds by transferring an electron (Berta et al., 2021). Polyphenolic compounds present an aromatic ring attached to OH^- groups and carbon atoms. Remarkably, the antioxidant activity tends to improve with a superior count of OH^- groups (Abuzeid et al., 2023).

Efficient inhibition against a large array of bacteria is greatly acknowledged for various nanosystems such as Fe_3O_4, TiO_2, CuO, and ZnO. These oxides possess greater durability, lower noxiousness and superior stability and selectivity in comparison with conventional organic antibacterial agents. NPs with dimensions < 20 nm are mostly more effective. They can infiltrate into bacterial cells and may release noxious MIs upon dissolution. MeO NPs with modifying physicochemical features can show various antibacterial mechanisms and consequences. Oxide NPs with a blend of two or three metals can be created for the effective removal of different bacterial strains (Sharma et al., 2019). Most MeO NPs (oxides of Al, Cu, Mg, and Fe) are also utilized in dermatological therapy as well as in promoting the healing of wounds. The applicability of these MeO NPs has boosted the innovative wound bandage, synthesis of bi-metal core-shell nanocomposites (NCs), prompting breaks in bacterial cellular membranes, hydrogen peroxide production, the high sorbing capacity of wound transudes, encouraging blood clots, etc. (Pan et al., 2021).

4.4. Gas sensing application of MeO NPs

Sensors as a technology have advanced and there is a greater need for precise data in many areas. They have become increasingly important in an array of industries, including aerospace, industrial engineering, environmental safety, ocean exploration, bio-engineering, and medical diagnosis (Annu and Ahmed, 2018). Gas sensors have gained a huge reputation for industrial and environmental atmosphere observation. These approaches are built on resistance measurement, liquid and gas chromatography, optical and electrochemical techniques and acoustic waves (Chavali and Nikolova, 2019). Based on MeO NPs, chemo-resistive sensors are the most extensively used gas sensors. These materials are semiconductors, and their non-stoichiometry defines their main charge carrier, as absolutely stoichiometric compounds, they are too resistant (Laurent et al., 2018).

The creation of anion (O_2) vacancies or the exchange with distinguished valence cations which enhances the number of free electrons defines the n-type semiconductor. While p-type semiconductor is ascribed to the generated holes either by interstitial anions addition or with lower valence cations substation. Based on the electronic structure, MeO semiconductors are grouped into transition MeO (hematite (Fe_2O_3), and TiO_2) and non-transition MeO which include pre-transition MeO like alumina, MgO, and post-transition MeO (Dadkhah and Tulliani, 2022).

The MeO gas sensitivity is controlled by the electronic structure and the pre-transition MeO are generally employed for gas sensors owing to their large E_g and incapacity of both electron and hole formation. The electronic configuration also guarantees transition MeO and post-transition MeO used in gas sensing. Based on MeO semiconductors, the operating principle of gas sensors on the adsorption of gas molecules on the surface of the sensing material (Dadkhah and Tulliani, 2022). With the exposing of the sensor to air at 100–500 °C, O_2 molecules are sorbed to the material surface. The O_2 chemisorption from the gas stage produces extrinsic surface acceptor states (O^-, O_2^- and O^{2-}), restraining the electrons in the conduction band from the region near the semiconductor surface. The O_2 species on the MeO surface can be physiochemically sorbed as a result of temperature. Below 150 °C, the dominant form is molecules and O_2^- are physically sorbed (Eq. (19)). While above this temperature, the ionic species that prevail are O^-, and O^{2-} (Eqs. (20) and (21)) at temperatures below 250 °C and above 450 °C. Owing to the sorbed O_2 molecules from the air (under normal room temperature), a resistive electron depletion layer (EDL) is created on the sensing material surface (Fig. 11a). The sorption of O_2 anions results in the creation of a hole accumulation layer (HAL) at the exterior surface (Fig. 11b) (Dadkhah and Tulliani, 2022).

$$O_{2(ads)} + e^- \rightarrow O^-_{2(ads)} \tag{19}$$

$$O^-_{2(ads)} + e^- \rightarrow 2O^- \tag{20}$$

$$O^-_{2(ads)} + e^- \rightarrow O^{2-}_{ads} \tag{21}$$

In n-type MeO semiconductors, the exterior resistive shell is accountable for the sensor resistance when the sensor is visible to air. But with samples exposed to a reducing gas (Fig. 12), the gas and ionic O_2 species reaction will lead to the acquired electrons emitted to the conduction band, leading to the reduction of the material resistance. With the introduction of oxidizing gas, there will be further oxidation of

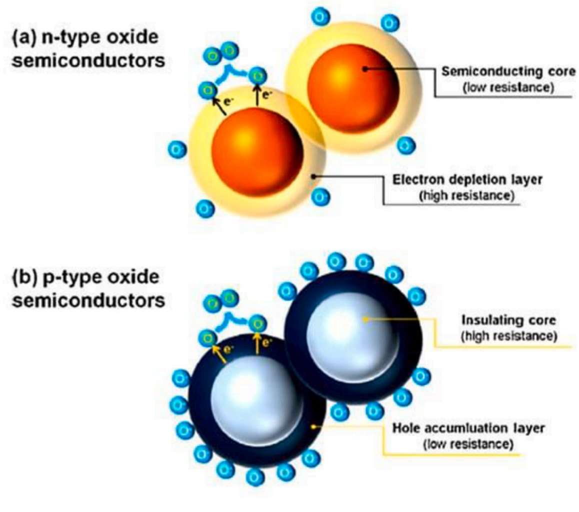

Fig. 11. The electronic core-shell structure of (a) n-type and (b) p-type MeO semiconductors (Dadkhah and Tulliani, 2022).

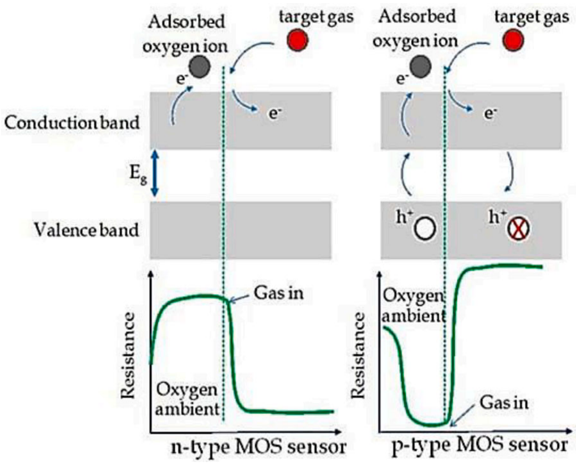

Fig. 12. A graphic representation for the alteration of sensor resistance when displayed to the reducing gas in the cases of n-form and p-form of MeO semiconductor sensors (Dadkhah and Tulliani, 2022).

the material and there will be an increase in the EDL and the material resistance. When the size of the grain of the sensing material is less than twice the Debye length (DL), the EDL will extend to the entire material and hence an electrical difference will be extreme (Eq. (22)) (Dadkhah and Tulliani, 2022).

$$DL = \sqrt{\frac{\varepsilon k_B T}{q^2 N_D}} \tag{22}$$

ε, kB, T, q, and ND represent the dielectric constant, Boltzmann's constant, the absolute temperature in Kelvin, the elementary charge, and the net density of dopants (either donors or acceptors) (Dadkhah and Tulliani, 2022).

For sensing materials, MeO NPs like CuO, copper (I) oxide (Cu_2O), ZnO, Fe_3O_4, nickel oxide (NiO), indium oxide (In_2O_3) and tungsten oxide (WO_3) are encouraging applicants that establish greater sensitivity, swifty response/recovery time, exceptional replicability and stability and cost-effectiveness with modest synthesis procedures in the detection of volatile organic compounds (VOC) gases and environmentally hazardous gases such as NO_2, NO, N_2O, H_2S, CO, NH_3, CH_4, SO_2, and CO_2. Established MeO-based sensors are mostly produced on rigid substrates owing to their extraordinary production temperature, which enhances energy consumption and production cost and forces restrictions in growing uses (Yoon et al., 2021; Chavali and Nikolova, 2019).

4.5. Bio-Imaging application of MeO NPs

Biosensors represent a critical component in environmental progress, energy-effective systems, chemical and agricultural industries, and medical care. The requirement for employing nonstop on-the-spot observation with adaptable and dependable features has suggested biosensors as an effective device for swift measurement and analysis. A particular case is exemplified by MeO materials, which have a great potential to become extremely reasonable materials in the biosensors market based on their structural resourcefulness, chemical stability, physicochemical interface features, and their capability to combine with composite structures (Şerban and Enesca, 2020). Advancements in luminous NPs with multi-functional properties like optical and magnetic variations are in great demand and they are employed to imagine complex cellular structures (organs and tissues), tumours, and receptors. Bio-fabricated NPs are required for bio-sensor use owing to their physiological competence, optical characteristics, and biocompatibility. Naturally, bio-sensors have receptor parts that act on particular analytes, which are generally of biologic sources such as viral DNA or bacteria, protein from antibodies or antigens, glucose molecules, or contaminants. Transduction (signal captured) is also enhanced with NPs, revealing extraordinary magnetic, optical, and electrochemical signals. Also, the bio-sensor sensitivity and lower detection time are improved with the effective immobilization of bio-receptor units on particles with ZnO and TiO_2 NPs (Jeevanandam et al., 2022).

4.6. MeO NPs application in defence

MeO NPs can be hypothetically utilized in the defence sector to safeguard high-value defence information. This is demonstrated by the MeO luminescent ink, which can be effortlessly utilized in a reasonable way on various surfaces and has been applied generally as safety inks to print security bars and codes for application in the defence sector. Furthermore, MeO NPs have been applied in other sectors to include smart coating, complex computing power for code-breaking and encoding, sensors to find life, safety and emergency signs, nanosensors in lightweight military outfits, dark setting image displays, as luminescent pigments employed as luminous paintings in watches and other devices dials (Gangwar et al., 2016; Sharon, 2019).

4.7. Optical application of MeO NPs

Light is an energy type that requires other energy forms supplied to create and harvest it. In luminescence, a selected energy resource stimulates electrons within a material from a lesser energy ground state to an advanced energy excited state and with a subsequent release of electrons to a lower energy state through the release of energy in light form. MeO NPs in optical use are incomparable and are recognized in different sectors. Among the different sectors, photoluminescence (PL) originates from photo-excitation (photon excitation) luminescence, which is generally acknowledged for insulators and semiconductor defects analysis. With the absorption or emission of photons by the defect, an optical alteration takes place. The observable emission is linked to revealing the associated emissions such as the O_2 vacancies and metal interstitials (Gangwar et al., 2016; Ma et al., 2020).

PL is employed as a non-critical, extremely sensitive, and direct optical device employed to research lattice defects, surface O_2 vacancies, self-trapped and localized excitons, and electronic energy band structure evaluation in MeO NPs. A critical parameter is the temperature, which is a carrier dynamic. Mostly, at ambient temperature, the MeO probability to show luminescence varies on the fundamental band structure and other peripheral/core factors (Gangwar et al., 2016).

Since crystalline defects are very effective trapping centers and are overshadowed by the minimal energy stages, which appear in the low-temperature PL spectrum, carriers are stuck at the surface or crystal defects at low temperatures. PL spectra gradually enhance with shrinking temperature owing to the declining non-radiative re-combination. MeO NPs properties are associated with the luminescence spectra and related decay times of luminescence. Material luminescence decay time is a fundamental parameter for determining its working and swift optical sensor uses. MeO NPs-based optical displays/sensors/switches need decay time to be in milli-seconds to pico-seconds limit and are generally employed in optoelectronics switching, bioimaging tools, and LED uses. MgO nanoflakes/fibers and Al_2O_3 NPs and nanowires show a swift decay time of luminescence of to a lesser extent than 10 ns, suggesting their use in white light production, solid state lighting uses, optical sensors, and different optoelectronic apparatus (Gangwar et al., 2016).

MeO semiconducting resources can sorb solar energy and use it for the movement of electrons from the valence band to the conduction band. This movement produces an electron-hole pair in the semiconductor materials. The occurrence is utilized to create the electric energy from the solar energy (Patel and Munjal, 2021; Calnan, 2014). MeO semiconductors have been utilized in photovoltaic technologies and their outstanding resourcefulness properties and the practicality to be produced by green, low-priced, and simply scalable production techniques confers a unique place in next-generation PV(s) (NGPVs). Their spectacular capability to sustain or enhance device properties, still as a non-crystalline (amorphous) material permits their use in flexible and semi-transparent PV systems and printed electronics. Improved lifetime stability to the up-to-the-minute PVs like organic (OPV) and halide perovskite solar cells (PSCs), which is an important phase towards NGPVs commercialization and industrialization has been provided by basic (doped and undoped) semiconductor oxides (Gershon, 2011).

In their complicated form, semiconductor oxides can also give magnetism, ferroelectricity, or pyroelectricity properties that cooperatively can produce unique and innovative features with most conventional materials. Transition MeO are a fascinating set of semiconducting materials, that have outstanding charge transport properties and can be regulated in different ways via dopant introduction, for the creation of nanostructures or surface modification. Due to their optical and electronic properties possessed by transition MeO, they play various parts within crossbreed carbon-based/inert PV devices (Gershon, 2011; Thu et al., 2018).

In organic-based PVs, MeO plays several different roles which include active materials (accountable for the sorption of light and photogeneration of charge carriers), transparent electrodes (owing to the relatively low conductivities of organic semiconductors, photogenerated charge carriers can only diffuse various hundred nanometers (nm) before they recombine, hence, transparent electrode are required, which will collect charges over the entire device area while permitting incident light to reach the active layer. Wide E_g transition MeO are suitable materials for this application owing to their excellent optical properties and their capability to tune their electrical features via doping), charge-blocking layers (charges injected at the electrodes recombine with photo-generated charges, hence decreasing the performance of the device, to decrease the leakage current, MeO is inserted as a blocking layer on any side of the active layer. Due to the energy level positioning difference, the transference of the hole is favored by one layer and the other layer favors electron transport), optical spacer (guarantees that the wavelength of light most effectively sorbed by the polymer have their maximum intensities in the active layer), intermediate coatings in tandem cells (to achieve this in an organic-based device, an intermediate layer is presented to protect the bottom cell from dissolving upon the successive cell deposition, ohmic contact between various cells and permits for the undesirable electrons from one layer and undesirable hole from another to re-combine) and stability enhancer (in light and O_2 presence, semiconducting polymers are unstable and to improve the organic layer stability, O_2 deficient oxides like TiOx ($x \approx 1.34$) are used) (Gershon, 2011; Thu et al., 2018; Calnan, 2014).

To curtail power loss processes in PV cells (Fig. 13), the first vital condition for high power conversion efficiency (HPCE) is that the photo-active (absorber) layer should have a reduced E_g of around 1 and 2 eV, to sorb photons with a large range of energies in the solar irradiance with elevated intensity range. The second vital condition is that there should be several potential incident photons entering the photo-active layer of the device to switch into charge carriers (Calnan, 2014).

4.7.1. *Applications of PV thermal systems (PVTs) of MeO NPs*

Solar energy is utilized to create thermal energy via solar thermal collectors (SC) and create electrical energy via PV collectors. Presently, it is a general procedure to set it up with two split solar collectors (one for the solar thermal collectors and the other for the photovoltaic components). It is an excellent concept to utilize solar energy for creating electrical energy and heating applications to meet the demand for both thermal and electrical energy requirements. When the SC and PV are combined, the total energy utilization efficacy is enhanced for combined solar collectors (Jia et al., 2019).

While the solar technology industry has seen a rise in throughput in recent times, the efficacy of viable PV materials remains a primary constraint. To tackle this constraint, novel PV materials and hybrid systems like concentrating PVTs are being created to enhance the efficacy of solar energy (Tunkara et al., 2019). Integration of the PV and SC components makes a PVT hybrid system and heat and electricity are created from this combined system. Electricity is created from the PV modules and concurrently, the sorbed thermal energy is transferred away by the working fluid. As a result, the PV effectiveness is enhanced. Solar energy can be utilized for the control of building temperature,

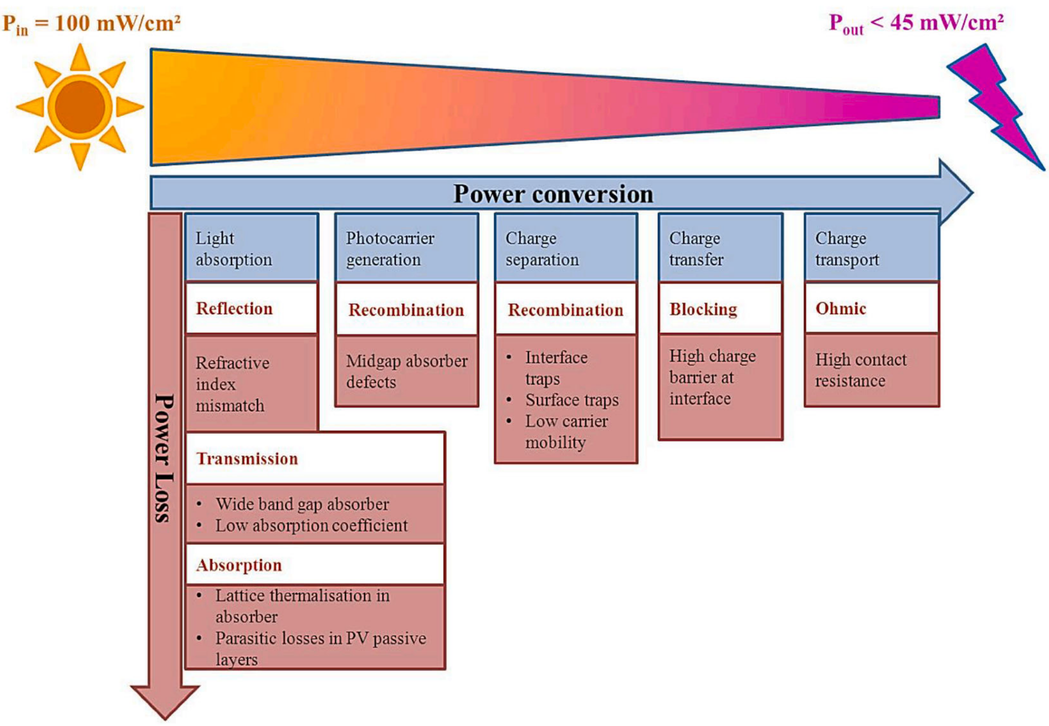

Fig. 13. Schematics of the power conversion and power loss processes in a PV cell (Calnan, 2014).

generation of heat for industries, refrigeration of food, water heating, irrigation systems, generation of power and other different processes. PVTs can be assessed from the thermodynamics and marketing viewpoints (Jia et al., 2019; Ramos et al., 2019). An increase in the cell temperature leads to reduced PV panel efficacy, to avoid the loss of efficacy, fluid is flowed via the collector to remove heat from the PV module (Noxpanco et al., 2020).

In energy storage technologies, MeOs are generally utilized because they are normally able to create charge carriers when energy is applied. PVTs technologies are primarily grouped into collector type, coolant type and material type (Ahmed et al., 2021). PVTs are grouped according to the medium for heat extraction, solar input, configuration etc. Water, air, air-water and nanofluid are the heat extraction medium (Mostakim and Hasanuzzaman, 2022).

PV cells are categorized based on the technology generation as first generation (crystalline silicon), second generation (thin films-amorphous silicon cells, Cadmium Telluride cells (CdTe), Copper Indium Gallium Selenide cells (CIGS) and Gallium Arsenide cells (GaAs)) and third generation cells (multi-junction such as GaAs multi-junction), the sensitized dye cells, organic (use organic materials, such as polymers) and inorganic (use inorganic substances) cells. Thermal SCs are grouped into concentrator collectors and flat collectors according to the presence or lack of solar radiation concentration devices. PVT collectors are grouped according to the working fluid utilized and the presence or lack of reflectors for the solar radiation concentration. Hence, these collectors are partitioned into liquid PVT collectors, air PVT collectors and PVT concentrators (Ramos et al., 2019). In recent years, a handful of researchers have tried to enhance the PVTs' performance by employing MeO-based nanofluids (NFs- Al_2O_3, TiO_2, SiO_2, Fe_3O_4, CuO, ZnO, and MgO-based NF) as coolants or optical filters or both at a similar time for improving the PVTs performance. The heat transfer via the fluid can be enhanced along with the thermal working of the whole system by using NF and the NF heat transfer capability depends on their thermophysical characteristics as shown in Table 1 (Ahmed et al., 2021).

By fitting in a thermal collector with a PV unit, the efficiency of the unit, and the general system energy output comprising the thermal energy is improved and increased. This novel device is known as the PVTs. In the research work by Abadeh et al. (2018), various nanofluids such as TiO_2/water, Al_2O_3/water and ZnO/water were employed as coolants for a PVT system. The electrical output of the PVT/nanofluid system was reported to improve by 7 % compared to traditional PV units (Abadeh et al., 2018). Al_2O_3-ZnO-Fe_3O_4 ternary hybrid NFs were synthesized via a two-step process. Using the hybrid NFs, an effective heat transfer application and cooling medium in PVT applications was reported in this study. The ideal relative electrical PVT efficacy against that of the PV is 8.13 %, while the thermal and electrical enhancement was assessed to be 19.06 % and 1.79 % for the NFs-based PVTs (Adun et al., 2021). ZnO NPs were prepared by mixing tomato (Lycopersicon esculentum) extract with zinc nitrate (precursor) in a 3:1 ratio, which was subjected to heating at 80 °C for 5 min. The same ratio of solutions was also subjected to microwave irradiation at different power. Absorption peaks of 322 and 334 nm were noticed for the UV–Vis spectra of ZnO NPs using microwave irradiation power of 360 and 540 W. No definite SPR phenomenon was observed at low microwave power of 180 W, which was suggestive that low microwave power was not adequate for ZnO NPs development within 5 min. With increased microwave power, a surface plasmon peak was reported, with a well-defined and substantial peak reported at a microwave power of 540 W. The determined E_g of ZnO NPs at a microwave power of 360 and 540 W were 3.50 and 3.38 eV. Based on the nanocomposite (ZnO/TiO_2/graphene oxide (GO)) prepared, an improved power conversion efficiency of 6.18 % was reported (Sutradhar and Saha, 2016).

Table 1
MeO NPs' thermophysical Characteristics (Ahmed et al., 2021).

MeO	Thermal Conductivity (k/(W.(m.K)$^{-1}$)	Specific Heat (C_p/(J.(Kg.K)$^{-1}$)	Density (ρ/(kg.m^{-3}))
Al_2O_3	40.0	773	3960
TiO_2	8.3	692	4230
Fe_3O_4	9.7	670	5180
CuO	33.0	551	600
ZnO	13.0	495	5600
SiO_2	1.4	745	2220
MgO	8.15 (at 699.5 K)	925.92 (at 300 K)	3650 (at 298 K)

4.8. Application of MeO NPs in storage devices

Shortage of worldwide energy and environmental contamination have raised a red flag for humankind, forcing us to switch our conventional energy acquisition approaches and as an alternative employ green energy sources like wind energy, solar energy, tidal and geothermal energies. These energies are generally accumulated in electrical energy form and delivered to users via energy storage devices like batteries especially the lithium-ion battery (LIB) (He et al., 2019).

Currently, energy storage devices like Li-ion batteries (LiBs), supercapacitors and sodium-ion batteries (SiBs) are surpassing the tremendous requirement for energy-based devices to manage our everyday activities. Batteries are based on their storage principles and classified as primary or non rechargeable batteries and secondary or rechargeable batteries which LIBs come under the last classification (Nichelson et al., 2022). Their exclusive properties like power rate, life cycle, fast charging with better load capacity, extended cycle and self-life, less maintenance, high energy competence, huge coulombic efficiency, low self-discharge, great energy density, huge operating temperature range, low self-discharge rate make them superior to other rechargeable batteries like lead acid, NiCD and NiMH. Device energy performance in terms of energy density against power density, fuel cells have huge energy density with reduced power density whereas conventional capacitors have extreme power density as shown in Fig. 14a (Nichelson et al., 2022).

A battery is a transducer that produces electrons by electrochemical reactions and comprises of positive (cathode) and negative (anode) terminals (Sharon, 2019). Fig. 14b shows the LiBs charging mechanism, where the electrolyte (liquid electrolyte, solid polymer electrolyte, solid ceramic electrolyte, gel polymer electrolyte, and ionic liquids), which acts as a charge carrier and provides the practical transfer of Li^+ to travel spontaneously from the anode to the cathode and the other way around. To avoid the direct interaction of the cathode and anode accessible for liquid electrolyte or solid electrolyte, a separator is included in the LiBs battery component. As the battery is powered, oxidation and reduction take place at the anode and cathode, with the loss of an electron by the anode and the gain of an electron by the cathode creating electrical energy, indicative of a LiBs system reversible reaction mechanism at the cathode and anode partitions (Nichelson et al., 2022).

LiBs are currently the primary power source for portable electronic devices such as cell phones, laptops, and notebooks and are projected for electric automobiles (hybrid electric vehicles (HEVs), plug-in hybrid electric vehicles (PHEVs) and electric vehicles (EVs)) in the near future owing to their high energy density, remembrance effect, lifetime and sustainability considerations (Shobana, 2019). The electrochemical behavior and LiBs performance are subject to the negative electrode called the anode. The nature of the metals used and, the compound's chemical and physical properties control LiBs performance. In the past decades, Li metal and graphite were generally used as anode materials for LiBs owing to their remarkable explicit capacities and huge energy density. Graphite has a spectacular Li storage capacity of 4200 mAh/g at room temperature and was deemed as a possible high-performance anode contender for LiBs. However, the deformation of shape when Li^+ and electrons are contained in the graphite structure results in reduced columbic efficiency and impacts the battery charge storage mechanism. Currently, to overcome such shortcomings, different potential electrodes such as silicon anodes, transition MeO, their alloys and

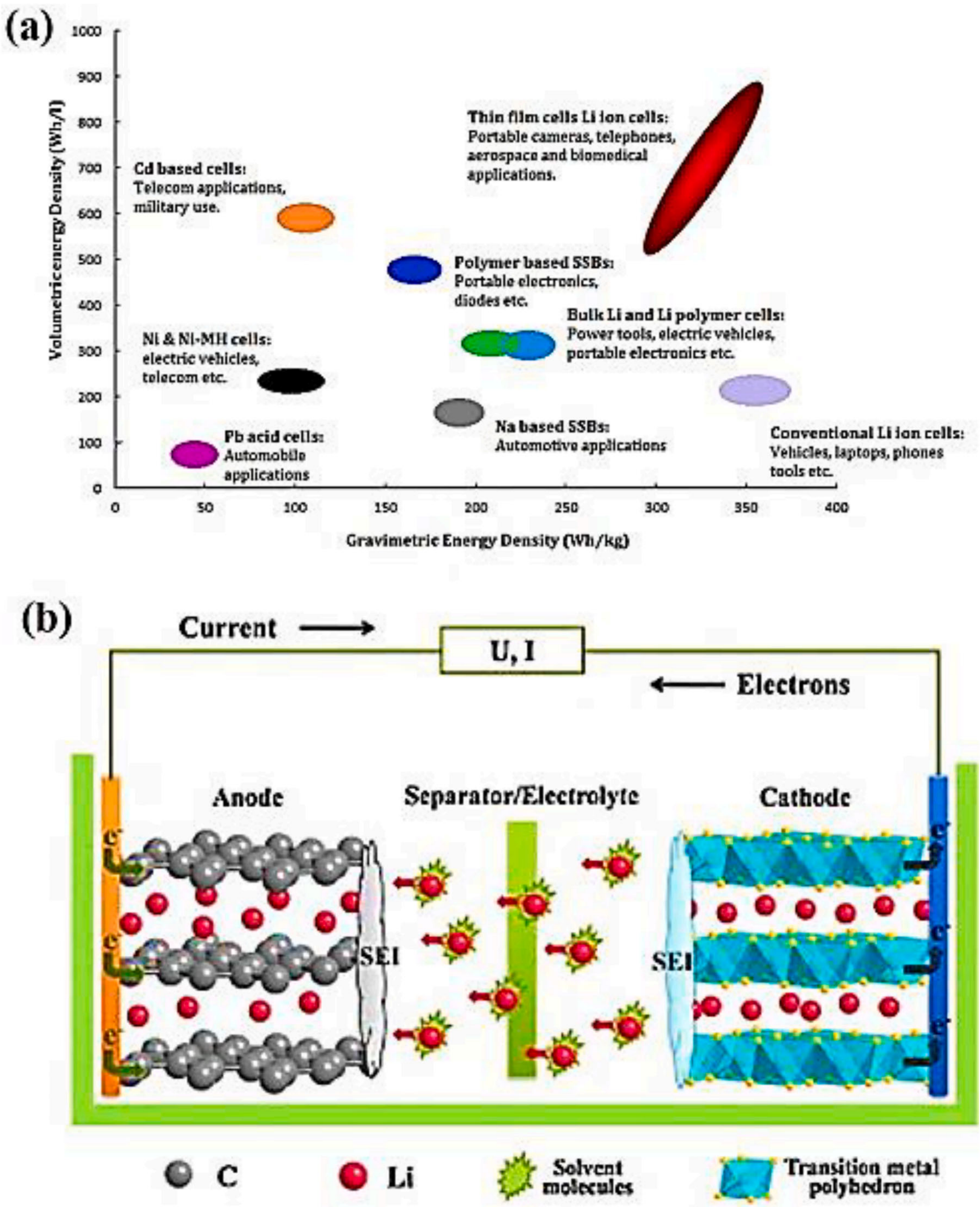

Fig. 14. (a) Different battery energy densities and (b) LiBs charging mechanism (Nichelson et al., 2022).

composites are used. Silicon and MeO-based anode issues of volumetric change and low coulombic efficiency limit their commercialization (Nichelson et al., 2022).

MeO NPs' hollow structures have led to their significant use as electrode material for Li batteries (LiBs). Their hollow structures present high specific capacity, superior rate capacity, and improved cycling operation as electrode materials for LiBs. By concentrating on the hollow-based structures of certain dual mixtures of MeO such as TiO_2, Fe_2O_3, Co_3O_4, SnO_2 and MeO complexes, the electrochemical performance is improved. Li-based MeO with +ve redox potentials, which is a composition of different blends of metals such as $LiCo_{1-x}M_xO_2$, $LiMn_{1-x}M_xO_2$, $LiMn_{2-x}M_xO_4$, $LiMPO_4$ (M = Fe, Co, Ni) are commonly utilized as cathode materials in LiBs. At high current rates of 1 − 10°C, they can distribute capacities of 100–200 mAh/g. LiBs anode is primarily composed of carbon-based materials with a prolonged cycle and the Li storage capacity is greater than 372 mAh/g. Owing to the high capacity of 1000–4000 mAh/g, Sn, Si, Al and their alloys are intended as anode in LiBs (Khan et al., 2022).

The storage technologies that guarantee energy security and tackle the basic constraint of occasional accessibility are Li batteries and supercapacitors (SCs). SCs are thought of as sustainable protection to save the exclusive Li batteries from shock linked with unexpected changes in demand and supply. The long cycle life has made SCs appealing for automobiles, electric vehicles, smartphones, shoes of soldiers, sensors, and load-level applications (Sharma et al., 2018).

Yet, minimal power density, cyclic stability and safety are substantial limitations linked with the LIB system for their advancement. In spite of these downsides and new energy storage systems like fuel cells, battery devices are deemed the most important energy storage technologies. Fuel cells are power production systems that transform chemical energy into electric energy and thus, have efficient energy conversion potentials, they are selected over batteries owing to their extraordinary power density. They are energy systems that are well-known for their improved power density and efficacy, sturdy ecological responsiveness, fuel multiplicity, variable installation and prompt load responses. Fuel cells are incapable of satisfying the sustainable advancement domain of lower cost owing to the elevated cost of setting up, sluggish starting speeds than internal combustion engines, undependable hydrogen storage expertise, scarce infrastructure and other problems (Shaheen et al., 2023).

An important alternative source of energy to fuel cells is the electrochemical capacitor known as a supercapacitor (SC), which shows features midway between those of a conventional capacitor and a battery. Owing to the comprehensive diversity of SC prospective properties such as sustained electrochemical cycle stability, wider operating range and better power density, SC has drawn a lot of research consideration over the years. The general pros of SCs over fuel cells and batteries are their power density (high as 102–104 W/kg), their extended charge-discharge cycles (higher performance and capacity and lower internal resistance up to a million speed, deeper charging and discharge), an extensive functioning temperature range, operation without maintenance and eco-friendly (green power source) (Shaheen et al., 2023).

Based on the charge storage mechanism, they are generally grouped as electric double-layer capacitors (EDLCs) and pseudocapacitors. EDLCs were originally created employing various carbon forms. Saturation in the device performance was due to the low specific capacitance, energy density and intricate procedures involved in achieving extraordinary surface area active materials. The pseudocapacitors are produced utilizing MeO, hydro-oxides or conducting polymer, which mostly show much more advanced specific capacitance than EDLCs. The performance of pseudocapacitors can be enhanced by incorporating redox additives into the electrolyte and their capacitance is driven by the faradaic redox reaction at the surface of the material. Currently, less costly and eco-friendly MeO (MnO_2, V_2O_5, SnO_2, Fe_2O_3, Co_3O_4 and Cu_2O and CuO-batteries and SCs) have been investigated and become scientifically acceptable for SC production due to the cost factor and climate mitigation laws (Sharma et al., 2018).

$NiFe_2O_4$ were bio-synthesized adding green tea extract to the precursor solution of $Ni(NO_3)_{2\cdot 6}H_2O$ and $Fe(NO_3)_{3\cdot 9}H_2O$. This approach was also applied in the synthesis of $NiFe_2O_4$CNT. The capacitance retention and the capacitance rate capability were forecast as 78.8 and 90.1 % and 65.1 % (5–17 A/g) and 62.4 % (5–17 A/g) for the $NiFe_2O_4$ and $NiFe_2O_4$CNT (Bashal et al., 2023). Bengal gram beans (Cicer arietinum *L.*) extract was employed in the bio-synthesis of a Co-doped TiO_2 NP-based anode in a Li-ion battery. As depicted in Fig. 15a, which shows the cyclic voltammetry (CV) analysis of TiO_2 and 3 %, 5 % and 7 % of Co-doped TiO_2 NPs at a scan rate of 0.2 mV/s and potential range of 0.01–3 Vs Li/Li^+, it was reported that the CV curves nature were that of TiO_2 and Co-doped TiO_2 NPs with similar redox couple peaks at ~1.68 and ~2.17 Vs Li/Li^+. This corresponds to the Li-ion intercalation into and deintercalation from the interstitial sites of TiO_2. The oxidation peak of the CV curve was noticed to decrease with a peak shift to the lower voltage as the Co doping concentration was increased, the most observed shift in 7 % Co-doped TiO_2 NPs. This was indicative of enhanced wetting and improved Li-ion insertion kinetics with an improvement in the doping concentration of Co and was attributed to reduced E_g. The relative first galvanostatic charge/discharge profile of TiO_2 and Co-doped TiO_2 NPs is displayed in Fig. 15b. A significant irreversible capacity of 27 mAh/g (discharge capacity of 183 mAh/g, and charge capacity of 156 mAh/g) was exhibited by TiO_2. While a low irreversible capacity of 3 mAh/g (discharge capacity of 160 mAh/g, and charge capacity of 157 mAh/g), 1 mAh/g (discharge capacity of 188 mAh/g, and charge capacity of 187 mAh/g) and 14 mAh/g (discharge capacity of 221 mAh/g, and charge capacity of 205 mAh/g) was displayed by 3 %, 5 % and 7 % Co-doped TiO_2. The decrease in the irreversible capacity of Co-doped TiO_2 signifies improvement in the

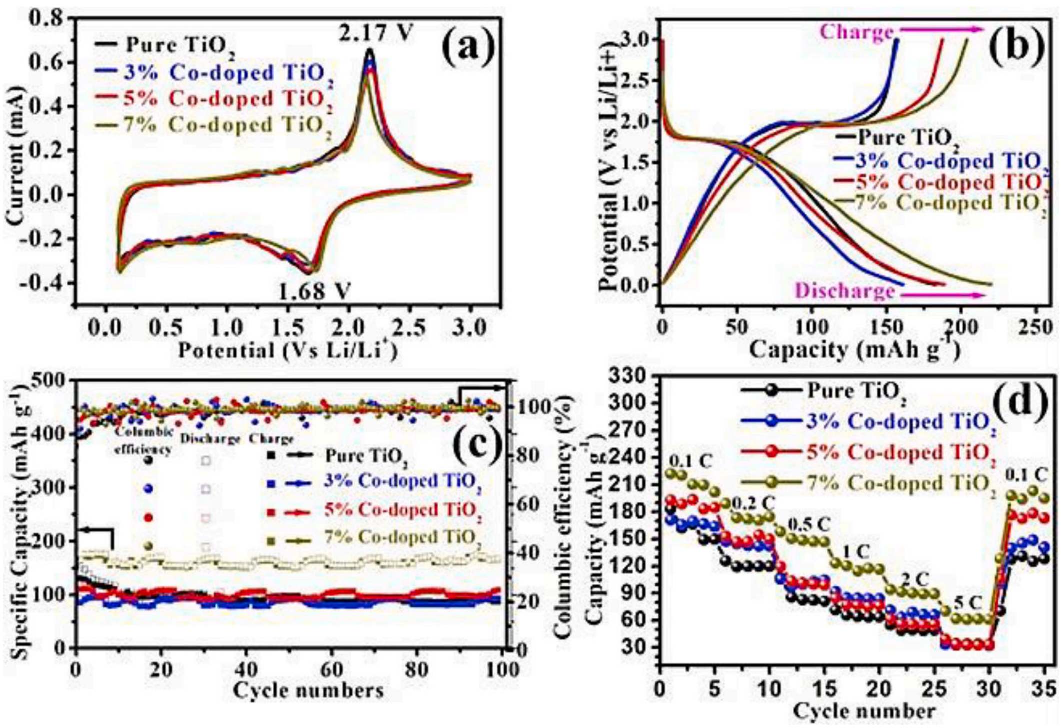

Fig. 15. (a) CV curves at a scan rate of 0.2 mV/s, (b) charge-discharge profile cycle at a current density of 0.1 C, (c) cycle performance and (d) rate performance of TiO_2 and Co-doped TiO_2 at various C-rate (Kashale et al., 2019).

electrode and electrolyte interaction, reduction in the solid electrolyte interface (SEI) production and improvement in the electrochemical reversible reaction of TiO_2. In Fig. 15c, a gradual reduction in the capacity with an improvement in the cycle number was reported for TiO_2. But for Co-doped TiO_2, there was relatively less reduction of the specific capacity. The 7 % Co-doped TiO_2 anode was reported to exhibit the ultimate capacity of 167 mAH/g (88.3 %) after 100 cycles at 0.5 C current density. The Co-doped TiO_2 was also reported to show elevated and stable coulombic effectiveness of up to 10 GCD cycles, which is indicative of good reversibility. From the rate performance of TiO_2 and Co-doped TiO_2, a gradual reduction in certain capacity during the first five original cycles of all electrodes of TiO_2 at 0.1 C was reported and was attributed to the loss of symmetry during phase transition complemented by a reduction in the unit cell along the c-axis. The successive improvement of the unit cell volume along the b direction resulted in capacity fading and further 0.2–5 C-rates, the specific capacitance of the TiO_2 electrode was stable. 7 % Co-doped TiO_2 NPs showed better rate performance and high specific capacitance according to Fig. 15d (Kashale et al., 2019).

The green synthesis approach was used to create lithium titanate (LiTO) NPs and the Aloe Vera extract was employed as a reducing and capping agent for this process. The assessed specific capacitances of 91 F/g were determined for LiTO at a scan rate of 5 mV/s. The reason for the low specific capacitance was ascribed to the higher value of peak separation potential. Based on the CV analysis, the LiTO NPs sample showed a thin potential window of -0.4–0.2 V in an aqueous electrolyte solution. The anodic peak is attributed to Ti ions oxidation by the lithiation process of LiTO matrix while the cathode peak was due to the delithiation. LiTO anode showed symmetrical anodic and cathodic peaks which showed good electrochemical reversibility. The peak saturation potential was assessed to be 192 mV (Perumal et al., 2020). TiO_2 NPs explored as a potential electrode material for effective next-generation electrochemical energy storage devices in this study were bio-prepared using Calotropis Gigantea plant and Ocimum Tenuiflorum plant extracts. The optical E_g of the anatase and rutile phase TiO_2 were assessed to be 3.2 and 3.0 eV at sturdy adsorption and edge peaks of 344 and 334 nm (Fig. 16a-b). The sample was reported to show an extraordinary specific capacitance of 224 and 105 F/g at 0.5 A/g with a 71 % and 55 % capacitive retention rate after 5000 cycles for Calotropis Gigantea and Ocimum Tenuiflorum plant extracts (Reddy et al., 2019).

Employing Calotropis Gigantea plant extract, TiO_2 NPs were biosynthesized. From the BET and BJH analysis, the TiO_2 NPs had a specific surface area of 129.4 m^2/g and average pore diameter and volume of 5 nm and 0.086 cm^3/g. A high specific capacitance of 804 F/g at a current density of 1 A/g and a capacity of 96 % after 5000 cycles were retained by the bio-synthesized TiO_2 NPs acting as an SC electrode (Reddy et al., 2021). Extract of gram seeds (Cicer arietinum. L) was used in the green synthesis of TiO_2, which was co-doped with rGO-nanosheet. The determined specific capacitance and energy density at a current density of 1 A/g were 599.9 F/g and 83.31 Wh/kg using this nanosheet (Anwer et al., 2023). ZnO NPs and CuO NPs bio-synthesized using Ficus benghalensis (banyan tree) extract, were assessed for their high-performance SC application. The specific capacitance obtained using the bio-prepared ZnO and CuO NPs were in a range of 2.97–4.36 F/g at a scan rate of 20–100 mV/s and a range of 1.73–2.14 F/g at a scan rate of 20–100 mV/s. The assessed energy for ZnO and CuO NPs at a scan rate of 20–100 mV/s was in a range of 0.50–1.06 mV/s and 0.15–0.19 mV/s (Yadav et al., 2022). Utilizing Piper nigrum (Indian black pepper) dried fruit extract as a reducing agent, CuO NPs were bio-prepared. The specific surface area of the obtained CuO NPs was 81.23 m^2/g. The specific capacitance obtained using the bio-prepared CuO NPs was determined to be 238 F/g at 5 mV/s. The green synthesized nanoporous CuO NPs could be utilized as a high-performance SC material for extraordinary energy storage devices (Murphin Kumar et al., 2020).

4.9. *Electrochemical application of MeO NPs*

Highly sensitive unique electroanalytical devices built on nanostructured MeO are cost-efficient and enhanced selectivity when coupled to bio-recognition molecules. MeO NPs with various morphologies have been prepared via adaptable techniques and they show different forms of electrical and photochemical characteristics owing to their size, stability and elevated surface area. Their major functions in electroanalysis include the strengthening of the conductive sensing interface, NPs catalytic characteristics permitting their expansion with metals and the electrical contact of the redox centers in proteins and transducer surfaces (George et al., 2018).

They are considered electronic wires and electrocatalysts owing to the fast electron transfer between the transducer and analyte molecules in the existence of metal NPs and their nano-size and structure. Biocompatible MeO NPs are normally utilized to immobilize biomolecules for the creation of immunosensors, enzyme sensors, and DNA sensors. Semiconducting NPs are generally utilized as markers and tracers in electrochemical research. The sturdy affinity of MeO NPs to the working electrode surface can be attained by different approaches such as electrodeposition, chemical covalent bonding, physical adsorption and electropolymerization (George et al., 2018). A key disadvantage of MeO NPs utilization as electrochemical sensor is their wide E_g, which makes them semiconductors or even insulators, their reduced ion transport kinetics and the pulverization of the electrode film resulting from the pronounced volume expansion and contraction during the charging and discharging processes. Through the hybridization with carbonaceous materials or matrix, other metal NPs and polymers, these problems can be overcome (Agnihotri et al., 2021).

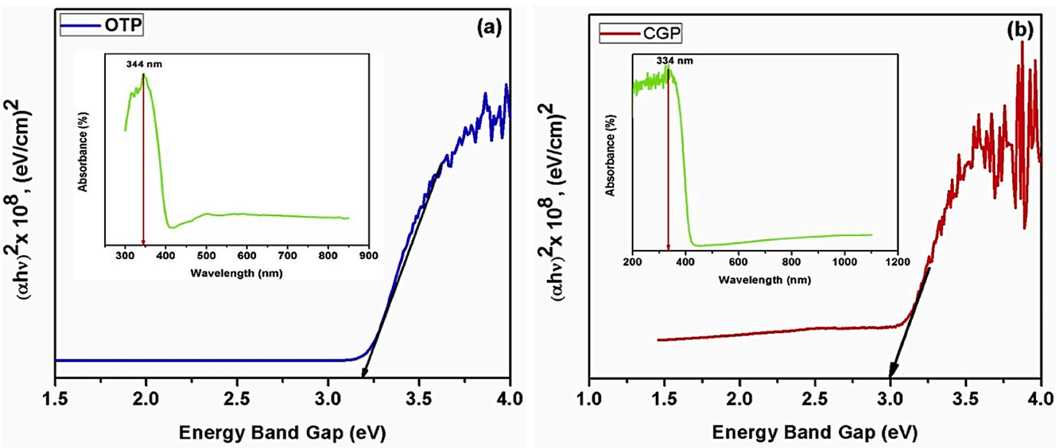

Fig. 16. (a). UV–Vis and absorption spectra (inset) of TiO_2 derived from Ocimum Tenuiflorum plant and b) Calotropis Gigantea plant extracts (Reddy et al., 2019).

For MeO deposition, voltammetric and Amperometric approaches are generally employed for the electrochemical procedures for MeO creation. Cyclic, linear sweep and square wave voltammetry are types of voltammetric approaches that are suitable for MeO NPs deposition. The improved qualities of the electrochemical approach include reactions at low temperatures and pressure, good control of morphology, MeO size, low cost and relatively eco-friendly. MeO electrochemical deposition can be achieved with a two or three-electrode system. This approach is suitable for MeO deposition on the substrate for modified glassy carbon electrodes (Althomali and Adeosun, 2023). MeO such as MgO, TiO_2, NiO and ZnO are finding wider practical use as catalysts in the detection of heavy metals, environmental pathogens, and organic and inorganic contaminants owing to their high reactivity, high specific surface area, controlled size and distribution (Fuku et al., 2018).

NiO, ZnO and CuO NPs were bio-synthesized employing Centella asiatica plant extract. The mixtures were preheated in a muffle furnace at 400 ± 10 °C and further calcinated at 800 °C to obtain the final product. According to the calculations carried out using the Debye-Scherrer equation, the crystalline size of the MeO NPs was determined to be in the range of 25–30 nm. Broad absorption peaks reported at 360 nm, 350 and 370 nm and 366 nm were ascribed to the absorption spectra of NiO, CuO and ZnO NPs (Fig. 17a). Based on the diffuse reflectance spectrometer (DRS) analysis, the calculated E_g of ZnO, NiO and CuO NPs were 3.4, 4.2 and 1.63 eV (Fig. 17b).

A moderated photodegradation of AR88 dye was shown using various MeO NPs. The photocatalytic activity of CuO, NiO and ZnO NPs on AR88 dye was 44 %, 46 % and 51 %. The electrochemical behavior (reduction-oxidation) of the electrodes was determined using the CV approach. Zn^0, Ni^0 and Cu^0 resulted in Zn^{2+}, Ni^{2+} and Cu^{2+}, owing to electrons being given out, leading to an anodic peak being created as noticed in Fig. 18a–c. A cathodic peak is created when Zn^{2+}, Ni^{2+} and Cu^{2+} are reduced to Zn^0, Ni^0 and Cu^0. The reduction peak potentials for ZnO, NiO and CuO NPs were -0.81, 0.16 and -0.6 V and -0.19, and 0.28 and -0.37 V. With increased scan rate, the peak currents of the oxidation and reduction peaks were noticed to be improved. The oxidation peaks were reported to shift slightly to the +ve side of the potential while the reduction peaks shifted marginally to the -ve side of the potential (Alam et al., 2021).

CuO NP was bio-synthesized utilizing Ficus elastica extract as a reducing and stabilizing agent. The bio-prepared CuO NPs were doped with graphite powder modified with polyaniline (PANI) (CuO/PANI-CPE sensor) to create the carbon electrode and employed as sensors for the detection of Cu(II), Pd(II) and Hg(II). It was reported in the findings of this study, that the CuO/PANI-CPE sensor was able to detect low concentrations of Cu(II), Pd(II) and Hg(II) in HCl at low limits of detections of 0.11, 0.16, and 0.07 μg/L. The accomplished sensor was found to show good selectivity, reproductivity and stability (Ali et al., 2023). Green synthesized Fe_2O_3/CuO NPs using Ocimum sanctum Linn (Tulsi) leaf extract. They were utilized for the electrochemical detection of amiprofos-methyl (APM)-an organophosphorus. The electrochemical sensor depicted a linear range of 0.05–30 μg/mL with a limit of detection of 0.0065 μg/mL. The established electrochemical sensor was effectively utilized for APM detection in various water and soil samples with recoveries ranging from 96 to 99 %, with good stability and reproductivity over 10 days (Puthalapattu et al., 2023). $ZnFe_2O_4$ NCs were bio-synthesized using Moringa Oleifera extract. The time constant and exchange current of $ZnFe_2O_4$ NCs from the electrochemical impedance spectroscopy (EIS) analysis were assessed to be 5.2×10^{-4} s/rad and 6.6×10^{-6} A. The $ZnFe_2O_4$ electrode showed a good voltammetric response, extraordinary electroactivity and outstanding electrochemical working (Matinise et al., 2018).

5. Synthesized MeO via green technique and their applications

5.1. Green synthesis of TiO_2 NPs and their applications

Titania occurs as a titanium oxide, which is documented as NPs of MeO forming distinctive thermal, optical, electric, and magnetic properties (Irshad et al., 2021). TiO_2 is created by the element's titanium with atomic number 22 from group IV B and oxygen with atomic number 8 from group VI A (Abisharani et al., 2019). They are n-type semiconductors, having an energy E_g of 3.2 eV. Owing to this justification, TiO_2 employs UV-light rather than visible-light (Jassal et al., 2022).

Anatase TiO_2 takes up a body-centered tetragonal shape [space group I4l/amd] with lattice-parameters (LPs) of 0.377 and 0.944 nm. The brookite and rutile TiO_2 NPs are orthorhombic crystal shapes [space group Pbca and space group P42/mnm] with LPs of 0.515, 0.546, and 0.919 nm and 0.295 and 0.458 nm. The way the three polymorphs of TiO_2 share their adjacent TiO_6 octahedral coordination differs. In anatase and brookite TiO_2 NPs, The TiO_6 units are linked via the neighbouring unit edges, while nearby octahedral units share a corner in (Krishnan et al., 2023) direction for the rutile TiO_2 and their E_g slightly differ (3.15 eV-anatase and 3.0 eV-rutile-TiO_2 NPs). Owing to the varied features of TiO_2 NPs, their application in various fields is influenced by the surface area, E_g, porosity, and crystal structure (Gangwar et al., 2016). Fig. 19 shows the building blocks of rutile and anatase.

This metal does not occur in a metal state owing to its extraordinary affinity to oxygen and other elements. Under the regular form, TiO_2 is insoluble in water, nonflammable, extremely stable, and has an extreme refractive index of $n = 2.4$, making it appropriate as a white pigment. TiO_2 exists in brookite, anatase, and rutile forms at different temperatures and is naturally inert. But when its particles become smaller, their surface area develops, and their rutile form becomes more vulnerable to unsafe effects (Gebre, 2023; Irshad et al., 2021).

They also have extraordinary properties like non-wettability, considerable E_g, and hydrophobicity. Thus, TiO_2 NPs present a broad

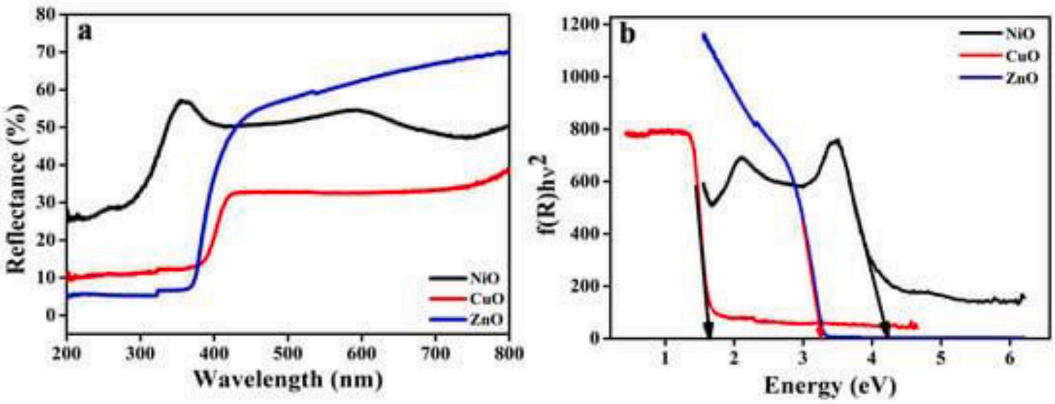

Fig. 17. (a). DRS spectra and (b) calculated E_g of NiO, ZnO and CuO NPs.

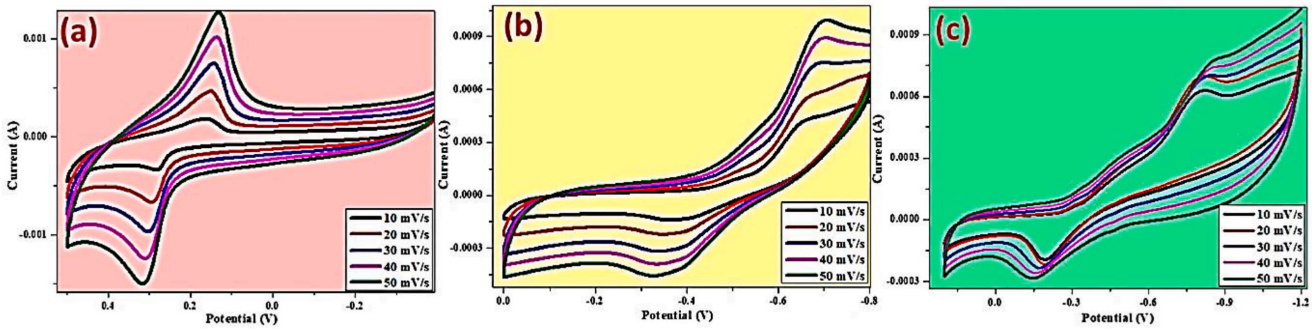

Fig. 18. Cyclic voltammetric research of (a) NiO, (b) CuO and (c) ZnO NPs (Alam et al., 2021).

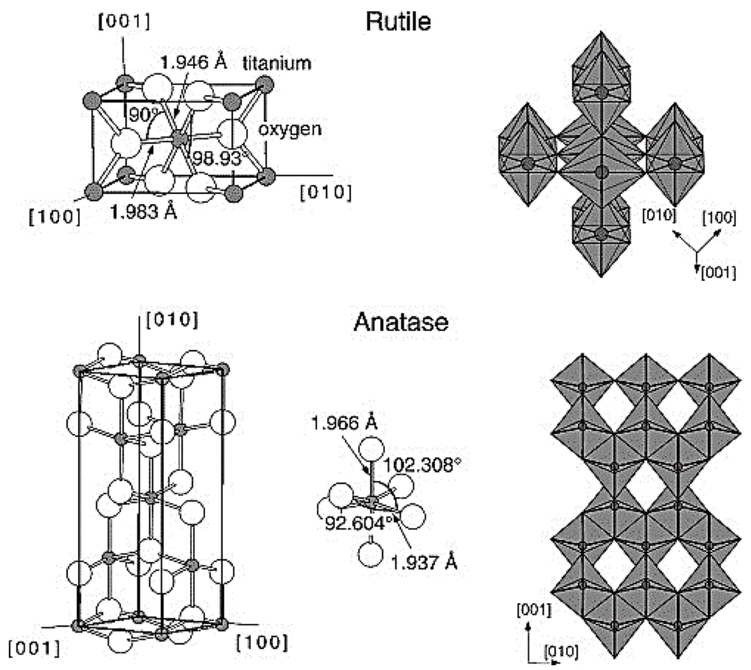

Fig. 19. Schematics of the bulk structures of rutile and anatase (Diebold, 2003).

scope of applications in medical, industrial, and environmental subjects. Their expanded application in different industries like photocatalysis, self-cleaning, dye-sensitized solar cells, charge-spreading devices, microelectronics, electrochemistry, chemical sensors, anti-bacterial products, and textiles (Arun et al., 2023; Malode et al., 2021). The sturdy oxidation potential, extensive photo-catalytic action, and remarkable optical and chemical stability are shown by the non-noxiousness of TiO_2 NPs. Furthermore, they have anti-bacterial and anti-microbial catalytic features which permit them to be utilized in a lot of manufacturing uses, involving catalyst support, pigment, and photocatalysts. They have also proven to be stable, and biocompatible, most especially owing to the capping agent on their surface. Among the other forms, anatase has astonishing physicochemical properties for ecological remediation. Owing to the varied features of TiO_2 NPs, their application in various fields is influenced by the surface area, E_g, porosity, and crystal structure (Gangwar et al., 2016; Abisharani et al., 2019; Alabdallah et al., 2021).

They are currently fabricated naturally employing microorganisms, PEs, and algae (Gebre, 2023). These NPs are the most generally created MeO NPs owing to primarily their multipurpose features arising from the chemical stability, physical, optical, and electrical properties (Annu and Ahmed, 2018). Using Caricaceae (Papaya) shell extracts, TiO_2 NPs were produced and assessed for seed germination as well as antifungal study. Fig. 20 shows the color change with the introduction of the shell

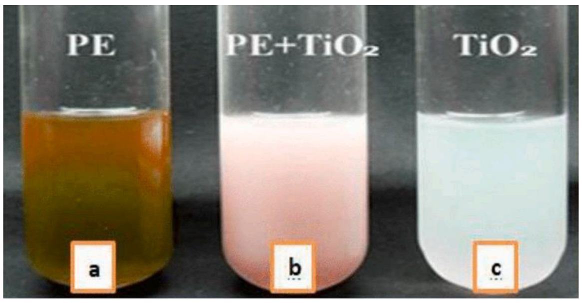

Fig. 20. Colour changes in the green synthesis of TiO_2 NPs using Caricca papaya shell extracts (a) Ti isoprop-oxide solution (b) introduction of the shell extracts to the MeO solution and (c) TiO_2 NPs (Saka et al., 2022).

extract into the MeO solution (Ti isoprop-oxide solution). XRD analysis of the prepared NPs shows diffraction peaks at 2θ (12.76, 18.2, 20.01, 28.34, 32.91, 35.32, 36.57, 40.21, 49.74, 58.34, 64.56 and 70.5° were matched to 100, 002, 101, 102, 101, 102, 110, 111, 102, 111, 101, and 111 crystal planes) which were ascribed to the crystalline plane of TiO_2 NPs. These peaks were indexed to the hexagonal phase of the rutile and anatase of TiO_2 NPs (JCPDS No.80-0075) (Fig. 21). It was reported that

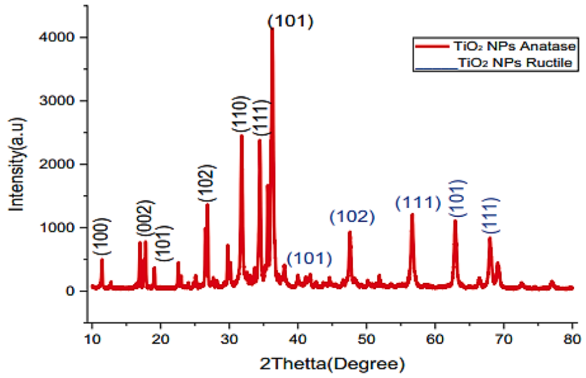

Fig. 21. XRD diffraction spectra of green synthesized TiO_2 NPs (Saka et al., 2022).

there was superlative germination of seeds, as well as roots and plant growth, noticed with the treatment with TiO_2 NPs (Saka et al., 2022).

TiO_2 NPs were created through the green synthesis route using three natural sources orange peel, aloe vera, and hibiscus rosa sinensis as reducing and stabilizing agents. The produced TiO_2 NPs were in the anatase phase (Santiago et al., 2023). Syzygium cumini leaf extract as a capping was used in the synthesis of TiO_2 NPs. It was further explored for the degradation of Pb(II) ions. The prepared TiO_2 NPs were in the anatase phase with an extraordinary BET surface area of 105 m^2/g. It was noticed that 75.5 % and 82.5 % of chemical oxygen demand (COD) and Pb(II) ions were sequestered using the prepared TiO_2 NPs (Sethy et al., 2020). TiO_2 NPs were created using kitchen waste (Bengal gram beans) extract and further calcinated at 500 °C to remove organic contaminants. It was reported in this study that the prepared TiO_2 NPs had uniform particle size distribution owing to the stabilization molecules naturally existing in the extract. The bio-prepared TiO_2 NPs and Li incorporation properties as an anode in the half-cell formation (Li/TiO_2) were found to show reversible insertion of 0.61 mol at a current density of 33 mA/g. The half-cell was found to exhibit reliable cyclability and with 98 % initial reversible capacity noticed after 60 galvanostatic phases (Kashale et al., 2016). The rutile phase of TiO_2 NPs was bio-produced using jasmine flower extract as a reducing and stabilizing agent. The prepared NPs were of spherical shape morphology and had an average crystalline size of 31–42 nm according to the SEM and XRD analysis. The prepared TiO_2 NPs were explored for the confiscation of methylene blue dye. It was found to be effective in the photodegradation of the dye molecules with a 92 % efficiency degradation achieved. The bio-prepared TiO_2 NPs were also found to be enhanced inhibition against Gram +ve and Gram -ve strains as indicated by Fig. 22 (Aravind et al., 2021).

Fig. 22. shows (a) the bio-prepared TiO_2 NPs' anti-bacterial activity and (b) the chemical route synthesized TiO_2 anti-bacterial activity (Aravind et al., 2021).

TiO_2 NPs were created using the bio-production approach using Calotropis gigantean medicinal PEs. The reduced particle size and the enhanced E_g energy were reported in this study using the extract of Calotropis gigantean medicinal plant for TiO_2 NPs production. The calculated E_g of TiO_2, flower- TiO_2 (F-TiO_2), seed-TiO_2 (S-TiO_2) and leave- TiO_2 (L-TiO_2) according to this study was determined to be 2.59 eV, 2.68 eV, 2.83 eV and 2.88 eV (Fig. 23). The determined E_g of the semiconductor were particle size conditional and found to increase with reducing particle size due to electron transition energy. This establishes quantum confinement of the TiO_2 by the active biomolecule inclusion. The prepared NPs were subsequently applied and found to be effective in the degradation of methylene blue (MB) dye within 60 min, with 96 % of MB degraded owing to the low re-combination of photo-created holes and electrons (Pavithra et al., 2023). The absorption edge was noticed to shift to higher energy (blue-shift) with reduced particle size.

Bengal gram beans extract *(*Cicer arietinum L.*)* was used in the bio-synthesis of TiO_2 NPs, which was calcinated at 500 °C to remove organic contaminants. The Li incorporation properties were assessed as anode in the half-cell configuration (Li/Bio-TiO_2) and were reported to show reversible insertion of 0.61 mol at a current density of 33 mA/g. The half-cell showed excellent cyclability and held 98 % of its initial reversible capacity after 60 galvanostatic cycles (Kashale et al., 2016). Table 2 gives a summary of the bio-synthesis approach for TiO_2 NPs production and their different uses.

5.2. *Green synthesis of ZnO NPs and their applications*

ZnO has a wurtzite crystal shape [shape group P63mc] with LPs of 0.325 nm and 0.520 nm having a series of irregular planes of four-fold coordinates of O^{2-} and Zn^{2+} ions, stacked instead along the c-axis, with an extraordinary density of 5606 kg/m^3. ZnO-based 1-D nanostructures have intensified extensive research attention due to their large volume and their actual benefits like great contrast ratio, ambient visibility, image resolution, effective heat resistance, and minimal outgassing, achieving improved photonic and electronic devices for sensing use (Gangwar et al., 2016).

ZnO NPs are NMs studied extensively for various applications like cosmetics, photocatalysts, gas sensing, electronics, pharmaceuticals, and energy. Bulk ZnO is known also for its extreme chemical and thermal stabilities. Additionally, bulk ZnO NPs show piezoelectric properties, creating electrical charges under mechanical stress. This feature is employed in sensor and energy-harvesting tools. They are n-form semiconductors with a direct E_g of 3.37 eV with tunable properties, extraordinary exciton binding energy (60 MeV), and excellent bond strength (Gebre, 2023; Kumbhakar et al., 2021; Yu et al., 2022; Kulkarni et al., 2020; Ali et al., 2023). ZnO NPs are employed as biocidal agents owing to their UV adsorption capability and excellent photostability. ZnO NPs show anti-bacterial and anti-cancer properties (Alabdallah et al., 2021). These NPs have sturdy adsorption and catalytic abilities as oxide semiconductors and as a result, they are used as a multiplicity of sensors, electrochemical sensors, biosensors and environmental applications (Shetti et al., 2019). Fig. 24 shows the ZnO NPs crystal structure (wurtzite).

ZnO NPs fabricated via the green route are the most useful MeO NPs owing to their swift rate of formation, non-noxiousness, considerable biocompatibility, antimicrobial action, and photocatalytic activity. In the synthesis of ZnO NPs, PEs are used as a biologic reducing and stabilizing agent. While Fungi and other microorganisms have also been employed for ZnO NPs synthesis. They are deemed as the most considerable NPs owing to their improved proportion to their surface area to volume and employed in different engineering and science fields like medical devices, the textile industry, electrochemistry, cleaning agents, catalysis, etc. (Annu and Ahmed, 2018).

ZnO NPs were fabricated using the green synthesis technique utilizing rhizophytic bacteria Paenibacillus polymyxa strain Sx3 as a

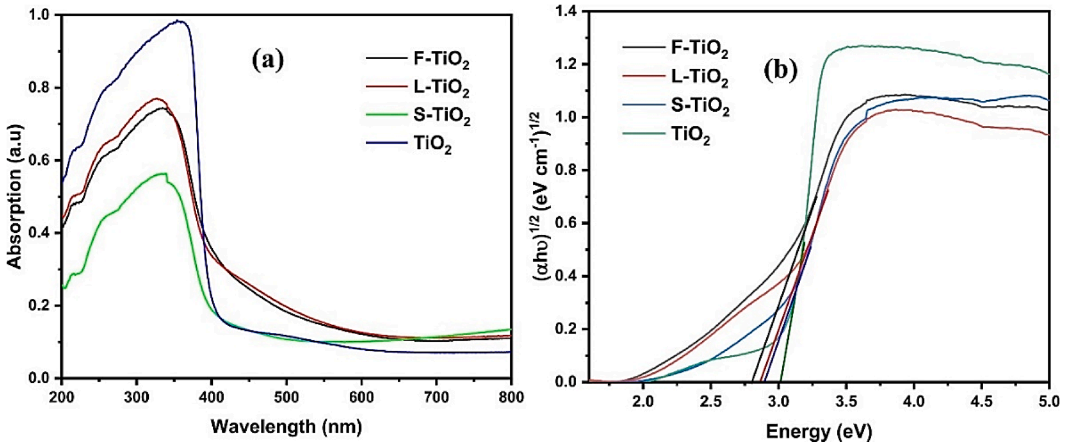

Fig. 23. (a) Plot of absorbance against wavelength and (b) $(\alpha h\gamma)^{1/2}$ against Eg (eV) of TiO_2, F-TiO_2, L-TiO_2 and S-TiO_2 (Pavithra et al., 2023).

reducing agent. UV–Vis reflectance of the fabricated NPs had a peak at 385 nm with an average crystalline size of 62.8 nm. It was also found that ZnO NPs produced via the biogenic process did show substantial inhibition impacts against the Xanthomonas oryzae pv. oryzae (Xoo) strain GZ ooo6 at a 16.0 µg/ml concentration and formation of biofilm reducing by 74.5, 74.4, and 80.2 % (Ogunyemi et al., 2020). ZnO NPs were successfully produced through the green route using the yeast strain Pichia kudriavzevii. Fig. 25A-C shows the TEM images of the produced ZnO NPs which were substantially developed, and the crystal size of the NPs was found to increase as the incubation time was increased. This was attributed to the NPs' slow rate of formation in the medium of reaction, thereby affecting the growth processes and nucleation. Based on the Kubelka-Munk model, the calculated E_g(s) were determined to be 3.39, 3.30, and 3.18 eV at incubation times of 12, 24, and 36 hr. The E_g was noticed to increase as the size of the NPs decreased from ZnO/T1-ZnO/T3 (Fig. 26). The sizable E_g was ascribed to quantum confinement impact (Boroumand Moghaddam et al., 2017).

Fungal cell filtrate of a strain of Trichoderma harzianum was used as a reducer and stabilizer agent in the bioproduction of CuO and ZnO NPs. The bio-produced NPs were assessed for the reduction of the growth of fungal phytopathogens as Alternaria alternata (A. alternata), Pyricularia oryzae (P. oryzae), and Sclerotinia sclerotiorum. There is a reduced mycelial outgrowth of A. alternata and P. oryzae in a dosage-related routine using the prepared ZnO NPs (Consolo et al., 2020). While Coleus amboinicus extract was explored as a reducing and stabilizing agent in the bio-production of ZnO NPs. The particles of ZnO NPs were reported to be polydisperse, with a typical particle size of 15–20 nm. According to the elementary composition, the main elements of the bio-prepared ZnO NPs were O_2 and Zn. Other notable elements in the prepared ZnO NPs were carbon (C), and chlorine which were ascribed to the bio-molecular capping. The XRD diffraction pattern (77.03°, 72.5°, 69.0°, 67.9°, 66.3°, 62.8°, 56.5°, 47.5°, 36.2°, 34.4° and 31.7°) with characteristic planes linked to 202, 004, 201,112, 200, 103, 110, 102, 101, 002 and 100- JCPDS NO: 89-7102) were attributed to ZnO NPs. The acquired results also confirm the wurtzite structure of bio-prepared ZnO NPs. The determined crystalline size of the ZnO NPs was 15 nm according to the Debye Scherrer equation using a diffraction peak intensity of 111. The bio-prepared ZnO NPs were reported to show superb antimicrobial over Gram+ve and Gram -ve microbial pathogens (Wang et al., 2020).

ZnO NPs were bio-produced using *Catharanthus roseus* (L.) G. Don leaf extracts and the produced NPs were explored for nano-priming agents for enhanced seed germination and seedling development. An extraordinary concentration of phytochemicals in the extract of the leaf serves as an effective reducing and stabilizing agent. These phytochemicals are comprised of biologic antioxidants that contain anionic radical that causes the Zn salt to be reduced to ZnO NPs. With the mixture's alkalinity being high, OH^- generated will be relatively substantial, leading to the attraction between OH^- and positively charged Zn^{2+} and thereby resulting in the enhanced ZnO NPs crystallization and the creation of miniature ZnO. A non-spherical shape bio-produced ZnO, with an average particle size of 44.5 nm was revealed by the TEM analysis. Also, XRD diffraction analysis confirmed that the crystalline size of the ZnO NPs was 35.19 nm. It was revealed in this study that the seed germination improved with the priming with the ZnO NPs comparable to the hydropriming (control) (Mishra et al., 2023).

While extracts of Phoenix dactylifera L. and Averrhoa bilimbi were applied in the bio-production of ZnO NPs. The prepared ZnO NPs had spherical shapes with an average particle size of 16–35 nm and 35.4–59.5 nm. A substantial improvement in shoots and callus was found with the ZnO bio-produced with extracts of Phoenix dactylifera L. The prepared ZnO NPs bio-synthesized using Averrhoa bilimbi extract was also found to be an effective antibacterial property against planktonic and biofilm E. coli (Salih et al., 2021; Rahayu et al., 2020). ZnO NPs were created using the extract from Bixa Orellana plant parts (leaf-L, seed-S and seed coat-SC). The prepared NPs were assessed as potential molecule carriers in drug delivery applications and antibacterial activity. Using the bio-synthesized L-ZnO, S-ZnO NPs and SC ZnO NPs, the presence of antibacterial activity against S. aureus and Bacillus subtilis, E. coli and S. aureus was noticed (Gharpure et al., 2022). ZnO NPs were green synthesized using *Mariposa Christia vespertilionis* (MCV) leaf extract. The pore size and pore volume of the green synthesized ZnO NPs were found to decrease with increased calcination temperatures. The ZnO NPs calcinated at 700°C were found to show an elevated preliminary discharge capacity of 591 mAh/g at 0.1 C and an excellent rate capacity (Idris et al., 2023). ZnO NPs were bio-synthesized using Spirogyra hyaline algae extract. The bio-synthesized ZnO NPs demonstrated great antibacterial activity against Gram+ve and Gram-ve bacteria (Hameed et al., 2023). The green synthesis approach was employed in the production of ZnO NPs using Averrhoa bilimbi (L) fruit extract in the study by Ramanarayanan et al. (2018). Based on the Linear Sweep Voltammetry (LSV) and Electrochemical Impedance Study carried out in this study, an improvement in the electrode photocurrent density with improved +ve bias which was suggestive of the n-type nature of the electrode materials was observed. As depicted in Fig. 27a, improvement in the photocurrent with illumination due to photogeneration and conduction of carriers was recorded. A decrease in the arc diameter in light in the EIS Nyquist plot was observed in Fig. 27b and this was attributed to the effective transfer of charge at the electrode-electrolyte surface under the illumination of visible light. Hence, ZnO electrodes used in this study showed outstanding current with less impendence under visible light illumination.

The antibacterial activity of ZnO NPs prepared with the aid of Cymbopogon citratus extract was explored in this study. The prepared

Table 2
Shows the bio-synthesis approach for MeO NPs production and its different uses.

MeO NPs	Biologic Parts	Particles Size (nm) /Morphology	Applications	Refs.
TiO_2	Plum, Kiwi, and Peach fruit extract	47.1–63.2, 54.1–85.1 and 200/cylindrical	In vitro antibacterial and antioxidant activities	Ajmal et al. (2019)
TiO_2	Aqueous leaf extract of Datura innoxia	36–42	Antibacterial analysis	Rajput et al. (2018)
TiO_2	Root Extract of Kniphofia foliosa	-/spherical	Drug resistance bacteria	Bekele et al. (2020)
TiO_2	Extracts of black pepper (Piper nigrum), coriander (Coriandrum sativum), and clove (Syzygium aromaticum).	5–20/spherical	Therapeutic applications	Bhullar et al. (2021)
TiO_2	Trigonella foenum-graecum extract	20–90/spherical	Antimicrobial activity	Subhapriya and Gomathipriya (2018)
TiO_2	Ocimum Basilicum leaf extract	Spherical	Degradation of MB and antimicrobial activity	Maheshna et al. (2022)
TiO_2/CuO	Mucuna seeds extract	28.4 and 14.15/rod and spherical	Anticancer	Gamedze et al. (2022)
TiO_2	Grapefruit extract	Spherical	Antimicrobial and catalytic applications	Ouerghi et al. (2023)
TiO_2/g-C_3N_4	Guava leaf extract	14.4/spherical	Degradation of rhodamine b (Rhb) and MB dye	Madima et al. (2022)
TiO_2	Leaf extract of Tulbhagia violacea	5–15.1/spherical	Antioxidant and anticancer activity	Mbenga et al. (2023)
ZnO NPs	Fruit extracts of Myristica fragrans	43.3–83.1/ hexagonal-shaped	Antibacterial, antidiabetic, antioxidant, antiparasitic, larvicidal properties and photocatalytic agents	Faisal et al. (2021)
ZnO NPs	Strawberry fruit extract	50/spherical shape	–	Khan et al. (2023)
ZnO NPs	Extract of Garcinia mangostana (G. mangostana) fruit pericarp	21/spherical shape	Degradation of malachite green dye	Aminuzzaman et al. (2018)
ZnO NPs	Extract of Allium sativum	5.95–15.66/ spherical shape	Antibacterial effects	Majeed et al. (2022)
ZnO NPs	Plant extract of chamomile flower (Matricaria chamomilla L.), olive leaf (Olea europaea), and red tomato fruit (Lycopersicon esculentum M.)	40.5–124.0/ spherical-shape	Antibacterial activity against Xanthomonas oryzae pv. oryzae	Ogunyemi et al. (2019)
ZnO	Eucalyptus globulus Labill leaf extract	27–35/spherical-shape	–	Barzinjy and Azeez (2020)
CuO	*Sesbania grandiflora* (Sg) (Hummingbird tree) leaves extract	33/needle shape	Anti-diabetic, cytotoxic, anti-microbial, and anti-inflammatory activities	Ramasubbu et al. (2023)
CuO	Terminalia phanerophlebia extract	Spherical	Electrochemical study	Keabadile et al. (2020)
CuO	Serratia sp. ZTB29 strain	20–40/spherical	Antimicrobial agents and plant growth stimulants	Singh et al. (2023)
CuO	leaf extract of Justicia adhatoda	45.07	antibacterial coatings	Islam et al. (2021)
CuO	Berberis vulgaris leaf extract	20	Antibacterial activity	Derakhshani et al. (2023)
CuO	Extract of Momordica charantia	61.48/spherical	Antimicrobial activity	Qamar et al. (2020)
CuO	Mulberry plant extract	40–60	Antibacterial, antioxidant, and photocatalytic activity	Shkir, 2022)
CeO_2	Calotropis procera flower extract	7/cubic	Photocatalytic degradation and antibacterial activity	Muthuvel et al., 2020)
CeO_2	Moringa oleifera leaf extract	17/spherical	Antimicrobial activity	Putri et al. (2021)
CeO_2	Moringa oleifera peel extract	45/spherical	Photocatalytic and antibacterial activity	Surendra and Roopan (2016)
CeO_2	E. tirucalli plant latex	20–25/cubic fluorite phase with flaky structure	Photoluminescent	Malleshappa et al. (2014)
CeO_2	Leucas aspera leaf extract	spherical	Structural, photoluminescent, photocatalytic, and antibacterial activity	Malleshappa et al. (2015)
CeO_2	*Acalypha indica* leaf extract	25–30	Antibacterial activity	Kannan and Sundrarajan (2014)
CeO_2	Extract of Salvadora persica.	10–15/spherical	Anticancer activity	Miri et al. (2020)
CeO_2	Root extract of Polygonum bistorta Linn	18.53/spherical	Electrochemical analysis and multifaceted biomedical applications	Khan et al. (2023)
FeO	Moringa oleifera extract	16/spherical	–	Kiwumulo et al. (2022)
FeO	Artocarpus heterophyllus peel extract	33/spherical	Degradation of Fuchsin Basic dye	Jain et al. (2021)
FeO	Aspalathus linearis (rooibos)	3–31/spherical	Sorghum seed growth and preventative oxidative damage of biomolecules	Ndou et al. (2023)
FeO	Eucalyptus globulus Extract	2.34	Removal of heavy metals from agricultural soil	Andrade-Zavaleta et al. (2022)
FeO	Platanus orientalis leaf extract	38/spherical	Antifungal activity	Devi et al. (2019)
FeO	Bacillus megaterium	20–30	Hyperthermia therapy	Hajiali et al. (2022)
FeO	Psidium guajava leaf extract	–	Antimicrobial and degradation activity	Adhikari et al. (2022)
FeO	Ceratonia siliqua L. aqueous extract	Spherical	Antibacterial activity	Aksu Demirezen et al. (2022)
FeO	Melia azedarach flower extract	231.43/spherical	Antimicrobial and antioxidant activities	Muzafar et al. (2022)
FeO	Agenaria Siceraria	30–100/cubic	Antimicrobial activity	Kanagasubbulakshmi and Kadirvelu (2017)
FeO	Aegle marmelos Extracts	–	Photocatalytic, antimicrobial and antifungal activity	Sriramulu et al. (2021)
FeO	Phyllanthus reticulatus leaf extract	185	Antimicrobial, phytotoxicity, and photodegradation of MB	Dharshini et al. (2021)

(*continued on next page*)

Table 2 (*continued*)

MeO NPs	Biologic Parts	Particles Size (nm) /Morphology	Applications	Refs.
TiO_2	Calotropis gigantea (CG) plant leaf extract	Non-uniform spherical and flowerlike shape/ 100	Supercapacitor	Reddy et al. (2021)
ZnO/rGO	Eclipta prostrata leaf extract	500	Supercapacitor	Kalaiarasi et al. (2021)
ZnO	Hyptis suaveolens leaf extract	10–200	Supercapacitor	Raja et al. (2019)
ZnO@PdO/Pd	E. cognata leaves extract	Spherical	Supercapacitor	Shaheen et al. (2021)
CuO	Amaranthus dubius leaf extract	Agglomerated shape	Glucose sensor and photodegradation of MB	Ansari et al. (2023)
Fe_3O_4	Artocarpus heterophyllus seeds extract	Spherical/34	Electrochemical sensor	Rajiv et al. (2022)
FeO	Orange-peel extract	–	Electrochemical sensor	Sieugaing Tamwa et al. (2023)
Fe_3O_4	Azadirachta indica (Neem Leaves) extract	20–40	Electrochemical sensor	Ijaz et al. (2022)
Ag-ZnO/rGO	Ceratophyllum demersum L. leaf extract	19.47	Photocatalytic degradation of RhB	Kadhem and Alshamsi (2023)
AC/ZnO	Pontiteria crassipes leaves extract	2.16	Adsorption of CR and MG	Allah and Alshamsi (2023)
ZnO/AC	Pontederia crassipes leaf extract	69.2	Photocatalytic degradation of CR	Hay Allah and Alshamsi (2023)

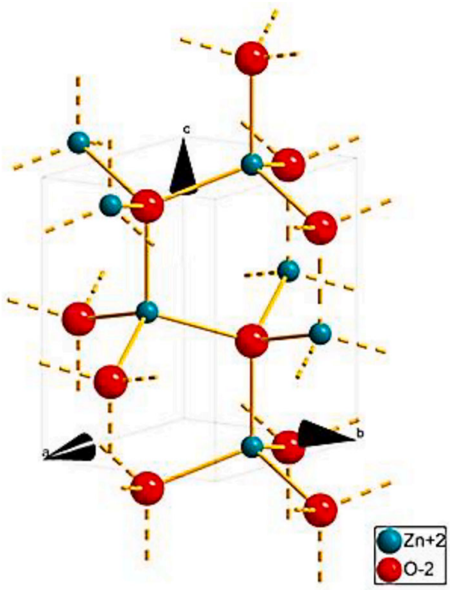

Fig. 24. Schematic of ZnO NPs crystal structure (Stefaniuk et al., 2018).

ZnO NPs were reported to have a particle size range of 20–24 nm and a distinguished crystalline wurtzite structure. At different concentrations of ZnO NPs, the growth of E. coli and S. aureus was noticed to be reduced, with the least inhibitory concentration values of ZnO NPs against E. coli and S. aureus were reported to be 92.07 $\pm$ 0.13 and 88.13 $\pm$ 0.35 μg/mL, at a concentration of 2 mg/mL (Mohammed et al., 2023). Mariposa Christia vespertilionis (MCV) leaf extract was used as a reducing and capping agent in the preparation of ZnO NPs calcinated at various temperatures of 700, 800 and 900 °C, and was explored as an anode in sodium-ion batteries (SIBs). The ZnO NPs prepared using the leaf extract and calcined at 700 °C were found to show a remarkable initial discharge capacity of 591 mAH/g and an improved rate capacity (Idris et al., 2023). Table 2 gives a summary of the bio-synthesis approach for ZnO NPs production and their different uses.

5.3. *Green synthesis of CuO NPs and their applications*

Cu is a primogenial metal utilized by humans, as it was initially used for water and wound sterilization in about 2000 BCE by the Egyptians (Naseem and Durrani, 2021). An uncommon earth metal with anti-ferromagnetic spin ordering is CuO. It is the most stable form of oxidized Cu which has increased consideration in current times owing to its p-type semiconductor nature (Kumbhakar et al., 2021). They have monoclinic crystal shapes [space group C2/c] with LPs (LPs) of 0.342, 0.468, and 0.513 nm, $\beta = 99.549°$ Different from other 3-D transition metal mono-oxides which have a cubic rock salt crystal shape with octahedral coordination. It is an exceptional mono-oxide with square two-dimensional coordination of the Cu atom to the adjoining O_2 atoms (Gangwar et al., 2016).

Among semiconductor materials, CuO is distinctive owing to its magnetic, optical, and electrical properties. They are utilized for different biotic and biocidal purposes. They also have wide use in the energy sector (storage and conversion), superconductors, biological purposes, and catalysts. They occur in two stoichiometries of oxides such as cuprous oxide (Cu_2O)-cubic structure and E_g of 2.0–2.5 eV and cupric oxide (CuO)-monoclinic structure and lower E_g of 1.3–1.7 eV. CuO NPs have been synthesized using different biomolecules from plants and microorganisms (Gebre, 2023).

It has the capacity to be applied in photoconductors, solar cells, gas sensors, catalysis, etc. (Kumbhakar et al., 2021). Fabricated biogenic CuO NPs are naturally benign with a variable size depending on the source of the plant (Annu and Ahmed, 2018). CuO NPs were produced using Parthenium hysterophorus plant extract as a capping, stabilizing, and reducing agent. Fig. 28a shows the schematic involved in the synthesis of CuO NPs using the plant extract. FTIR peaks at 3284, 1600, 1368, 1278, 1084, 820, 522, and 590 cm^{-1} were ascribed to CuO NPs, and the peak in the range of 3371–3212 cm^{-1} was attributed to the O—H group which was representative of phenol in the extract and also present in CuO NPs spectra (Fig. 28b). The produced NPs were found to be effective in the degradation of rifampicin antibiotics (Nzilu et al., 2023).

CuO NPs bio-fabricated using the Abutilon indicum (A. indicum) leaf extract, were assessed for their antibacterial activity against human pathogenic organisms of Gram-ve (E. coli and Salmonella typhi) and Gram+ve (Bacillus subtilis and Staphylococcus aureus (S. aureus)) bacteria and degradation of malachite green (MG) dye molecules. The bio-fabricated CuO NPs were found to show more capability antibacterial activity against the Gram+ve bacteria (Fig. 29a and d). The prepared CuO NPs also showed anticancer activity against human lung A549 and breast MDA-MB-231 cancer cell lines. The cells' sustainability was noticed to reduce gradually with an increasing concentration of CuO NPs. The bio-prepared CuO NPs were also found to effectively degrade MG dye molecules, with an efficient removal % of 78 % (Fig. 30a and b) (Sathiyavimal et al., 2022).

The green synthesis approach was employed to produce CuO NPs using water extract of papaya (Carica papaya L.) peel biowaste as reducing and stabilizing agents. The prepared CuO NPs were spherical particles with particle sizes ranging from 85 to 140 nm. The prepared CuO NPs were found to be effective in the degradation of palm oil mill

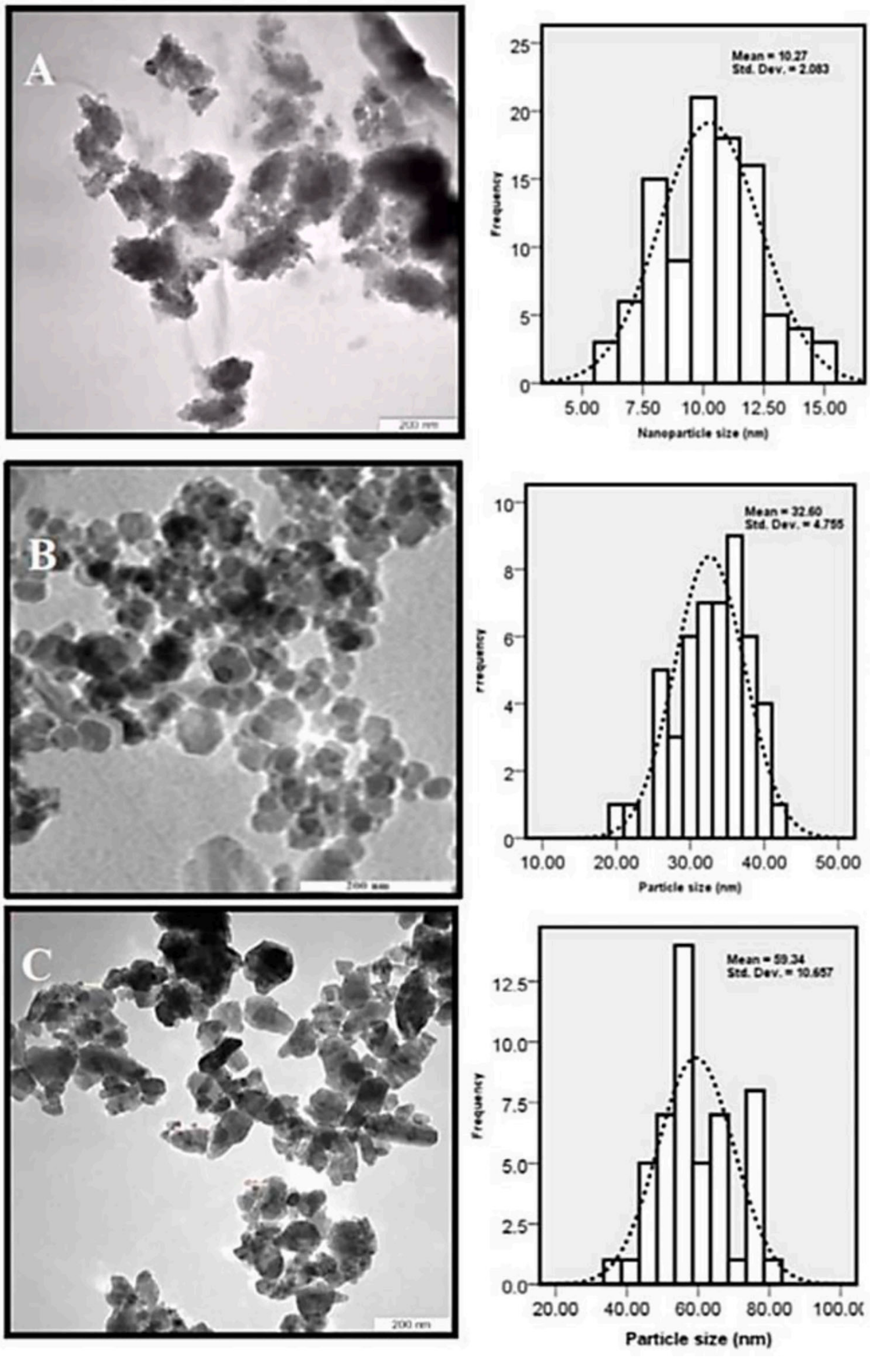

Fig. 25. TEM images of ZnO NPs at different incubation times (A) 12; (B) 24 and (C) 36 h (Boroumand Moghaddam et al., 2017).

effluent (POME) under ultraviolet light, with a 66 % degradation (Phang et al., 2021). Two plant pathogenic fungi (Botrytis cinerea and Alternaria alternata), which were isolated from plants were used for the bio-production of CuO NPs. The pathogenic fungus was found to bio-transform Cu salt into CuO NPs (Kovačec et al., 2017). In Alhalili's study (2022), Eucalyptus Globoulus extract was used as a reducing and stabilizing agent for the bio-production of CuO NPs. According to the XRD analysis, the crystalline size of the CuO NPs was determined to be 85.80 nm using the Debye Scherrer equation. According to SEM analysis, the average particle size of the spherical CuO NPs was 88 nm, which was comparable to the XRD result. The prepared CuO NPs were tested for the sorption of methyl orange dye (MO) and it was found to be effective in the biosorption of these dye molecules, with optimum removal noticed at pH 6.5. The biosorption process was best defined using the Langmuir (LNRM) and Pseudo-second-order models (PSOM). The determined sorption capacity was 95 mg/g. The main mechanism for CuO NPs bio-fabrication was attributed to phytochemicals presence (polyphenols) in the plant extract, which was responsible for the

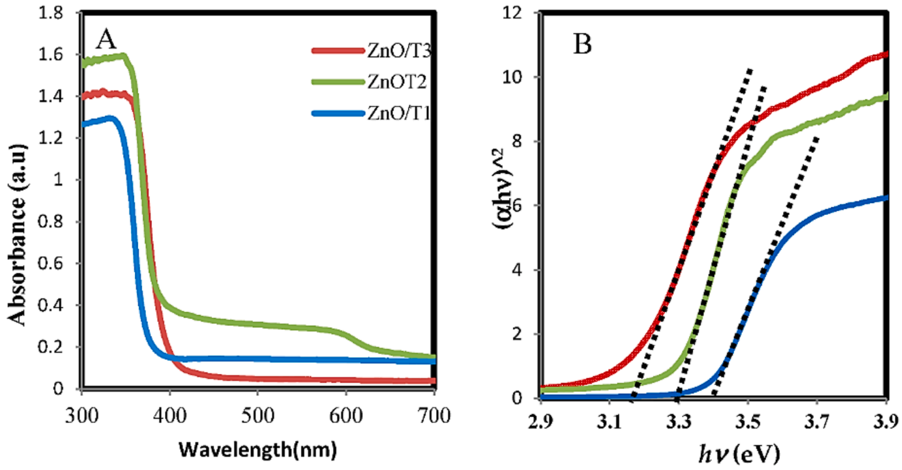

Fig. 26. (A) UV spectra plot for the produced ZnO NPs and (B) determined E_g(s) for ZnO NPs at various incubation times of 12–36 h. (Boroumand Moghaddam et al., 2017).

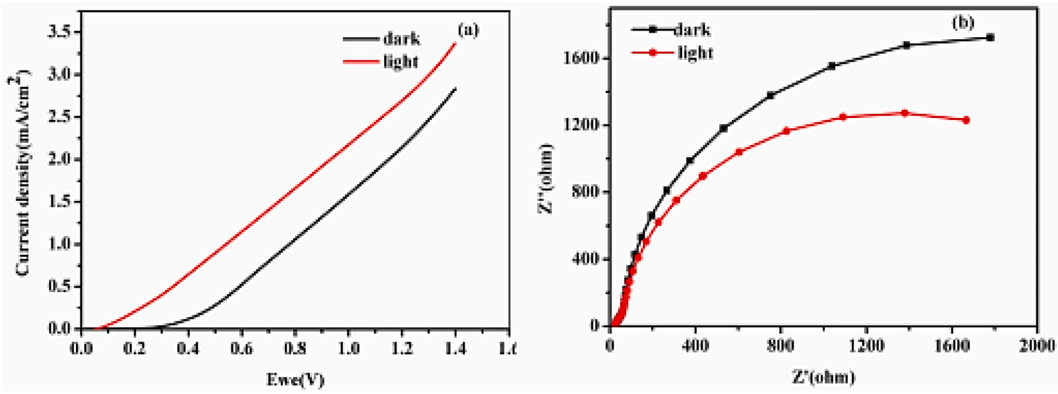

Fig. 27. Photoelectrochemical study of ZnO NP using (a) LSV curves and (b) EIS Nyquist plot (Ramanarayanan et al., 2018).

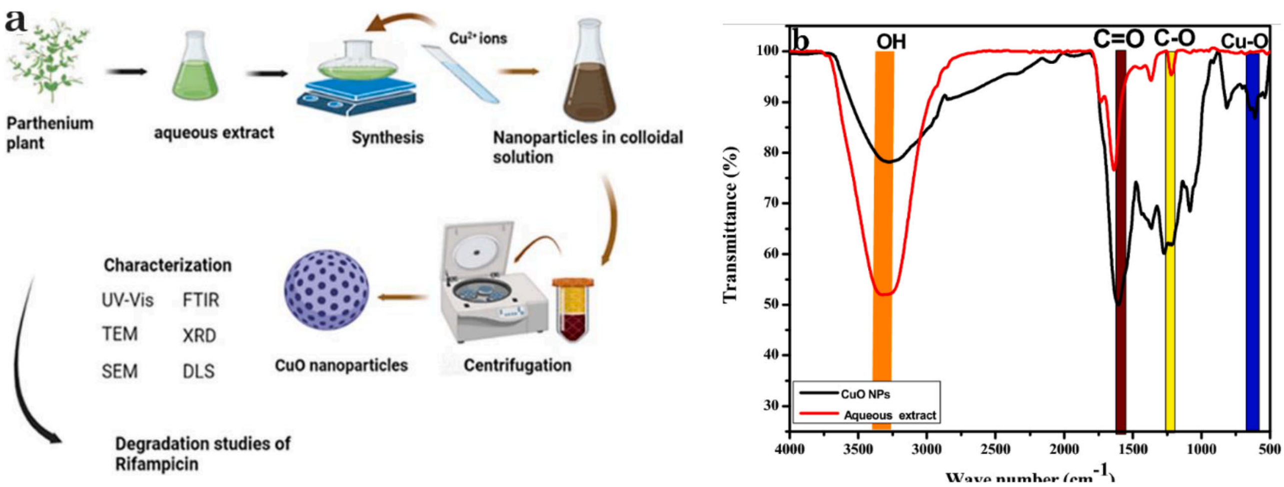

Fig. 28. (a) Schematic showing the production of CuO NPs from *Parthenium hysterophorus* extract and (b) IR spectra of produced CuO NPs (Nzilu et al., 2023).

bio-reduction and stabilization of the CuO NPs through the formation of metals complexes and subsequent reduction of the metal complexes to CuO seed particles. The CuO seed particles undergo aggregation, and this is followed by nucleation (Alhalili, 2022).

Aerva javanica leaf extract was used as a reducing and stabilizing agent in the bio-preparation of CuO NPs. The bio-produced CuO NPs had an average particle size of 15–23 nm and had a spherical morphology. The prepared CuO NPs were found to have antimicrobial potential against various bacterial and fungal pathogens. The minimum inhibitory (MIC) and bactericidal concentrations (MBC) of CuO NPs were reported to be 128 μg/mL. While the MIC of fungus and minimum fungicidal concentration (MFC) of CuO NPs were 160 µg/mL (Amin et al., 2021). Mint leaves and orange peel extracts were explored for the bio-synthesis of CuO NPs. The SEM images of bio-produced CuO NPs using both PEs

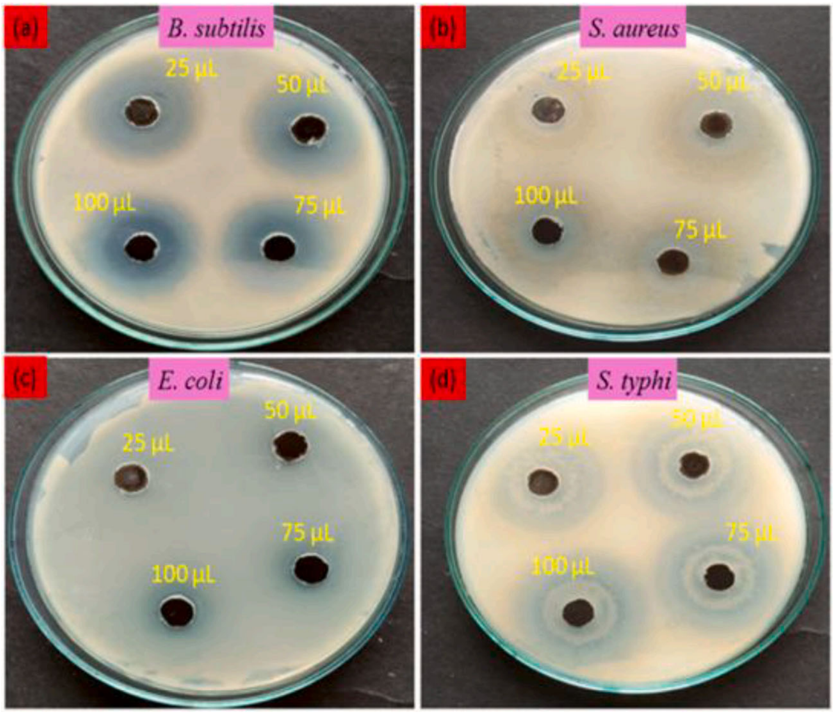

Fig. 29. Antibacterial activity against (a and b) Gram+ve bacteria and (c-d) Gram-ve bacteria using bio-produced CuO NPs (Sathiyavimal et al., 2022).

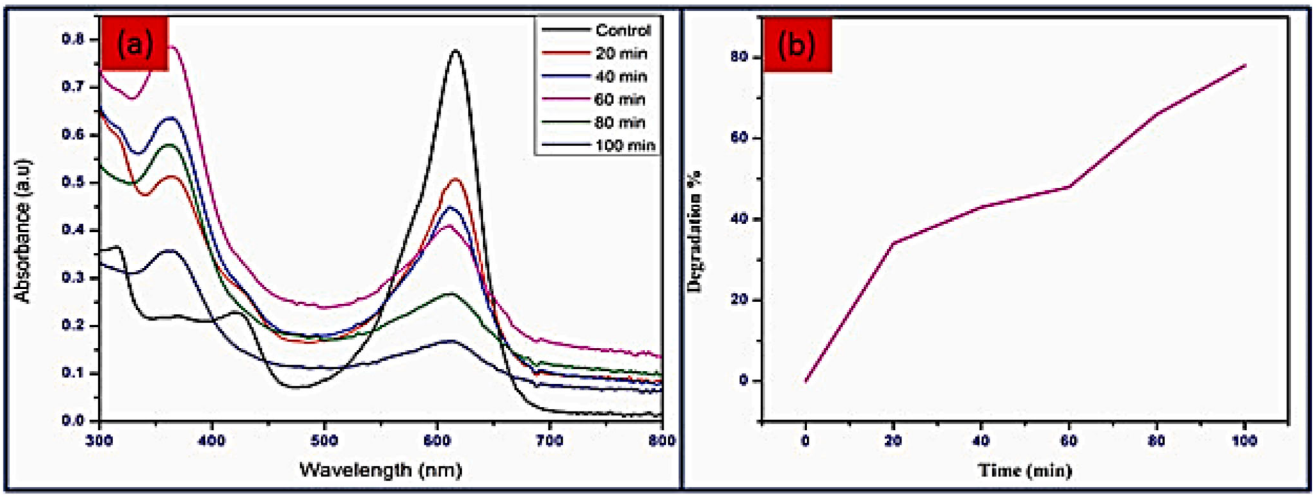

Fig. 30. (a) Photodegradation of MG dye using CuO NPs under sunlight irradiation and (b)% of degradation (Sathiyavimal et al., 2022).

show the spherical morphology of CuO NPs with an average particle size of 150 nm (Fig. 31). The optimum sorption capacities at pH 6 using CuO NPs for Pb(II), Ni(II), and Cd(II) ions were 88.8, 54.9, and 15.6 mg/g. The biosorption process was generally described by the Freundlich model (FRHM) and PSOM (Mahmoud et al., 2021).

CuO NPs were bio-synthesized employing Caesalpinia bonducella seed extract and assessed for electrocatalytic properties by carrying out electrochemical detection of riboflavin (vitamin B2 (VB_2)). The CuO NPs were integrated into graphite permeated electrode surface (CuO NP/PIG-modified electrode) and used as an electrochemical sensor for VB_2. A detected linear range of 3.13–56.3 nM with a limit of detection of 1.04 nM for VB_2 by the modified electrode. The electrode depicted excellent stability and reproductivity over 120 days (Fig. 32). The bio-produced CuO NPs were also observed to have high antibacterial activity against Gram+ve and Gram-ve bacteria (Fig. 33). The excellent activity of the NPs towards the bacteria was ascribed to ROS generation from CuO. The obtained inhibition zone that was measured is presented in Fig. 34, which is a mean ± standard deviation value of three parallel experiments. The VB_2 electrocatalytic redox reaction comprises of two protons that are linked with two electrons. The probable mechanism of VB2 reduction at the CuO NPs modified electrode (Fig. 35) (Sukumar et al., 2020).

Pumpkin seed extract was used to bio-synthesize CuO NPs and assessed for anticancer activity against the human colorectal cancer cell line (HCT-116) in this study. The bio-synthesized CuO NPs displayed 50 % repressive concentration at 25 µg/mL against the HCT-116 cell line. This led to significant cancer cells shrinking, detachment, membrane bleeding and shape distortion (Tabrez et al., 2022). Using Annona muricata L plant extract, CuO NPs were bio-synthesized and their anticancer effect was assessed. The spread of breast cancer cell lines (AMJ-13 and MCF-7) was reduced by the prepared CuO NPs. Minor colony creation by the cancer cells was also observed after sustained

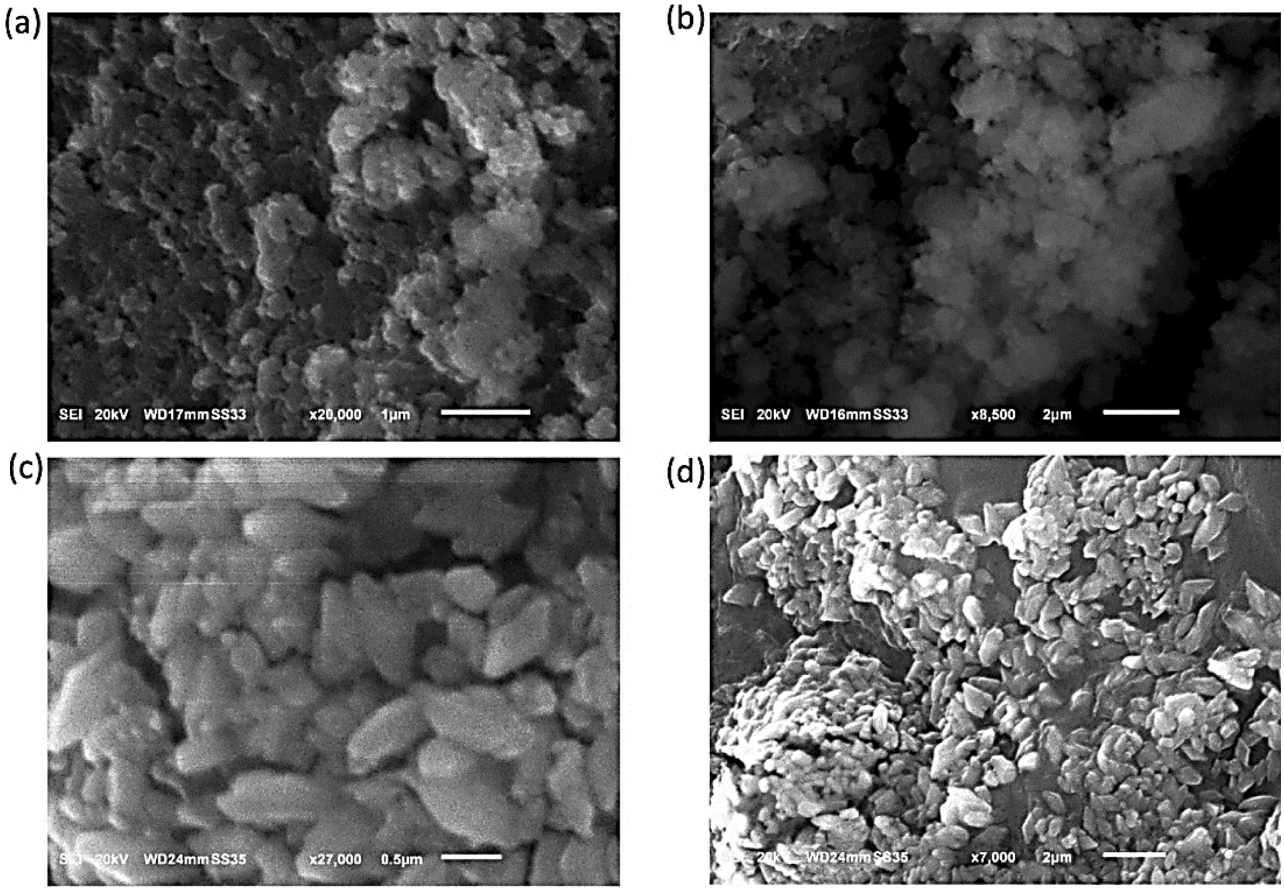

Fig. 31. (a–d) SEM micrograph of CuO NPs produced using mint leaves and orange peel extracts (Mahmoud et al., 2021).

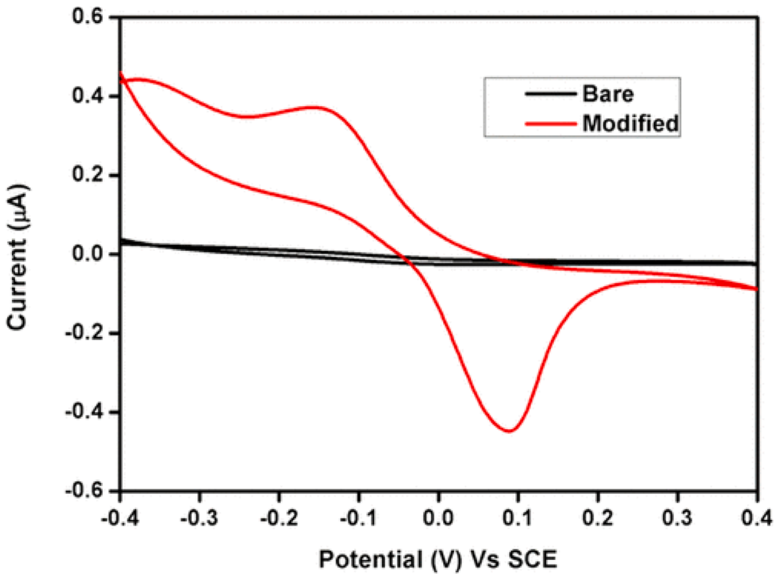

Fig. 32. Cyclic-voltammograms of plain and modified electrodes with 30 μM riboflavin (Sukumar et al., 2020).

exposure of the cancer cells to CuO NPs and this led to programmed cell death (Mahmood et al., 2022). Employing the green synthesis approach, CuO NPs were created using a water-soluble extract of Cystoseira myrica. The prepared CuO NPs were found to inhibit the growth of cancer lines like HepG2 and MCF-7. Cell viability was reported to reduce with increasing NPs concentration, with 100 μg/ml concentration of CuO NPs having the lowest percentage of cell viability in HepG2 and MCF-7 (18,7 % and 19.3 %) (Mohamed et al., 2021). Moringa stenopetala seed extract was employed as a reducing and stabilizing agent in the green synthesis of CuO NPs. The prepared CuO NPs were reported to have an average particle size of approximately 6.6 nm and were crystalline NPs according to the SEM and XRD analysis. From the UV analysis, the calculated E_g was determined to be 1.73 eV. The CuO NPs bio-synthesized using an extract of Moringa stenopetala seed were

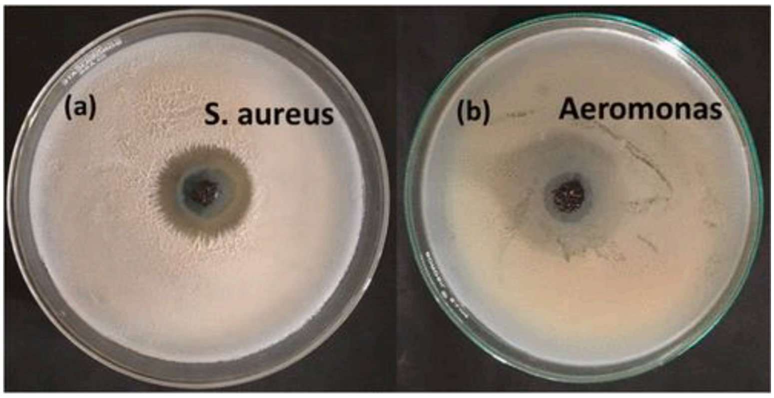

Fig. 33. Antibacterial activity of CuO NPs against (a) S. aureus and (b) Aeromonas (Sukumar et al., 2020).

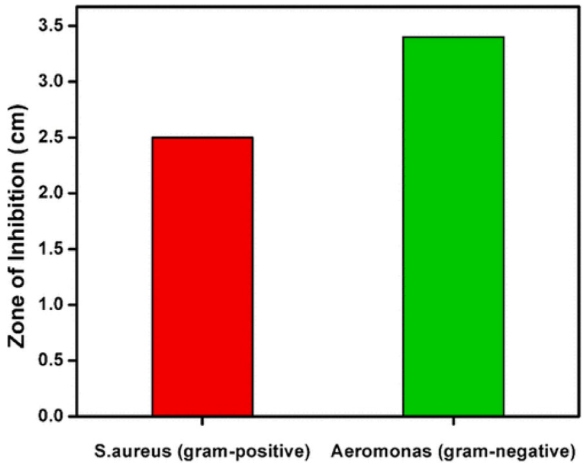

Fig. 34. CuO NPs zone of inhibition against S. aureus and Aeromonas (Sukumar et al., 2020).

reported to photodegrade 98.4 % and 95.4 % of congo red and Alizarin red S dyes at pH 5 and 4.5. The bio-prepared CuO NPs were reported to be reused or recycled for five cycles, which was indicative of the high stability of CuO NPs (Aaga and Anshebo, 2023). Table 2 gives a summary of the bio-synthesis of CuO NPs using the green approach and their different uses.

5.4. Green synthesis of CeO_2 NPs and their applications

CeO_2 NPs have generally been developed owing to their exceptional surface chemistry, biocompatibility, and great stability (Nadeem et al., 2020). Cerium (Ce) is a lanthanide metal class and in its oxide form, it has a fluorite structure. In bulk materials, CeO_2 can have two different forms of oxides, CeO^2 (Ce^{4+}) and Ce_2O_3 (Ce^{3+}). O defect concentration increases with a decrease in the size of the particle. Hence, CeO_2 NPs have enhanced redox features regarding their mass materials. While mixed valence state existence plays a critical part in foraging reactive O and nitrogen groups. In nano-scale form, the fluorite structure with oxygen (O) deficiencies is maintained by cerium oxide NPs (CeO_2). This gives CeO_2 with vacancies ($CeO^{2\text{-}x}$), thereby providing sites for reduction oxidation reactions. The catalytic performance of these NPs is determined by the surfaces of the fluorite structure arrangement. The (100), (110), and (111) are functional viable surfaces on CeO_2 nanocrystals as depicted in Fig. 36, which represent the lattice ions arrangement (Ce^{3+} and O^{2-}) in the fluorite structure. The (100) and (111) have the O terminal endings and the (111) layout displays the Ce center and the O ions. These characteristics facilitate the utilization of these NPs in carbon monoxide, hydrocarbon, and nitric species removal from the used gas. This feature is eased by Ce ability to occur in

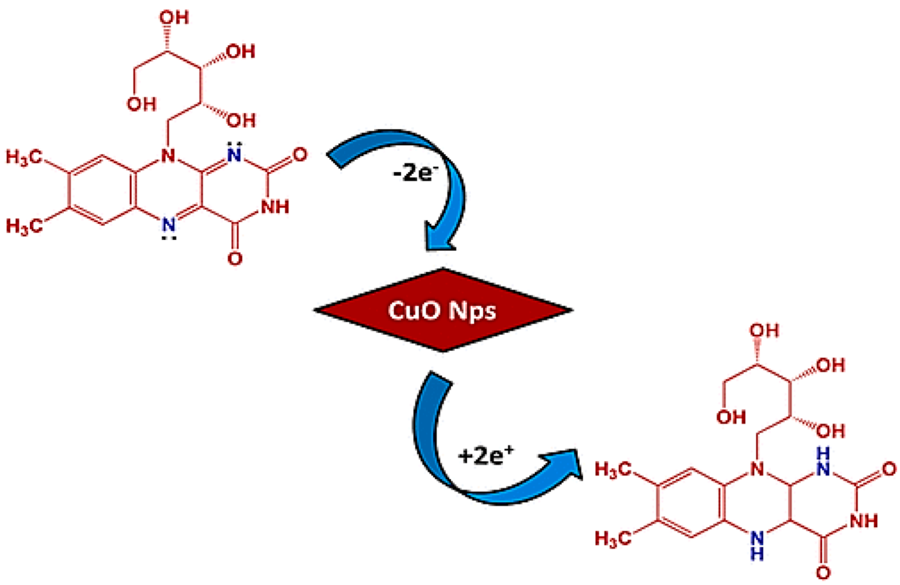

Fig. 35. The probable mechanism of VB_2 on the CuO NPs modified electrode (Sukumar et al., 2020).

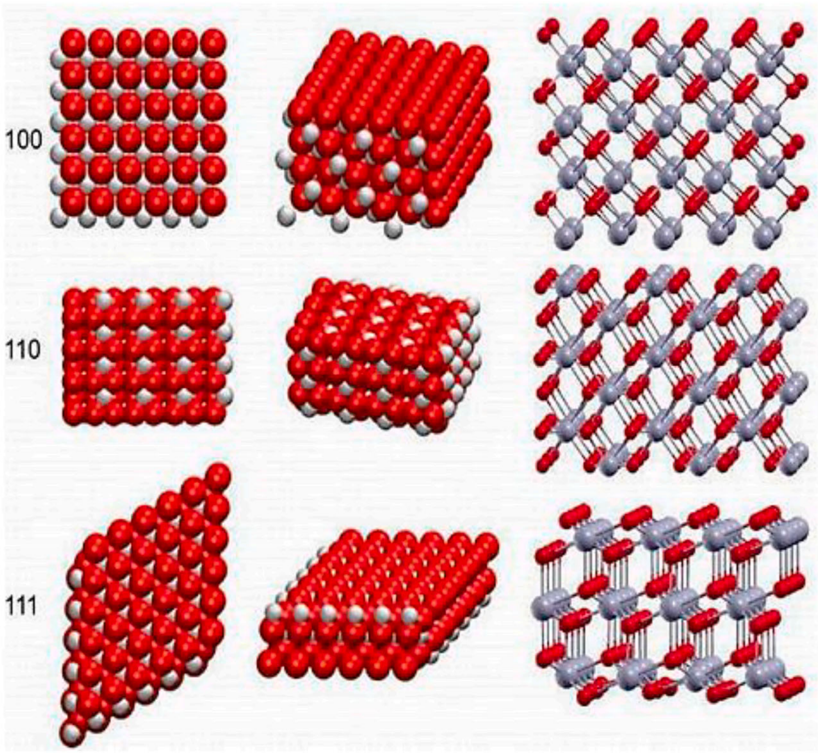

Fig. 36. Crystal lattice and surfaces (100, 110, and 111) of CeO_2 NPs (Nyoka et al., 2020).

tetravalent (Ce^{4+}) and trivalent (Ce^{3+}) phases (Nyoka et al., 2020; Charbgoo et al., 2017)

CeO_2 NPs' functional purpose in fuel cells, catalysts, and antioxidants in biologic systems has received great attention in NT (Charbgoo et al., 2017). They are also employed in sensor fabrication, therapeutic agents, drug delivery carriers, anti-parasitic ointments, catalysis, and cells (Nadeem et al., 2020).

This is an exceptional earth semiconductor oxide with a broad E_g of 3.0–3.2 eV and UV wavelength at about 370 nm. From room temperature to its melting point of 2700 °C, no crystallographic modification is observed for this material. These NPs have multi-enzymes namely oxidase, superoxide oxidase, catalase, and mimetic features, which have shown various biologic effectiveness like antioxidant activity towards almost all harmful intracellular ROS (Annu and Ahmed, 2018).

Preparing CeO_2 NPs via conventional techniques has various weaknesses such as noxious solvents and reagent usage, extreme pressure and temperature, and external additives such as stabilizing or capping agents' requirement during the reaction. The biological route is very important since NPs' physicochemical properties generally vary on the procedure of synthesis, and the NPs fabrication technique. Physical features like surface charge, aggregation status in coating and liquid, size, and residual contamination of the surfactant on the surface of the NPs generally affect nano-bio interface interactions (Charbgoo et al., 2017).

CeO_2 synthesis via the use of PEs, microbial and other biologic products has been reported, with plants being the most effective source owing to the large quantity, safe nature, and rich source of stabilizing and reducing agents. Different plant sources have been utilized for CeO_2 NPs synthesis owing to their rich source of metabolites/phytochemicals like phenols, ketones, ascorbic acid, and carboxylic acids for the stabilization and reduction of bulk metal salt. The reduction of the metal salt into NPs is confirmed by the color change from colorless to yellowish, whitish, or brownish. Microbial metabolites like enzymes, heterocyclic derivatives, and proteins play a crucial part in bulk salt of CeO_2 reduction and stabilization into respective NPs. CeO_2 synthesized using microbial shows enhanced stability, water dispensability, displays great fluorescent properties, and is less clustered (Nadeem et al., 2020).

Utilizing extracts of Artabotrys hexapetalus leaf CeO_2 NPs were fabricated via the green route. XRD diffraction pattern of the fabricated NPs showed a faced-centered cubic phase of CeO_2 NPs which corresponds to the JCPDS data file No 34-0394. The surface morphology of the NPs shows a mesh-like structure (Fig. 38a–c). The direct E_g of the NPs was estimated from the UV–Vis spectra to be 3.15 eV. The fabricated NPs were explored for antibacterial activity and the cytotoxic impacts of the NPs were noticed in the culture human breast cancer cell line (MCF-7) (Fig. 37a and c) (Parvathy et al., 2022).

While CeO_2 NPs were effectively synthesized using an extract of Origanum Majorana L. leaf. The prepared was explored as an antioxidant and cytotoxic impact of the NPs in human breast carcinoma cells (MDA-MB-231 cell line) and human umbilical endothelial cells (HUVEC) assessed in this study (Aseyd Nezhad et al., 2020). To enable the creation of CeO_2 NPs, Colocasia Esculenta leaf extract was utilized employing the sol-gel method. Fig. 38 shows the steps involved in the synthesis of the NPs and their use in mung bean seed germination. The CeO_2 NPs formation mechanism using the extract from the leaf is given by Eqs. (23)–(27) (Monica Ahmad and Hasan, 2023).

$$C_e(NO_3)_3.6H_2O \rightarrow Ce^{3+} + 3NO_3^- + 6H_2O \quad (23)$$

$$Ce^{3+} + H_2O \rightarrow C_e(OH)^{3+} + H^+ + e^- \quad (24)$$

$$Ce^{4+} + 4OH^- + xH_2O \rightarrow C_e(OH)_4.xH_2O \quad (25)$$

$$C_e(OH)_4.xH_2O \rightarrow C_e(OH)_4 + xH_2O \quad (26)$$

$$C_e(OH)_4 \rightarrow C_e2 \ + 2H_2O \quad (27)$$

While extracts of Dillenia indica aqueous fruit, Azadirachta indica leaf, and Origanum majorana L. leaf were found to be effective in the bio-synthesis of CeO_2 NPs, which were used for antioxidant, antibacterial, and anticancer purposes (Das et al., 2022; Manimaran, 2023; Aseyd Nezhad et al., 2020). Acorus calamus extract was used in the green production of CeO_2 NPs and explored for antibiofilm activity against

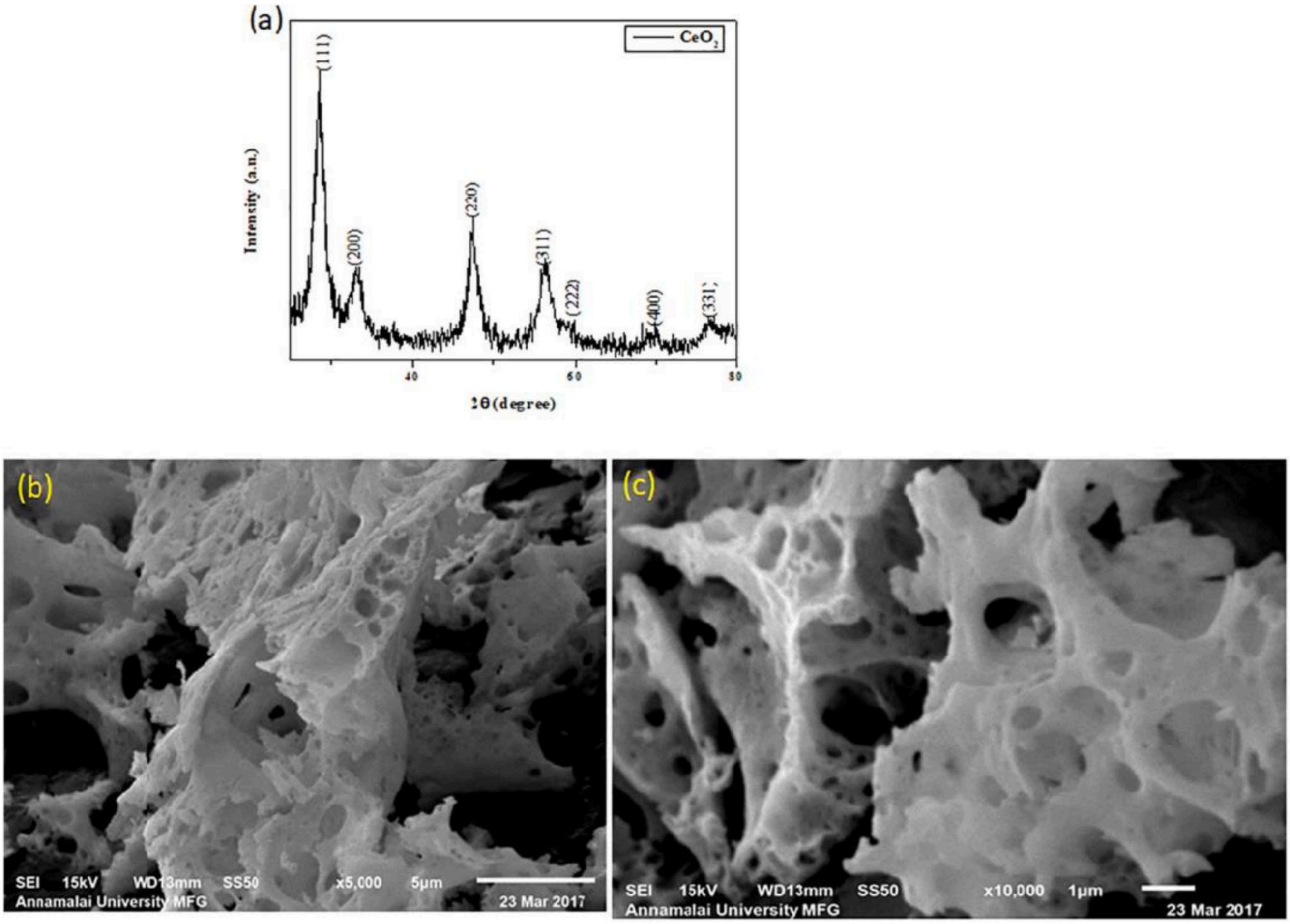

Fig. 37. (a) XRD pattern of prepared CeO_2 NPs and (b and c) SEM images of the CeO_2 NPs (Parvathy et al., 2022).

Gram+ve and Gram-ve bacteria. The produced CeO_2 average size was 22.03 nm. 75 % of the treated biofilm of the test bacteria was inhibited by the produced CeO_2 NPs (Altaf et al., 2021). CeO_2 NPs were prepared via the green synthesis route using bacterial cellulose matrix (BCX) in the aerogel and hydrogel forms. It was explored for antioxidant properties and found to reduce MDA levels in rat blood and increase the activities of antioxidant defence enzymes (Melnikova et al., 2023). CeO_2 NPs were bio-synthesized using egg white and tested for antibacterial properties in solid and liquid development medium against S. aureus and E. coli bacteria. The TEM image of the produced CeO_2 NPs shows single-phase NPs with a spherical shape and uniform size distribution of 5–7 nm. The characteristic peaks are insightful of the CeO_2 NPs with an E_g of 2.80 eV (Kumar et al., 2021). CeO_2 NPs were bio-fabricated using Kochiae Fructus PEs and assessed for anticancer activity against HeLa cancer cells in an MTT assay (two normal cell lines-3T3 and hMSC) and antibacterial and biofilm inhibition against Gram+ve and Gram-ve multi-drug resistant (MDR). The biofilm of the MDR bacteria was suppressed using the CeO_2 NPs. Substantial cytotoxic impacts were shown by the CeO_2 on the HeLa cancer cells (Lu et al., 2022). Aspergillus niger culture filtrate was explored in the bio-production of CeO_2 NPs. The morphology of the CeO_2 NPs showed cubic and spherical morphologies with a regular size distribution of 10 nm. While the CeO_2 NPs selected-area electron diffraction (SAED) patterns show ring pattern features of fluorite cubic structure (Fig. 39a–c). The CeO_2 NPs showed inhibition activities against Gram+ve bacteria (Streptococcus pneumoniae and Bacillus subtilis) (Gopinath et al., 2015).

Employing the green synthesis approach, CeO_2 NPs were created using the extract from part of Propopis farcta above ground as a reducing agent. The produced CeO_2 NPs were further calcinated at 300, 400 and 500 °C. Bio-synthesized CeO_2 NPs electronic spectra showed optimum absorbance at 312, 317 and 33 nm at calcination temperatures of 300, 400 and 500 °C (Fig. 40). The absorption peaks were ascribed to the intrinsic E_g that is confirmed via the electron transition from the valence band to the conduction band.

Based on the cytotoxic effect of CeO_2 NPs on the HT-29 cell line, it was reported that the treated cells did not show any substantial noxiousness in comparison to the control (Miri and Sarani, 2018). Table 2 gives a summary of the bio-synthesis of CeO_2 NPs using the green approach and their different uses

5.4.1. *Green synthesis of Al_2O_3 NPs and their applications*

Al_2O_3 NPs or alumina is the most utilized oxide porcelain material due to its superior features like crystalline and amorphous phases, considerable electronic E_g ($E_g \sim$ 8.8eV), remarkable sensitivity, and rapid response/regaining time humidity, outstanding dielectric features, high thermal, chemical, and mechanical stability; make it an outstanding material of performance. These NPs have various metastable structural phases like $\gamma-$ Al_2O_3, and $\eta - Al_2O_3$ (cubic-spinel shape), $\theta - Al_2O_3$ (monoclinic shape), k-Al_2O_3 (orthorhombic shape), $\delta - Al_2O_3$ (tetragonal shape), $\beta - Al_2O_3$ (hexagonal shape), $\alpha - Al_2O_3$ (corundum shape-a stable phase with the rhombohedral shape) and $\chi -$ Al_2O_3 (hexagonal or cubic shape). Unstructured Al_2O_3 generally consists of haphazard Al distribution (Al^{3+}) ions and vacancies over tetrahedral (AlO_4), octahedral (AlO_6), and polyhedral (AlO_5) sites. The unstructured Al_2O_3 NMs show bright bluish white emission, with a high sensitivity and swift response/recovery time to humidity and elevated thermal conductivity in their glycol-based fluid. Only Al^{3+} ions in the AlO_6 unit that gives the thermodynamically stable $\alpha - Al_2O_3$ crystal

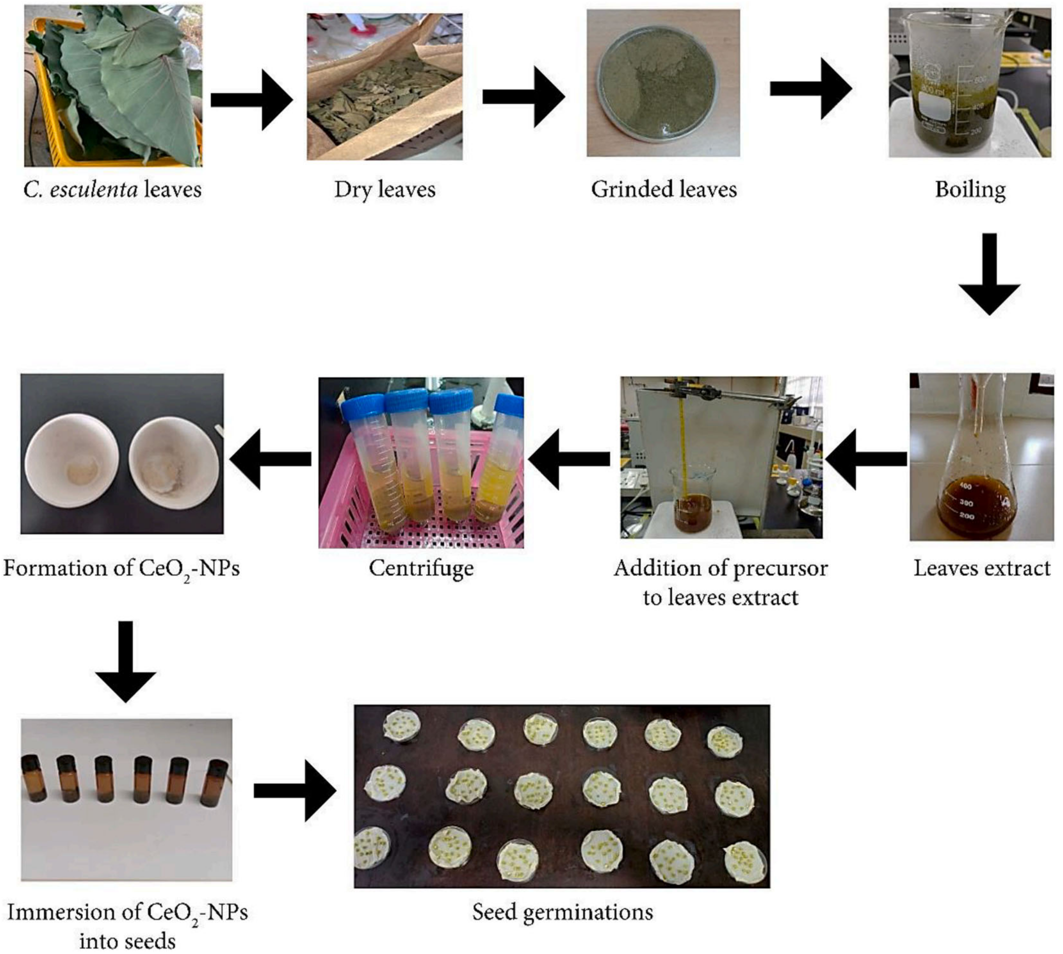

Fig. 38. Process of CeO_2 NPs synthesis and their application in mung bean seed germination (Monica Ahmad and Hasan, 2023).

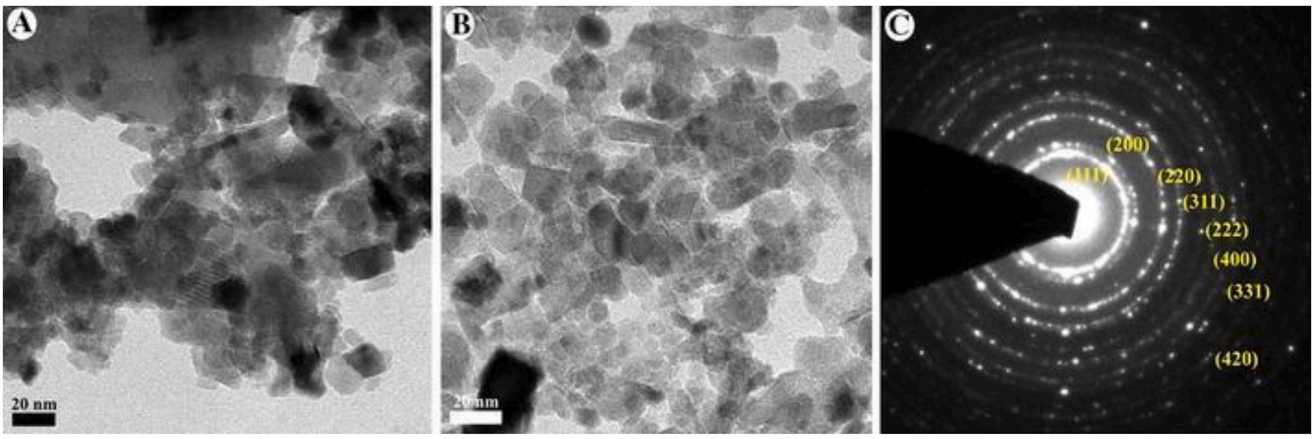

Fig. 39. (a and b) TEM images of CeO_2 NPs biosynthesize using Aspergillus niger culture filtrate and (c) SAED of CeO_2 NPs (Gopinath et al., 2015).

phase. Sensing, optical, thermal, and other performance of Al_2O_3 NMs rely on their crystal phase as well as the definite crystal facet shown by their structure (Gangwar et al., 2016).

These NPs are passive at ambient temperature and are intricate in all conventional chemical reagents. It shows exceptional wear resistance and enhance surface finish. Among the different allotropes of Al_2O_3 NPs, α- Al_2O_3 form is thermodynamically extremely stable. Owing to their stability, traditional techniques have been utilized for Al_2O_3 NPs synthesis. But most of these approaches are not sustainable and to accomplish a naturally benign, non-noxious, cost-efficient, and swift approach, phyto-mediated fabrication of Al_2O_3 NPs has been highlighted by nano-technologists. These NPs show favorable features like superior stability, catalytic, stiffness, insulation and surface protective coverings. As composite materials, they have tuneable mechanical features that are beneficial in the engineering sciences disciplines (Annu and Ahmed, 2018). According to the study by Gudkov et al. (2022), the key mechanism of recognition of the bacteriostatic impact on Al_2O_3 NPs production is the electrostatic interactions between the bacteria's

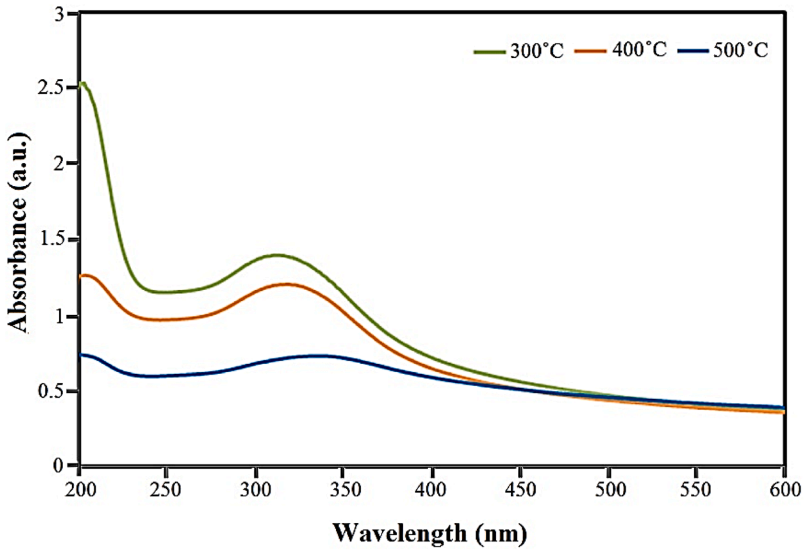

Fig. 40. UV–vis spectra of bio-synthesized CeO_2—NPs at various calcination temperatures of 300, 400 and 500 °C.

exterior membrane or cell wall and the NPs, which leads to the creation of Al cations that initiate the generation of ROS and oxidizing of bio-polymer (Gudkov et al., 2022).

Al_2O_3 NPs were bio-produced using Prunus × yedoensis leaf extract (PYLE) and the prepared NPs were assessed for the confiscation of nitrate and antibacterial activities. The creation of these NPs was via the MI reduction which was followed by nucleation as depicted in Fig. 41. According to SEM analysis, the particles had spherical and hexagonal shapes, and the size arrays were between 50 and 100 nm. Using Tauc plot relationships, the determined E_g was 3.1 eV at pH 7, which relates to the reflectance edge of 420 nm. Also, according to the BET result, the surface area of the NPs was 54.5 m^2/g. The bio-produced Al_2O_3 NPs were found to be highly efficient for nitrate confiscation at pH 7 under light irradiation (Fig. 42a and b). The antibacterial activity of the prepared Al_2O_3 NPs and the NPs was found to be very effective in inhibiting bacteria growth against Gram+ve S. aureus and Gram-ve E. coli (Fig. 43) (Manikandan et al., 2019).

Muntingia Calabura leaf extract was utilized in the bio-production of Al_2O_3 NPs. Al_2O_3 NPs were subsequently infused into sisal/banana and banana/coir to form a hybrid composite. Epoxy-based natural fiber composite was created using the compression moulding technique, with Al_2O_3 NPs added in weight (wt)% of 0, 1, 2, 3, and 4. The result from this study shows that the 3 wt% of Al_2O_3 NPs enhanced the tensile, and flexural properties of the hybrid fiber (Sumesh and Kanthavel, 2019). Exploring the extract of lemon, Al_2O_3 NPs were bio-produced in a 1.1 ratio under microwave irradiation of 600 W for 5 min. The prepared NPs were further stabilized using sodium citrate and the average size of the particles was 460 nm (Narayanan and Rakesh, 2018). Extracts of aerva lanta leaf and Terminalia chebula seeds were used in the bio-production of Al_2O_3 NPs as reducing agents. The produced NPs were spherically shaped, with a particle size of 50–70 nm (aerva lanta leaf extract) and 50–100 nm (Terminalia chebula seed extract). While the crystalline size according to the XRD result was 70 nm (Duraisamy, 2018). Leaf extracts of lemongrass were used as a reducing and stabilizing agent for the green production of Al_2O_3 NPs. It was further explored for its antibacterial activity against extended-spectrum β-lactamases and Metallo-β-lactamases clinical isolates of P. aeruginosa. According to the XRD analysis, the crystalline size was found to be 34.5 nm. The bio-prepared Al_2O_3 NPs were found to inhibit extended-spectrum β-lactamases and Metallo-β-lactamases clinical isolates of P. aeruginosa growth (Ansari et al., 2015). In the study of Haider et al. (2023), Al_2O_3, Cu-Al_2O_3, and Ni-Al_2O_3 were bio-synthesized using Hibiscus rosa-sinensis plant leaf extract. According to the XRD result, the crystalline sizes of Al_2O_3, Cu-Al_2O_3, and Ni-Al_2O_3 were 12.44, 34.61, and 31.63 nm. The optical E_g of Al_2O_3, Cu-Al_2O_3, and Ni-Al_2O_3 was calculated as 3.8, 3.2 and 3.65 eV. A cathodic peak (E_{pc}) was observed at 0.48 V with an anodic counterpart (E_{pa}) at 0.49 V ($E_{1/2}$ = 1.75 V) according to the cyclic voltammogram (Fig. 44) (Haider et al., 2023).

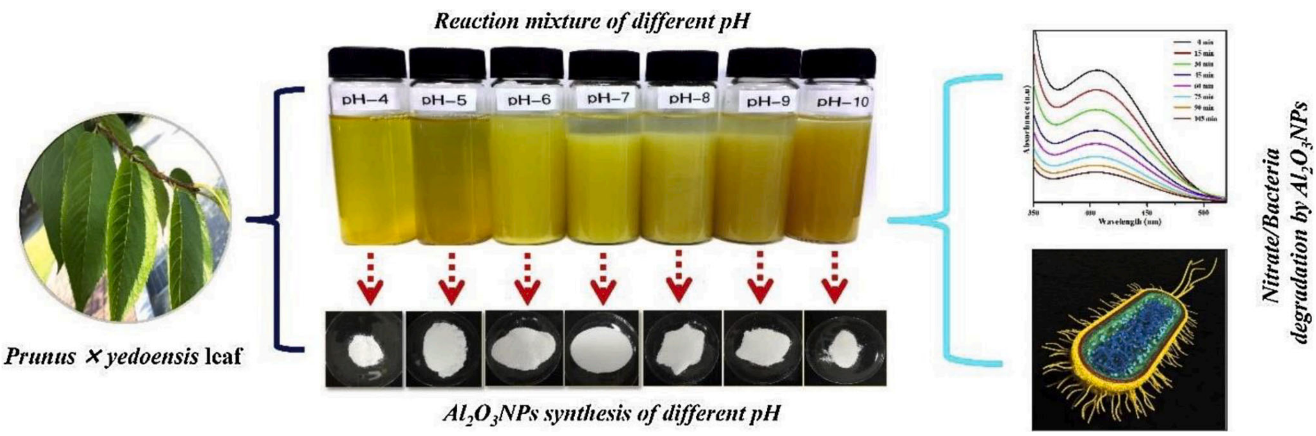

Fig. 41. Schematic of Al_2O_3 NPs bio-synthesis and its uses (Manikandan et al., 2019).

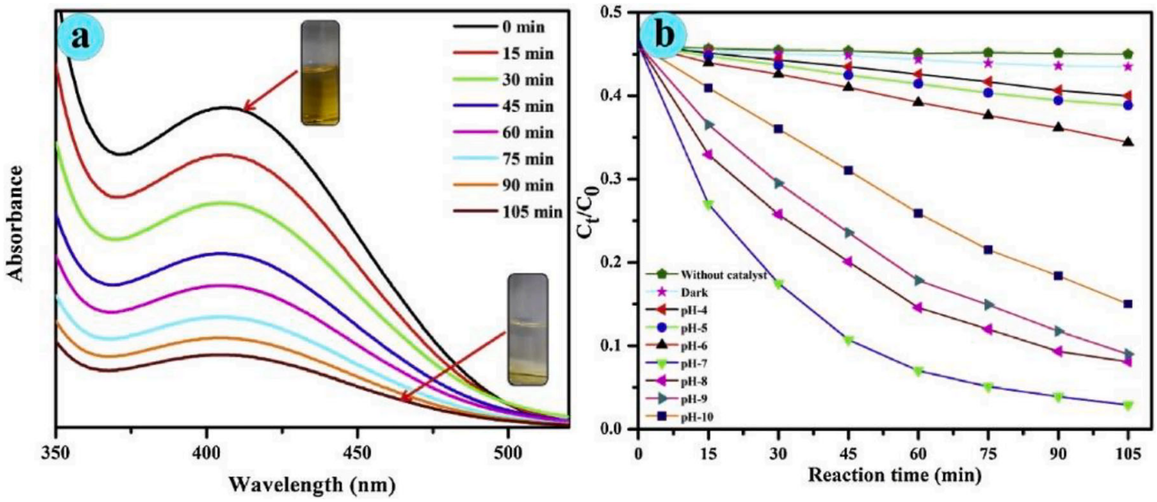

Fig. 42. (a) Absorption spectra of nitrate solution at pH 7 and varying time of interactions and (b) impact of nitrate molecules confiscated without, dark and pH 4–10 of Al_2O_3 NPs (Manikandan et al., 2019).

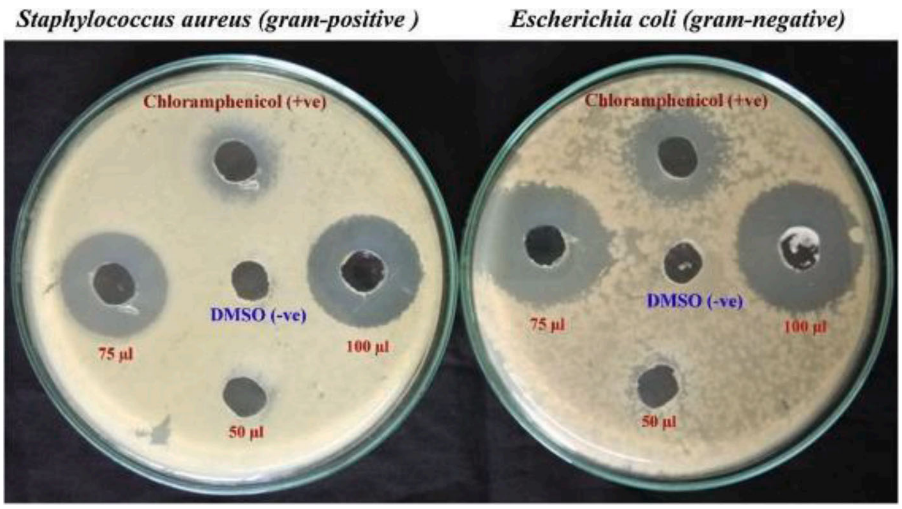

Fig. 43. The inhibition zone was tested at pH 7 using Al_2O_3 NPs against Gram+ve S. aureus and Gram-ve E. coli bacteria (Manikandan et al., 2019).

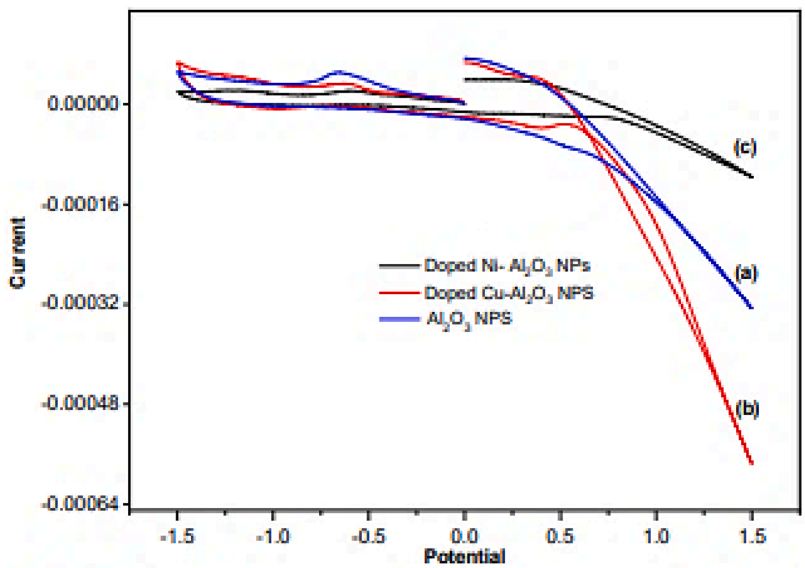

Fig. 44. Cyclic voltammogram of (a) Al_2O_3, (b) Cu-Al_2O_3, and (c) Ni-Al_2O_3 using a scan rate of 2 V/s (Haider et al., 2023).

5.4.2. Green synthesis of FeO NPs and their applications

FeO is a transition MeO that occurs in 16 states of FeO and oxyhydroxide polymorphs (Aigbe et al., 2023). The three forms of FeO NPs are magnetite (Fe_3O_4), Wustite or iron (II) oxide (FeO), and hematite or iron (III) oxide (Fe_2O_3), where each of them has its peculiar constructive functionality (Jeevanandam et al., 2022). Fe_2O_3 has four polymorphs which are α-, β-, γ- and ε-Fe_2O_3. α-Fe_2O_3 is a rhombohedral system that is employed as a basic material for magnetic resources, as a cathode for lithium-ion batteries, and as a color pigment in art. While γ-Fe_2O_3 has a spinel structure and is employed for magnetic storage material owing to their ferro-magnetic properties. ε-Fe_2O_3 is isostructural with $AlFeO_3$ and $GaFeO_3$ and potential use as magnetic materials. β-Fe_2O_3 has a bixbyite $(Fe, Mn)_2O_3$ structure form and shows anti-ferromagnetism with a 119 K Neel temperature (T_N). This oxide is less known among the polymorphs owing to it being an intermediary meta-stable form in the α-Fe_2O_3 evolution (Danno et al., 2013). Every polymorph depicts exceptional physicochemical characteristics that are practical for broader uses (Arularasu et al., 2018). As shown in Fig. 45, the FeO phase and the corresponding proportion of Fe^{2+} to Fe^{3+}, the FeO phase diagram can be separated into six segment sectors from right to left (Gareev, 2023).

Fe_3O_4 NPs a magnetic FeO, which has a cubic inverse spinel form. There is a widespread study and applications of Fe_3O_4 NPs owing to the transfer of electrons between Fe^{2+} and Fe^{3+} in the octahedral sites resulting in their exclusive magnetic and electrical properties and their low noxiousness. Fe_3O_4 NPs are recognized as superparamagnetic FeO NPs. They have been applied in bio-medical fields like cellular treatment, delivery of drugs, magnetic resonance imaging (MRI), hyperthermia, magnetofection, and tissue repair. The co-precipitation approach has been employed widely to produce FeO NPs. They have also found uses in sensors, catalysis, magnetic storage, wastewater treatment, ferrofluids, and the separation process owing to the extraordinary surface area, exclusive magnetic properties, bio-compatibility, and extraordinary chemical stability (Varghese et al., 2020; Jeevanandam et al., 2022). Apart from the traditional chemical route used for their synthesis, there is an extending development in the production of FeO NPs using the green synthesis route (Alabdallah et al., 2021; Aigbe et al., 2023).

An advancement in the production of Fe NMs like Fe and FeO NPs, by an easier, environmentally friendly procedure is a step further. Due to the stabilizing and capping effects of bio-molecules on various biological materials, particularly plants, green-produced NPs regularly show lower

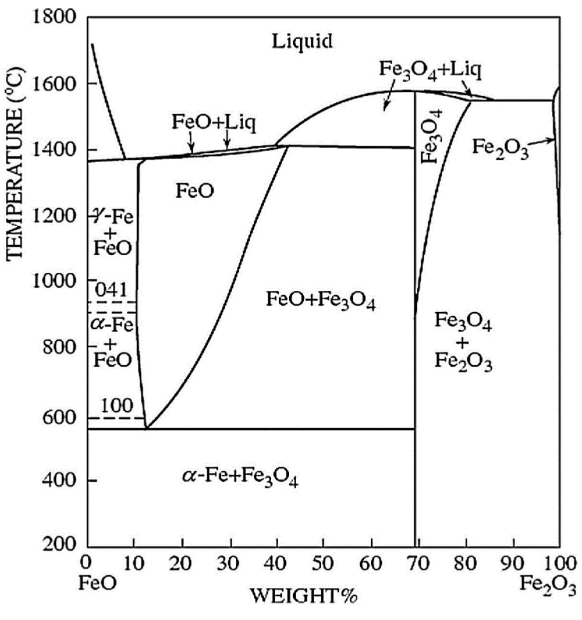

Fig. 45. FeO phase graph (Gareev, 2023).

noxiousness and aggregation with heightened stability. As opposed to bacteria, PEs are more repeatedly employed to make NPs since they take less time. Researchers have recently concentrated on PEs from various plant species, plant bio-mass that forestalls the aggregation and oxidation of FeO NPs, and synthesis by bio template due to the requirement to advance eco-friendly, affordable, and effective treatment solutions (Selvaraj et al., 2022). FeO NPs have outstanding chemical, optical, magnetic and electronic surface features like biocompatibility, low noxiousness, surface-to-volume ratio, superparamagnetic properties, exceptional electrocatalytic activity and suitable adsorption affinity, hence their application in sensor fabrication, antimicrobial agents, environmental remediation, food and agriculture, health care, energy, defence and aerospace technology, construction, textiles, automotive and electronics (Shetti et al., 2020; Attia et al., 2022).

FeO NPs (α-Fe_2O_3) were produced via the green synthesis route from hexahydrate ferric chloride ($FeCl_3{\cdot}6H_2O$) using papaya (Carica papaya) leaf extract as a reducing and stabilizing agent. The schematic for the steps and mechanism of α-Fe_2O_3 production is shown in Fig. 46(a and b) (Bhuiyan et al., 2020).

While α-Fe_2O_3 NPs were produced via the green route using an extract from the Hibiscus *rosa sinensis* flower plant. The produced NPs were found to be formed of an aggregate of spherical and mono-dispersed grains with an average size of particles of 51 nm according to TEM analysis (Fig. 47). The average crystalline size of the poly-crystalline NPs according to the XRD calculation was 36.4 nm (Buarki et al., 2022).

Fe_3O_4 NPs were also produced via the green route using Hibiscus rosa-sinensis extract and Ficus carica leaf extract as fortificants in wheat biscuits and antioxidants. The produced particles using Hibiscus rosa-sinensis extract and Ficus carica leaf extract were reported to have an average particle size of 65 nm and 43–57 nm according to SEM analysis (Razack et al., 2020; Üstün et al., 2022). Fe_3O_4 NPs produced using clove and green coffee (g-coffee) extracts through the green approach were explored for the adsorption of cadmium (II) (Cd^{2+}) and nickel (II) (Ni^{2+}) ions. The SEM images and the EDX reports (Fig. 48) show that the produced Fe_3O_4 NPs using the g-coffee extract show a pyramidal shape structure. The elemental composition of the NPs consists of the objective elements C, O, and Fe species with notable distinctions in Fe distribution in the produced NPs. The optimal sorption capacity for Cd^{2+} and Ni^{2+} were 78.0 and 74 mg/g and 64.8 and 80.0 mg/g using clove and g-coffee extracts in Fe_3O_4 production. The adsorption process of both HMs was defined by the pseudo-second order and Baudu and Fritz-Schlunder models. A broad spectrum of antibacterial activity was shown by the NPs against a Gram+ve (S. aureus) (25,932) than Gram-ve (E. coli) (25, 913) bacteria by the NPs created with the assistance of clover extract than g-coffee extract. The mechanism of antibacterial action of the extract of clove (Fig. 49) was influenced by the integrity of the bacteria cell, cell membrane destruction, nucleic acids, and protein release can affect bacteria growth, foil the reproduction of bacteria as well as antibacterial and sterilizing impacts. Fe_3O_4 NPs' antibacterial action may have been triggered by the instinctive release of free radicals such as ROS (Mohamed et al., 2023).

Extract of Graptophyllum pictum leaf (GPLE) was used in the bio-production of Fe_3O_4 NPs. Alkaloids from the leaf extract hydroxylated Fe^{2+} to create Fe_3O_4 NPs. The addition of the leaf extract to MSs resulted in a color change from pale yellow to dark brown. The prepared Fe_3O_4 NPs have a crystalline size of 23.17 nm according to the XRD result. The assessed E_g from the prepared Fe_3O_4 NPs was extrapolated to the x-axis and determined to be 1.56 eV (Sari and Yulizar, 2017). Water-soluble PEs were utilized to make extremely stable, biocompatible, and environmentally friendly MeO NPs in this study. FeO NPs were created using aqueous Ageratum conyzoides extracts, and their photocatalytic and antibacterial activities were evaluated. The extracts' GCMS– profile showed the occurrence of secondary metabolites, which were then calculated to determine the extracts' total phenolic and flavonoid contents. When compared to the antibiotic ciprofloxacin, the particles of

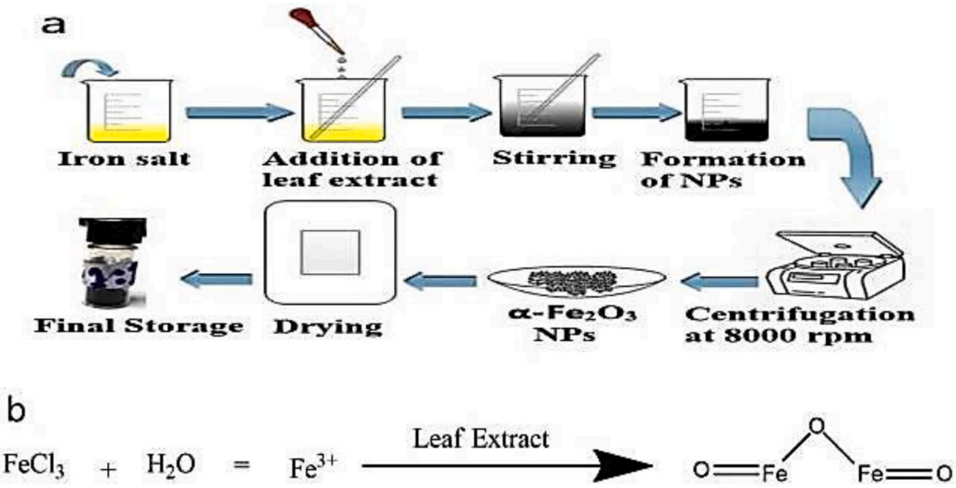

Fig. 46. Schematic of the (a) steps and (b) mechanism of α-Fe_2O_3 production (Bhuiyan et al., 2020).

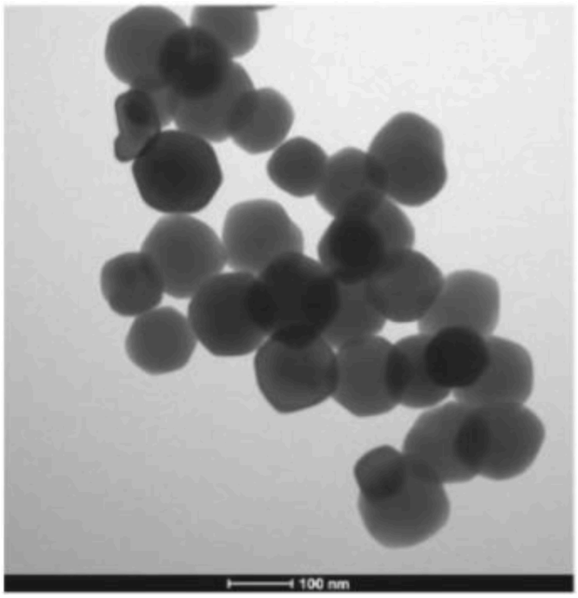

Fig. 47. TEM image of Fe_3O_4 NPs produced using extract of Hibiscus *rosa sinensis* flower plant (Buarki et al., 2022).

FeO NPs generated reasonable activity against the chosen microorganisms, according to the XRD data. With a 92 % effectiveness, the particles were able to photo-catalytically degrade MB molecules as depicted by Fig. 50. The findings of this work support the possibility that Ageratum conyzoides can play a significant role in the bio-reduction of Fe ions to FeO NPs, which have a modest antimicrobial action and can function as a photocatalyst to degrade dye molecules (Madivoli et al., 2019).

The use of bio-materials in the fabrication of NPs is a useful strategy in green NT. In this study, an easy and biologically acceptable process to create FeO NPs in the α -Fe_2O_3 phase via an aqueous extract of Laurus nobilis L. leaves. The findings demonstrated that the NPs, which have an average size of 8.03 nm, are crystalline, nearly spherical-like, and somewhat hexagonal according to the TEM result. Three bacteria and two fungi were used as test subjects for the bio-produced NPs' antibacterial properties. According to this study's findings, Listeria monocytogenes, a Gram+ve bacterium, and the fungus Aspergillus flavus and Penicillium spinulosum are all susceptible to the NPs' modest effectiveness. The environmentally friendly approach used to create these NPs has the prospective to make compounds that are antifungal and antibacterial, as well as gas sensors, light photo-catalysis, and semiconductors (Jamzad and Kamari Bidkorpeh, 2020).

Leaf extracts from Ficus carica (Fica) and Euphorbia amygdaloides (Euphorbia) were employed in the synthesis of γ-Fe_2O_3 NPs and used as a gas sensor for methane gas. Improved response, selectivity and short response time to methane gas were presented by the γ-Fe_2O_3 NPs synthesized using the extract of Fica leaf than the Euphorbia leaf extract. The resistance owing to grain boundaries was found to substantially contribute to the characteristics of sensing methane gas (Karaduman et al., 2017). The green production of FeO NPs was carried out using water-soluble spinach extract. The outcomes confirmed that the bio-prepared Fe_3O_4 NPs had a spherical structure. Following the spermine (SM) covering of the Fe_3O_4 NPs, the surface charge increased from -3.2 to 18.42 mV. The findings confirmed that during drought stress, antioxidant enzyme and secondary metabolite levels significantly improved. Furthermore, by enhancing the activity of respective antioxidant enzymes and secondary metabolites, the use of SM-coated Fe_3O_4 NPs can be effective in improving plant resilience to drought stress. An agarose gel electrophoresis assay was exploited to prove that Fe_3O_4-SM can reduce the effect of the negative charge of DNA and defend it from DNaseI and ultrasonic vibrations (Afrouz et al., 2023). The goal of this study was to assess the effectiveness of microalgal products containing FeO NPs (Fe_3O_4 NPs) as a promoter of plant growth and antifungal agents. Utilizing a 0.1 M of ferric/ferrous chloride solution (2:1 ratio; 65 °C) and a water-soluble extract of the green microalga Chlorella K01 was used in the bio-reduction MIs into Fe_3O_4 NPs. SEM and TEM were both utilized to examine the morphology of Fe_3O_4 NPs (Fig. 51). SEM images show that the bio-synthesis of Fe_3O_4 NPs in a mono-dispersed form, which is spherical and well separated, was a result of the outstanding capping capacity of the bio-molecules in the extracts of Chlorella K01 (Fig. 51a and b). The average particle size and morphology of the produced NPs were revealed by TEM check in the 50–100 nm range (Fig. 51c and d) (Win et al., 2021).

The rice, maize, mustard, green grams, and watermelons' germination and vigor indexes were significantly improved by the synthesized microalgal Fe_3O_4 NPs. Additionally, Fe_3O_4 NPs showed antifungal action against Fusarium oxysporum, Fusarium tricinctum, Fusarium maniliforme, Rhizoctonia solani, and Phythium sp. (Fig. 52) (Win et al., 2021).

$\gamma - Fe_2O_3$ NPs were bio-synthesized using ethyl acetate extract of fungus Chaetomium cupreum as a reducing agent. The prepared NPs potential against the human breast cancer cell line was assessed and significant inhibition of the cancer cell was reported at elevated concentrations in this study (Wani et al., 2020). A summary of FeO NPs bio-synthesized using the green approach and their various applications

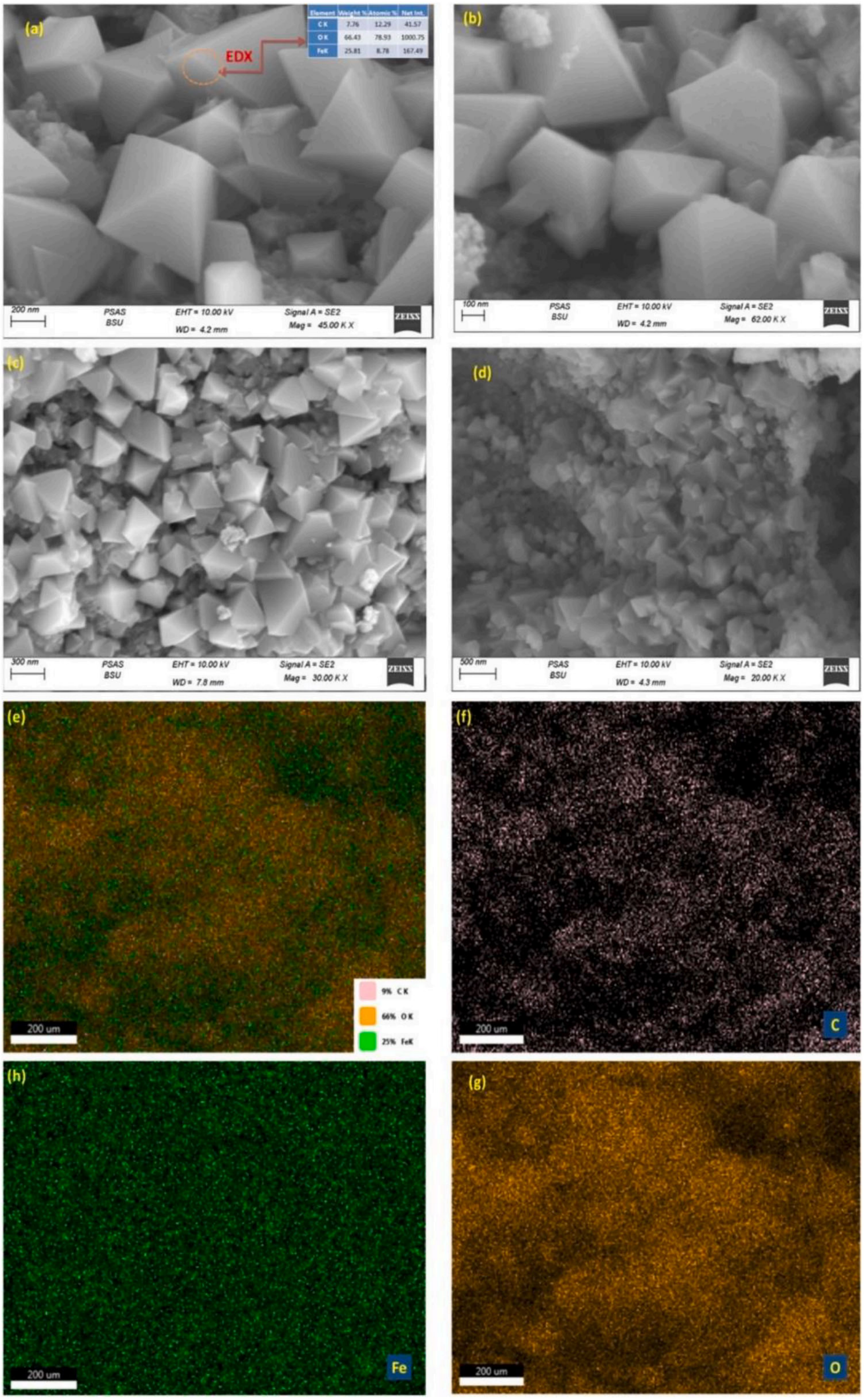

Fig. 48. (a–d) SEM images and (e-g) EDX of the produced Fe_3O_4 NPs using g-coffee extract (Mohamed et al., 2023).

is given in Table 2.

6. NPs noxiousness

Along with their existing and mounting uses, concerns about the unintentional health and ecological impacts of nanoscale materials have escalated. Valuable risk assessment considerations for engineered NMs include exposure assessment, noxiousness, extrapolation, biologic and ecological destiny, transportation, prolonged existence, transition, and general survival (Kurhade et al., 2021).

NPs can have -ve impacts on organ, tissue, cellular, sub-cellular, and protein stages because of their unusual physicochemical characteristics, such as their nanoscale, enormous surface area percentage, elemental composition, electronic properties, crystal structure, reactivity and

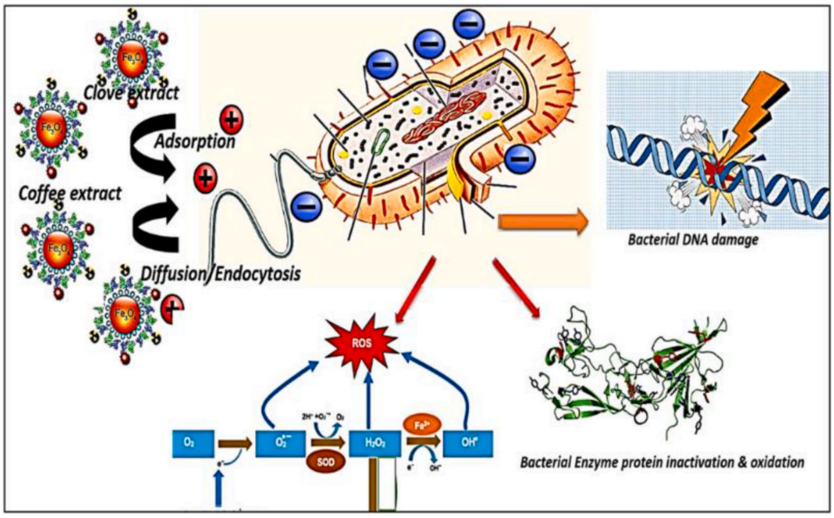

Fig. 49. Mechanism of antibacterial action of Fe_3O_4 NPs using clove and g-coffee extracts (Mohamed et al., 2023).

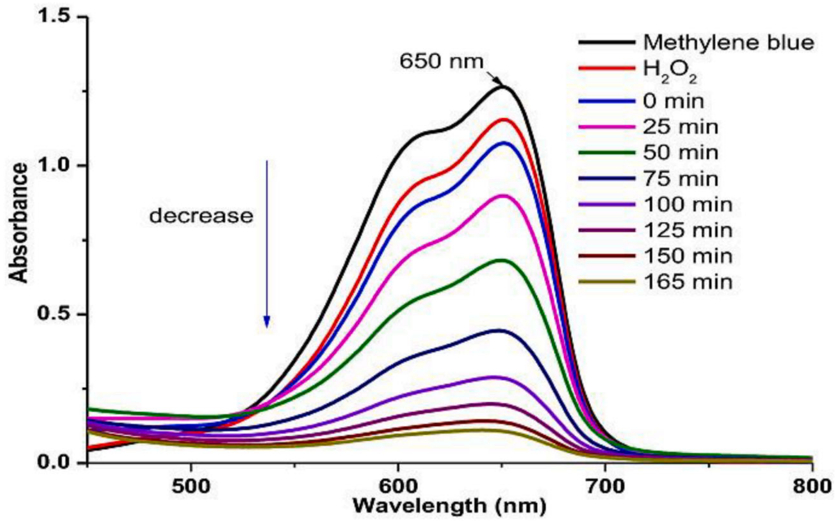

Fig. 50. Degradation of MB using bio-produced FeO NPs using Ageratum conyzoides extracts (Madivoli et al., 2019).

functional-groups, structure, inorganic or organic coverings, solubility, and aggregation actions. MeO NPs have received heaps of attention due to their massive use in medicine, the automobile industry, industry, and the military. Contrarily, it has been demonstrated that these MeO NPs are extremely unsafe, although a similar element is relatively benign in its bulk state (Kurhade et al., 2021).

Occupational and consumer contact with NPs is a risk given their growing production. Several research on exposure in the workplace has been initiated. Physical workplace assessments or estimates based on laboratory simulations are the two major procedures that can be utilized to produce realistic exposure approximations. The problem of background particles is considerable in both circumstances. Exposure to NMs can hypothetically take place at many phases of the life cycle of man-made NPs, including synthesis, handling of nanopowder handling, ready-to-use nano-product dispersion (such as spraying), and fracture and finishing product abrasion (Karlsson et al., 2022).

The design and modification of MeO NPs can be done through a diversity of surface functionalities, which improves their potential functions in bio-technology, drug and gene delivery, magnetic separation, and imaging. Nevertheless, despite their valuable properties, metallic NPs have the prospective to have -ve impacts if they encounter live biologic tissues and systems. Awkwardly, there are several routes for involuntary and unprompted NP entrance into the body, including via the air we inhale, the water we drink, foods, clothing, medications, and cosmetics. The three leading entrance approaches are through ingestion via the digestive tract, transudation via the skin, and breathing through the respiratory tract. Hence, it is fundamental to research the noxiousness-related issues of NMs as their release into the body environment appears expected and they may have some unexpected -ve impacts. If we consider their capability to enter different live tissues at the nanoscale and their prospective for interaction with correspondingly sized organs, such as those in the liver, raises the urgency of this topic (Attarilar et al., 2020).

Assessing NP noxiousness is characteristically done to address the danger and risk of NP exposure. In-vitro or *in-vivo* tests can be used to determine the noxiousness of a certain NP. For the noxiousness screening of NPs, *in-vitro* noxiousness approaches are regularly utilized since they are less expensive, take less time, and raise fewer ethical probes. These procedures allow for the assessment of the acute noxiousness of NPs towards different cell lines utilizing a variability of procedures and assays (Gakis et al., 2023). Nonetheless, since *in-vivo* methods assess absorption, distribution, metabolism, and excretion (ADME), which are fundamental for deciding how toxicants affect humans, animals, and other living things, they are the most reliable.

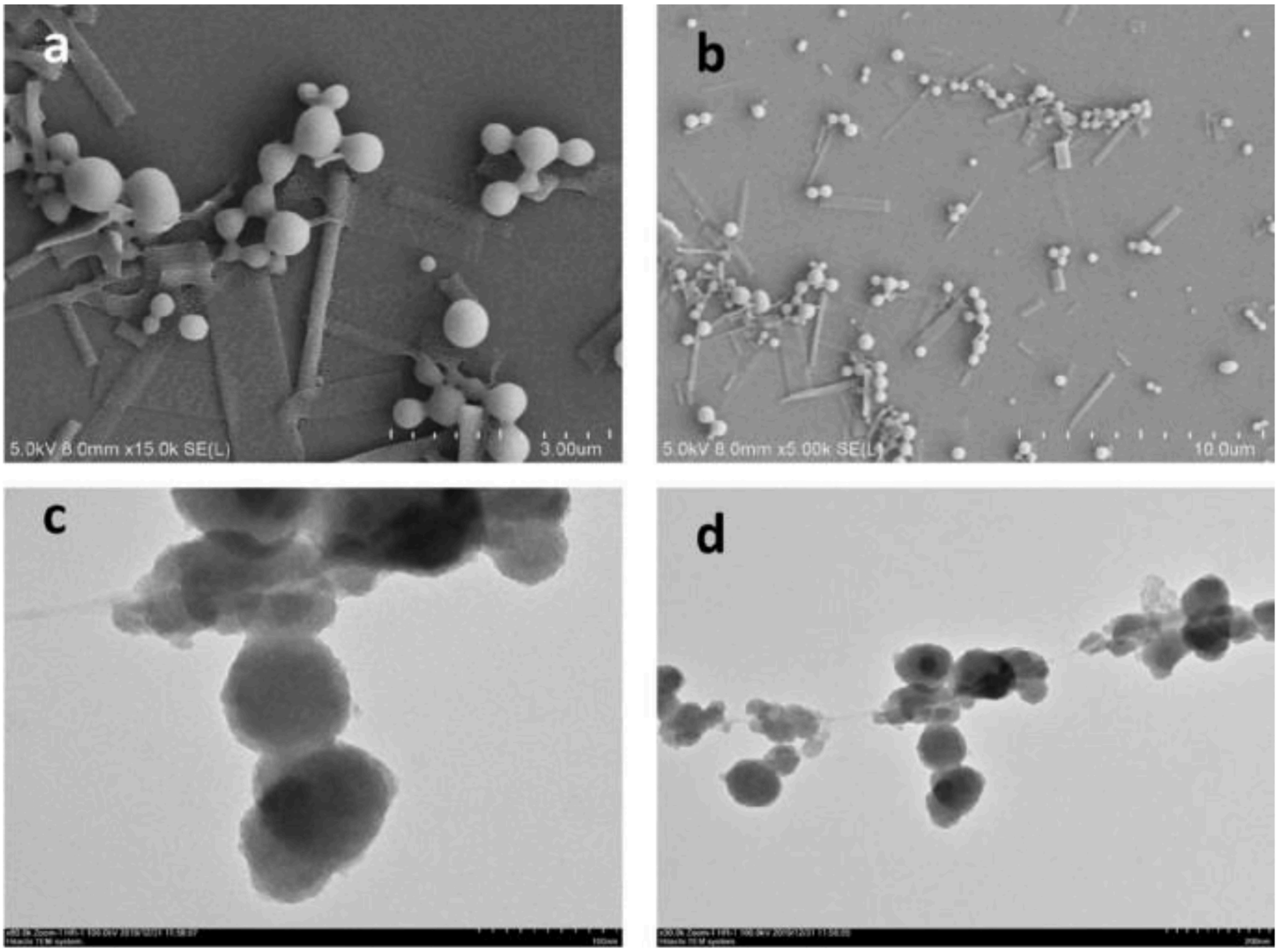

Fig. 51. (a and b) SEM images of Fe_3O_4 NPs and (c and d) TEM micrograph of Fe_3O_4 NPs (Win et al., 2021).

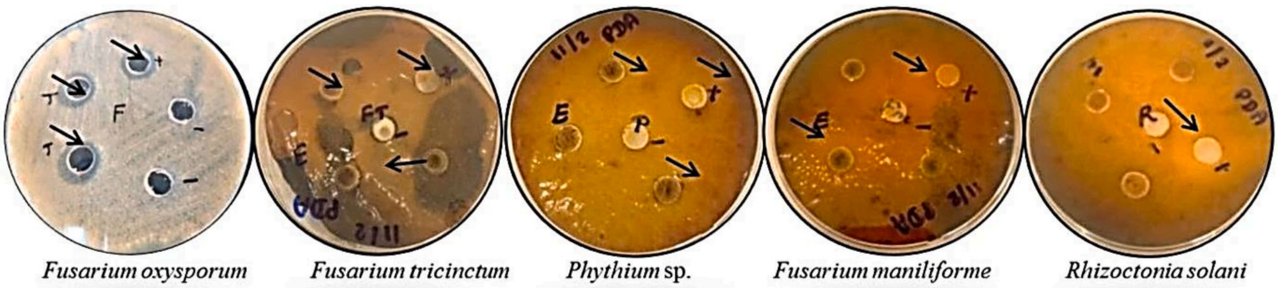

Fig. 52. Antifungal action of Fe_3O_4 NPs against Fusarium oxysporum, Fusarium tricinctum, Phythium sp. Fusarium maniliforme, and Rhizoctonia solani (Win et al., 2021).

However, *in-vivo* assessments are high-priced, take more time, and involve ethical issues with animal research. To decide the NP concentrations at which harmful effects show, dose-response analyzes are regularly conducted first *in-vitro* experiments before moving on to controlled *in-vivo* exposure tests. In any case, in comparison to the innovation and time-to-market of NMs, the noxiousness evaluation of a huge number of NPs, under a wide range of concentrations, towards numerous cell lines and creatures, is remarkably labor-exhaustive and experimentally challenging (Gakis et al., 2023).

However, regarding the NPs, the concentration, composition, size, charge, and other physicochemical factors are taken into consideration for material selection and their prospective use. Unfortunately, there have not yet been any widespread and comprehensive standard protocols for the cytotoxicity of different materials (Attarilar et al., 2020). Physicochemical features of related NPs influence the capability of NPs to enter specific organs via unique pathways and their tendency to collect in cell organelles or be reassigned to other organelles. Furthermore, as they can change the mechanism of the toxicologic response as well as the accumulation, absorption, and translocation of NPs, their physicochemical properties have a substantial influence on their noxiousness. For illustration, identical material with various sizes and shapes can substantially alter the reaction of live tissue and disclose whether NPs will have a safe or threatening consequence. The mass of NPs, precise chemical composition, concentration or dose of NPs, surface charge, hydrophilicity, solubility, and geometrical properties are amongst the sizeable physicochemical qualities related to the cytotoxicity of NMs. These attributes can also influence material behavior (Attarilar et al., 2020).

The surface area and size of the NPs also play a significant function in their interaction with live tissues. The NPs nanometric size level is nearly in the same array as protein globules ranging from 2 to 10 nm, DNA helix approximately 2 nm, and cell membrane thickness with 10 nm, so they can pass the walls of cells and enter cell organelles (Attarilar et al., 2020). Particularly for the cellular absorption of NPs, size matters. Furthermore, existing research suggests that the more hazardous impacts NPs have, the higher the intracellular dose at which they are present (Karlsson et al., 2022).

Furthermore, the size of the NPs can change the interactions between the transport and cellular defence systems, which in turn influences the NP kinetics concentration and distribution. It is pondered that sizeable NPs enter the cells by phagocytosis and other probable transport modes, whereas the trivial NPs are characteristically able to overcome cell entrance walls and can translocate across cell membranes. The *in-vivo* tests proved that the immune system can quickly identify big NPs and block their entry into the body. Successful adsorption of NPs on surfaces is necessary to decrease their cytotoxicity, with the surface area being one of the key factors (Attarilar et al., 2020).

Particle shape, as well as size, are important (Karlsson et al., 2022). The forms and geometries of NPs, such as cubes, spheres, ellipses, cylinders, sheets, spikes, and rods, have a substantial influence on their noxiousness. In this connection, NPs with fiber and tube geometry are less vulnerable to endocytosis than NPs with a spherical shape. Furthermore, it was revealed that plate- and needle-shaped NPs cause greater necrosis proportions than other spherical and rod-shaped NPs since they are better able to physically harm cells and live tissues when they come into touch with them (Attarilar et al., 2020).

Ionic charges can extensively impact noxiousness-associated routes by affecting how NPs interact with cells. Zeta (ζ) potential, which is identified as the difference in potential between the mobile dispersion medium and the stationary layer of the dispersion medium that is attached to the dispersed particle, can be utilized to explain the surface charge of NPs as shown in Fig. 53 (Attarilar et al., 2020).

The MeO NPs that enter the cell serve as a source of MIs and can distribute them nonstop into the surrounding cytoplasm. The pace at which the NPs dissolve defines how rapidly MIs are distributed. Despite having a low dissolving rate, some MIs can behave in a way that is exceptionally harmful in biologic mediums. It is assumed that NPs have elevated solubility than their mass counterpart. This finding can be true only for NPs in the unique size specification (less than 100 nm size), thus particles with sizes greater than 100 nm fail to improve their saturation solubility in the low solubility compounds, even if the dissolution rate is enhanced (Zhang et al., 2022).

NPs uptake is extensively influenced by surface charge. The general net -ve charge of cellular surfaces is mostly the rationale for why +ve-charged NPs are integrated by cells more quickly than -ve-charged ones. +ve charged NPs in general have heightened noxiousness due to their enhanced cellular absorption (Karlsson et al., 2022). ζ potential can be exploited to verify the consistency of particle dispersion. NPs with a zeta potential value higher than 130 mV or lower than 230 mV are improbable to aggregate, while NPs with lower zeta potential values are more likely to stick together, leading to either aggregation. The variance surface charge controls the cellular absorption and positively charged NPs show extreme noxiousness values than negatively charged NPs. +ve charged particles are more lethal (Attarilar et al., 2020).

NPs cause more cell damage in part owing to their robust electrostatic interactions with -ve charged cellular membranes, which increases their uptake by cells. This occurrence can be described by the higher +ve charge of NPs causing compelling electrostatic interactions with cells. The greater the NPs' electrostatic interactions with cells, the longer the endocytic uptake process of NPs into cells. and stronger the electrostatic contact between NPs and cells (Zhang et al., 2022; Manuja et al., 2021).

Due to their inherited chemical properties, different MeO NPs and their compounds, in particular oxides, show diverse harmful mechanisms and demonstrate different toxic effects. Cytotoxicity, genotoxicity, formation of ROS, oxidative stress and inflammation, regulation of cell signaling, apoptosis, cancer, etc. are a few examples of the typical activities of nano-noxiousness as shown in Fig. 54. When NPs are internalized, they activate the cellular process within membrane-based receptors, which causes the formation of ROS and oxidative stress. This occurs when it physically or chemically interacts with mitochondria, changing the way the oxidation of the phosphorylation membrane system after internalization. The level of NP concentration and its functionalization change this action (Manuja et al., 2021).

To avoid the unsafe impact of NPs, the NPs' morphology, size, concentration, charge, aggregation mode and surface features noxiousness must be considered. It is well known that MeO NPs' noxiousness is associated directly with their surface attributes, thus, NPs surface modification is an adequate idea for abating their potentially unsafe impacts. In this interest, different safe surface designs applied are doping-based approaches, coating of the surface, core-shell structures, geometric control, surface passivation approaches, and the utilization of metal-organic framework (MOF) and artificial intelligence-based computational methods (Attarilar et al., 2020; Manuja et al., 2021).

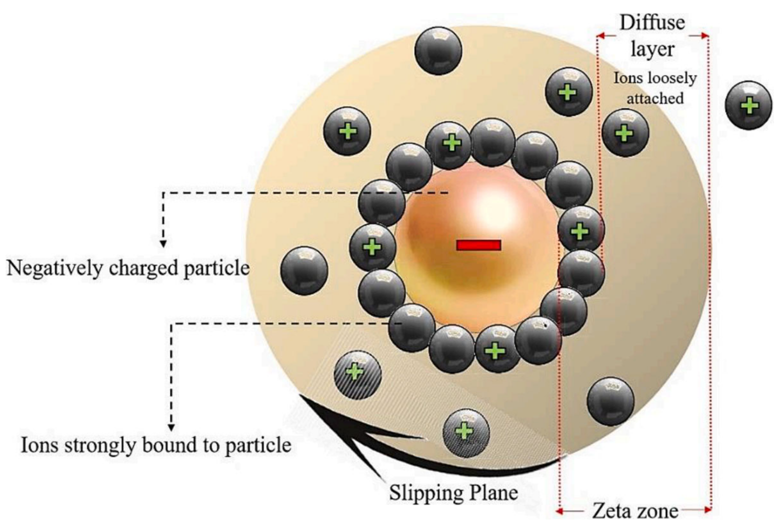

Fig. 53. Graphic illustration of the ζ potential zone and the electric double layer surrounding the charged NPs (Attarilar et al., 2020).

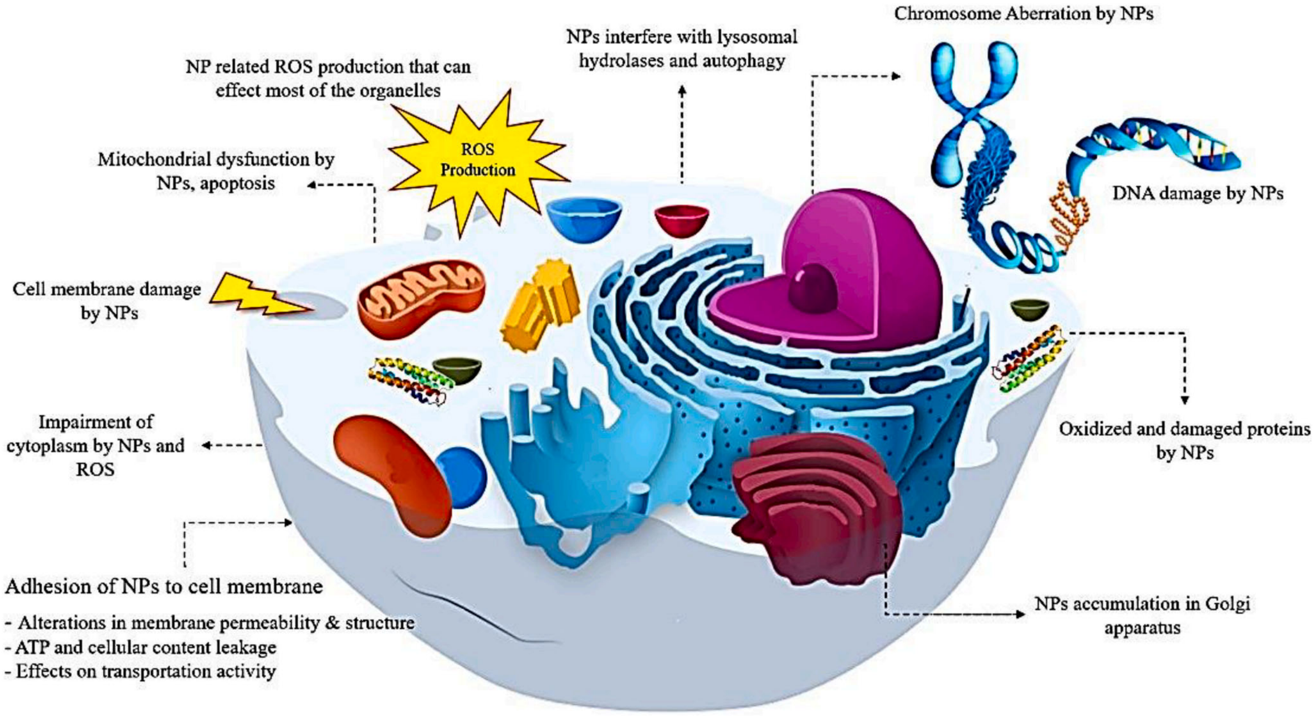

Fig. 54. NPs noxiousness mechanism (Attarilar et al., 2020).

7. Conclusion

The production of engineered NMs symbolizes a critical advancement in NT and material science, which involves the development of products further than the laboratory. The commercialization of successful unsettling technologies is necessary for various functioning of human and inclusive development, but significant relevance is a must for potential health assessment and environmental impacts of these materials. In recent years, the green or bio-production of MeO NPs has been an extensive research area owing to their eco-friendly approach. MeO is reckoned as a multipurpose material that has successfully been used in various environmental, medical, optical, and electronic applications. In recent times, MeO NPs have been bio-synthesized using green synthesis procedures, owing to it offering the potential to control the problems of traditional NPs creation approaches. NPs made using this approach have an ample range of characteristics, including excellent corrosion resistance, stability in oxidative settings, antifungal, antiviral, and antimicrobial actions, and magnetic, optoelectronic, and catalytic attributes. Most of the time, a complex comprising of the most effective and profuse chemical found in the biologic source is formed after an MSs is reduced into the appropriate MIs. Discussed in this review article are the green chemistry, as well as factors affecting the green bio-synthesis of MeO NPs. The various MeO NPs bio-synthesized using the approach owing to their bioavailability, stability, and dispersion in water-soluble solutions, their focused applications and their toxicity were revised in this article over the last ten years. Imperatively, it is suggested, that future research should focus more on the existing results of noxiousness of green-produced MeO NPs and their impacts on various applications especially in the medical field.

Funding information

The authors are grateful to the National Research Foundation and the Cape Peninsula University of Technology for the funding of this research.

CRediT authorship contribution statement

Uyiosa Osagie Aigbe: Writing – review & editing, Writing – original draft, Validation, Methodology, Conceptualization. **Otolorin Adelaja Osibote:** Writing – review & editing, Supervision.

Declaration of competing interest

The authors declare that they have no known competing financial interests or personal relationships that could have appeared to influence the work reported in this paper.

Data availability

Data will be made available on request.

Acknowledgment

The authors are grateful to the National Research Foundation and the Cape Peninsula University of Technology for the funding of this research.

References

Aaga, G., Anshebo, S., 2023. Green synthesis of highly efficient and stable copper oxide nanoparticles using an aqueous seed extract of Moringa stenopetala for sunlight-assisted catalytic degradation of Congo red and alizarin red s. Heliyon 9 (5).
Abadeh, A., Rejeb, O., Sardarabadi, M., Menezo, C., Passandideh-Fard, M., Jemni, A., 2018. Economic and environmental analysis of using metal-oxides/water nanofluid in photovoltaic thermal systems (PVTs). Energy 159, 1234–1243.
Abdal Dayem, A., Hossain, M., Lee, S., Kim, K., Saha, S., Yang, G., Choi, H., Cho, S., 2017. The role of reactive oxygen species (ROS) in the biological activities of metallic nanoparticles. Int. J. Mol. Sci. 18 (1), 120.
Abisharani, J., Devikala, S., Kumar, R., Arthanareeswari, M., Kamaraj, P., 2019. Green synthesis of TiO_2 nanoparticles using Cucurbita pepo seeds extract. Mater. Today Proc. 14, 302–307.
Abuzeid, H., Julien, C., Zhu, L., Hashem, A., 2023. Green synthesis of nanoparticles and their energy storage, environmental, and biomedical applications. Crystals 13 (11), 1576.

Adeola, H., 2023. Nanobiotechnology in regenerative dental medicine. Nanomaterials in Dental Medicine. Springer, pp. 141–157.
Adhikari, A., Chhetri, K., Acharya, D., Pant, B., Adhikari, A., 2022. Green synthesis of iron oxide nanoparticles using Psidium guajava L. leaves extract for degradation of organic dyes and anti-microbial applications. Catalysts 12 (10), 1188.
Adun, H., Mukhtar, M., Adedeji, M., Agwa, T., Ibrahim, K., Bamisile, O., Dagbasi, M., 2021. Synthesis and application of ternary nanofluid for photovoltaic-thermal system: comparative analysis of energy and exergy performance with single and hybrid nanofluids. Energies 14 (15), 4434.
Afrouz, M., Ahmadi-Nouraldinvand, F., Elias, S., Alebrahim, M., Tseng, T., Zahedian, H., 2023. Green synthesis of spermine coated iron nanoparticles and its effect on biochemical properties of Rosmarinus officinalis. Sci. Rep. 13 (1), 775.
Agnihotri, A., Varghese, A., Nidhin, M., 2021. Transition metal oxides in electrochemical and bio sensing: a review state-of-art review. Appl. Surf. Sci. Adv. 4, 100072.
Ahmed, S., Ahshan, K., Mondal, M., Hossain, S., 2021. Application of metal oxides-based nanofluids in PV/T systems: a review. Front. Energy 16 (3), 1–32.
Aigbe, U., Osibote, O., 2020. A review of hexavalent chromium removal from aqueous solutions by sorption technique using nanomaterials. J. Environ. Chem. Eng. 8 (6), 104503.
Aigbe, U., Das, R., Ho, W., Srinivasu, V., Maity, A., 2018. A novel method for removal of Cr (VI) using polypyrrole magnetic nanocomposite in the presence of unsteady magnetic fields. Sep. Purif. Technol. 194, 377–387.
Aigbe, U., Onyancha, R., Ukhurebor, K., Okundaye, B., Aigbe, E., Enaroseha, O., Obodo, K., Osibote, O., El Nemr, A., Noto, L., Atagana, H., 2023a. Utility of magnetic nanomaterials for theranostic nanomedicine. Magnetic Nanomaterials: Synthesis, Characterization and Applications. Springer Nature, pp. 47–86.
Aigbe, U., Maluleke, R., Lebepe, T., Oluwafemi, O., Osibote, O., 2023b. Rhodamine 6G Dye adsorption using magnetic nanoparticles synthesized with the support of vernonia amygdalina leaf extract (bitter leaf). J. Inorg. Organomet. Polym. Mater. 1–20.
Aigbe, U., Ukhurebor, K., Onyancha, R., Okundaye, B., Aigbe, E., Kusuma, H., Noto, L., Osibote, O., Atagana, H., 2023c. Applications of magnetic nanomaterials for wastewater treatment. Magnetic Nanomaterials: Synthesis, Characterization and Applications. Springer International Publishing, Cham, pp. 129–169.
Ajmal, N., Saraswat, K., Bakht, M., Riadi, Y., Ahsan, M., Noushad, M., 2019. Cost-effective and eco-friendly synthesis of titanium dioxide (TiO_2) nanoparticles using fruit's peel agro-waste extracts: characterization, *in vitro* antibacterial, antioxidant activities. Green Chem. Lett. Rev. 12 (3), 244–254.
Akintelu, S., Oyebamiji, A., Olugbeko, S., Folorunso, A., 2021. Green synthesis of iron oxide nanoparticles for biomedical application and environmental remediation: a review. Eclét. Quím. 46 (4), 17–37.
Aksu Demirezen, D., Yılmaz, Ş., Demirezen Yılmaz, D., Yıldız, Y., 2022. Green synthesis of iron oxide nanoparticles using Ceratonia siliqua L. aqueous extract: improvement of colloidal stability by optimizing synthesis parameters, and evaluation of antibacterial activity against Gram-positive and Gram-negative bacteria. Int. J. Mater. Res. 113 (10), 849–861.
Alabdallah, N., Hasan, M., Hammami, I., Alghamdi, A., Alshehri, D., Alatawi, H., 2021. Green synthesized metal oxide nanoparticles mediate growth regulation and physiology of crop plants under drought stress. Plants 10 (8), 1730.
Alam, M., Aamir, M., Farhan, M., Albuhulayqah, M., Ahmad, M., Ravikumar, C., Dileep Kumar, V., Ananda Murthy, H., 2021. Green synthesis of Ni-Cu-Zn based nanosized metal oxides for photocatalytic and sensor applications. Crystals 11 (12).
Alhalili, Z., 2022. Green synthesis of copper oxide nanoparticles CuO NPs from eucalyptus globoulus leaf extract: adsorption and design of experiments. Arab. J. Chem. 15 (5), 103739.
Alhalili, Z., 2023. Metal oxides nanoparticles: general structural description, chemical, physical, and biological synthesis methods, role in pesticides and heavy metal removal through wastewater treatment. Molecules 28 (7), 3086.
Ali, J., Bibi, S., Jatoi, W., Tuzen, M., Jakhrani, M., Feng, X., Saleh, T., 2023a. Green synthesized zinc oxide nanostructures and their applications in dye-sensitized solar cells and photocatalysis: a review. Mater. Today Commun., 106840
Ali, D., Krid, F., Nacef, M., Boussaha, E., Chelaghmia, M., Tabet, H., Selaimia, R., Atamnia, A., Affoune, A., 2023b. Green synthesis of copper oxide nanoparticles using Ficus elastica extract for the electrochemical simultaneous detection of Cd^{2+}, Pb^{2+}, and Hg^{2+}. RSC Adv. 13 (27), 18734–18747.
Allah, M., Alshamsi, H., 2023. Green synthesis of AC/ZnO nanocomposites for adsorptive removal of organic dyes from aqueous solution. Inorg. Chem. Commun. 157, 111415.
Alshammari, B., Lashin, M., Mahmood, M., Al-Mubaddel, F., Ilyas, N., Rahman, N., Sohail, M., Khan, A., Abdullaev, S., Khan, R., 2023. Organic and inorganic nanomaterials: fabrication, properties and applications. RSC Adv. 13 (20), 13735–13785.
Altaf, M., Manoharadas, S., Zeyad, M., 2021. Green synthesis of cerium oxide nanoparticles using Acorus calamus extract and their antibiofilm activity against bacterial pathogens. Microsc. Res. Tech. 84 (8), 1638–1648.
Althomali, R., Adeosun, W., 2023. Wet chemically synthesized metal oxides nanoparticles, characterization and application in electrochemical energy storage: an updated review. Synth. Met. 298, 117424.
Amin, F., Khattak, B., Alotaibi, A., Qasim, M., Ahmad, I., Ullah, R., Bourhia, M., Gul, A., Zahoor, S., Ahmad, R., 2021. Green synthesis of copper oxide nanoparticles using Aerva javanica leaf extract and their characterization and investigation of *in vitro* antimicrobial potential and cytotoxic activities. Evid. Based Complement. Altern. Med. 2021.
Aminuzzaman, M., Ying, L., Goh, W., Watanabe, A., 2018. Green synthesis of zinc oxide nanoparticles using aqueous extract of Garcinia mangostana fruit pericarp and their photocatalytic activity. Bull. Mater. Sci. 41, 1–10.
Andra, S., Balu, S., Jeevanandham, J., Muthalagu, M., Vidyavathy, M., Chan, Y., Danquah, M., 2019. Phytosynthesized metal oxide nanoparticles for pharmaceutical applications. Naunyn Schmiedeb. Arch. Pharmacol. 392, 755–771.
Andrade-Zavaleta, K., Chacon-Laiza, Y., Asmat-Campos, D., Raquel-Checca, N., 2022. Green synthesis of superparamagnetic iron oxide nanoparticles with eucalyptus globulus extract and their application in the removal of heavy metals from agricultural soil. Molecules 27 (4), 1367.
Andualem, W., Sabir, F., Mohammed, E., Belay, H., Gonfa, B., 2020. Synthesis of copper oxide nanoparticles using plant leaf extract of Catha edulis and its antibacterial activity. J. Nanotechnol. 2020, 1–10.
A. Annu and S. Ahmed, "Green synthesis of metal, metal oxide nanoparticles, and their various applications," Handbook of Ecomaterials, pp. 1–45, 2018.
Ansari, M., Khan, H., Alzohairy, M., Jalal, M., Ali, S., Pal, R., Musarrat, J., 2015. Green synthesis of Al_2O_3 nanoparticles and their bactericidal potential against clinical isolates of multi-drug resistant Pseudomonas aeruginosa. World J. Microbiol. Biotechnol. 31, 153–164.
Ansari, P., Muthukrishnan, R., Khan, R., Vedhi, C., Sakthipandi, K., Kader, S., 2023. Green synthesis of copper oxide nanoparticles using Amaranthus dubius leaf extract for sensor and photocatalytic applications. Chem. Phys. Impact 7, 100374.
Anwer, A., Abdulaziz, F., Latif, S., Alanazi, A., Sultana, S., Khan, M., 2023. Microwave assisted green synthesis of high capacitive TiO2 doped rGO nanosheets for supercapacitor applications. Mater. Sci. Eng. B 291, 116367.
Aravind, M., Amalanathan, M., Mary, M., 2021. Synthesis of TiO_2 nanoparticles by chemical and green synthesis methods and their multifaceted properties. SN Appl. Sci. 3, 1–10.
Arularasu, M., Devakumar, J., Rajendran, T., 2018. An innovative approach for green synthesis of iron oxide nanoparticles: characterization and its photocatalytic activity. Polyhedron 156, 279–290.
Arun, J., Nachiappan, S., Rangarajan, G., Alagappan, R., Gopinath, K., Lichtfouse, E., 2023. Synthesis and application of titanium dioxide photocatalysis for energy, decontamination and viral disinfection: a review. Environ. Chem. Lett. 21 (1), 339–362.
Arunadevi, N., Kirubavathy, S., 2022. Metal oxides: advanced inorganic materials. Inorg. Anticorros. Mater. 21–54.
Aseyd Nezhad, S., Es-haghi, A., Tabrizi, M., 2020. Green synthesis of cerium oxide nanoparticle using Origanum majorana L. leaf extract, its characterization and biological activities. Appl. Organomet. Chem. 34 (2), e5314.
Ashour, M., Mansour, A., Abdelwahab, A., Alprol, A., 2023. Metal oxide nanoparticles' green synthesis by plants: prospects in phyto-and bioremediation and photocatalytic degradation of organic pollutants. Processes 11 (12), 3356.
Attarilar, S., Yang, J., Ebrahimi, M., Wang, Q., Liu, J., Tang, Y., Yang, J., 2020. The toxicity phenomenon and the related occurrence in metal and metal oxide nanoparticles: a brief review from the biomedical perspective. Front. Bioeng. Biotechnol. 8, 822.
Attia, N., Abd El-Monaem, E., El-Aqapa, H., Elashery, S., Eltaweil, A., El Kady, M., Khalifa, S., Hawash, H., El-Seedi, H., 2022. Iron oxide nanoparticles and their pharmaceutical applications. Appl. Surf. Sci. Adv. 11, 100284.
Aziz, Z., Mohd-Nasir, H., Ahmad, A., Setapar, S.Mohd., Peng, W., Chuo, S., Khatoon, A., Umar, K., Yaqoob, A., Mohamad Ibrahim, M., 2019. Role of nanotechnology for design and development of cosmeceutical: application in makeup and skin care. Front. Chem. 7, 739.
Bagheri, A., Aramesh, N., Hasnain, M., Nayak, A., Varma, R., 2023. Greener fabrication of metal nanoparticles using plant materials: a review. Chem. Phys. Impact, 100255.
Bansal, V., Ramanathan, R., Bhargava, S., 2011. Fungus-mediated biological approaches towards 'green'synthesis of oxide nanomaterials. Aust. J. Chem. 64 (3), 279–293.
Barzinjy, A., Azeez, H., 2020. Green synthesis and characterization of zinc oxide nanoparticles using Eucalyptus globulus Labill. leaf extract and zinc nitrate hexahydrate salt. SN Appl. Sci. 2 (5), 991.
Bashal, A., Hefnawy, M., Ahmed, H., El-Atawy, M., Pashameah, R., Medany, S., 2023. Green synthesis of $NiFe_2O_4$ nano-spinel oxide-decorated carbon nanotubes for efficient capacitive performance—Effect of electrolyte concentration. Nanomaterials 13 (19), 2643.
Bathla, A., Vikrant, K., Kukkar, D., Kim, K., 2022. Photocatalytic degradation of gaseous benzene using metal oxide nanocomposites. Adv. Colloid Interface Sci. 305, 102696.
Bekele, E., Gonfa, B., Zelekew, O., Belay, H., Sabir, F., 2020. Synthesis of titanium oxide nanoparticles using root extract of Kniphofia foliosa as a template, characterization, and its application on drug resistance bacteria. J. Nanomater. 1–10.
Bensy, A., Christobel, G., Muthusamy, K., Alfarhan, A., Anantharaman, P., 2022. Green synthesis of iron nanoparticles from Ulva lactuca and bactericidal activity against enteropathogens. J. King Saud Univ. Sci. 34 (3), 101888.
Berta, L., Coman, N., Rusu, A., Tanase, C., 2021. A review on plant-mediated synthesis of bimetallic nanoparticles, characterisation and their biological applications. Materials 14 (24), 7677 (Basel).
Bhati, M., 2023. Biogenic synthesis of metallic nanoparticles: principles and applications. Mater. Today Proc. 81, 882–887.
Bhuiyan, M., Miah, M., Paul, S., Aka, T., Saha, O., Rahaman, M., Sharif, M., Habiba, O., Ashaduzzaman, M., 2020. Green synthesis of iron oxide nanoparticle using Carica papaya leaf extract: application for photocatalytic degradation of remazol yellow RR dye and antibacterial activity. Heliyon 6 (8).
Bhullar, S., Goyal, N., Gupta, S., 2021. Rapid green-synthesis of TiO2 nanoparticles for therapeutic applications. RSC Adv. 11 (48), 30343–30352.
Boholm, M., 2016. The use and meaning of nano in American English: towards a systematic description. Ampersand 3, 163–173.
Borah, R., Ninakanti, R., Nuyts, G., Peeters, H., Pedrazo-Tardajos, A., Nuti, S., Vande Velde, C., De Wael, K., Lenaerts, S., Bals, S., Verbruggen, S., 2021. Selectivity in the

ligand functionalization of photocatalytic metal oxide nanoparticles for phase transfer and self-assembly applications. Chem. Eur. J. 27 (35), 9011–9021.
Boroumand Moghaddam, A., Namvar, F., Moniri, M., Md. Tahir, P., Azizi, S., Mohamad, R., 2015. Nanoparticles biosynthesized by fungi and yeast: a review of their preparation, properties, and medical applications. Molecules 20 (9), 16540–16565.
Boroumand Moghaddam, A., Moniri, M., Azizi, S., Abdul Rahim, R., Bin Ariff, A., Zuhainis Saad, W., Namvar, F., Navaderi, M., Mohamad, R., 2017. Biosynthesis of ZnO nanoparticles by a new Pichia kudriavzevii yeast strain and evaluation of their antimicrobial and antioxidant activities. Molecules 22 (6), 872.
Buarki, F., AbuHassan, H., Al Hannan, F., Henari, F., 2022. Green synthesis of iron oxide nanoparticles using Hibiscus rosa sinensis flowers and their antibacterial activity. J. Nanotechnol. 1–6.
Cañas-Carrell, J., Li, S., Parra, A., Shrestha, B., 2014. Metal oxide nanomaterials: health and environmental effects. Health and Environmental Safety of Nanomaterials. Woodhead Publishing, pp. 200–221.
Caf, F., 2022. Biogenic synthesis of iron oxide nanoparticle using Padina pavonica extract: application for photocatalytic degradation of congo red dye, neurotoxicity and antioxidant activity. Turk. J. Fish. Aquat. Sci. 23 (2).
Calnan, S., 2014. Applications of oxide coatings in photovoltaic devices. Coatings 4 (1), 162–202.
Charbgoo, F., Ahmad, M., Darroudi, M., 2017. Cerium oxide nanoparticles: green synthesis and biological applications. Int. J. Nanomed. 1401–1413.
Chavali, M., Nikolova, M., 2019. Metal oxide nanoparticles and their applications in nanotechnology. SN Appl. Sci. 1 (6), 607.
Chopra, H., Bibi, S., Singh, I., Hasan, M., Khan, M., Yousafi, Q., Baig, A., Rahman, M., Islam, F., Emran, T., Cavalu, S., 2022. Green metallic nanoparticles: biosynthesis to applications. Front. Bioeng. Biotechnol. 10, 548.
Chouke, P., Shrirame, T., Potbhare, A., Mondal, A., Chaudhary, A., Mondal, S., Thakare, S., Nepovimova, E., Valis, M., Kuca, K., Sharma, R., 2022. Bioinspired metal/metal oxide nanoparticles: a road map to potential applications. Mater. Today Adv. 16, 100314.
Consolo, V., Torres-Nicolini, A., Alvarez, V., 2020. Mycosinthetized Ag, CuO and ZnO nanoparticles from a promising Trichoderma harzianum strain and their antifungal potential against important phytopathogens. Sci. Rep. 10 (1), 20499.
Dadkhah, M., Tulliani, J., 2022. Green synthesis of metal oxides semiconductors for gas sensing applications. Sensors 22 (13), 4669.
Danish, M., Estrella, L., Alemaida, I., Lisin, A., Moiseev, N., Ahmadi, M., Nazari, M., Wali, M., Zaheb, H., Senjyu, T., 2021. Photocatalytic applications of metal oxides for sustainable environmental remediation. Metals 11 (1) (Basel).
Danno, T., Nakatsuka, D., Kusano, Y., Asaoka, H., Nakanishi, M., Fujii, T., Ikeda, Y., Takada, J., 2013. Crystal structure of β-Fe_2O_3 and topotactic phase transformation to α-Fe_2O_3. Cryst. Growth Des. 13 (2), 770–774.
Das, M., Chatterjee, S., 2019. Green synthesis of metal/metal oxide nanoparticles toward biomedical applications: boon or bane. Green Synthesis, Characterization and Applications of Nanoparticles. Elsevier, pp. 265–301.
Das, S., Panicker, N., Rather, M., Mandal, M., Sahu, P., 2022. Green synthesis of cerium oxide nanoparticles using Dillenia indica aqueous extract and its anti-oxidant activity. Bull. Mater. Sci. 46 (1), 3.
de Marco, B., Rechelo, B., Tótoli, E., Kogawa, A., Salgado, H., 2019. Evolution of green chemistry and its multidimensional impacts: a review. Saudi Pharm. J. 27 (1), 1–8.
Demissie, M., Sabir, F., Edossa, G., Gonfa, B., 2020. Synthesis of zinc oxide nanoparticles using leaf extract of lippia adoensis (koseret) and evaluation of its antibacterial activity. J. Chem. 1–9.
Derakhshani, E., Asri, M., Naghizadeh, A., 2023. Plant-based green synthesis of copper oxide nanoparticles using berberis vulgaris leaf extract: an update on their applications in antibacterial activity. Bionanoscience 13 (1), 212–218.
Devi, H., Boda, M., Shah, M., Parveen, S., Wani, A., 2019. Green synthesis of iron oxide nanoparticles using Platanus orientalis leaf extract for antifungal activity. Green Process. Synth. 8 (1), 38–45.
Dharshini, R., Poonkothai, M., Srinivasan, P., Mythili, R., Syed, A., Elgorban, A., Selvankumar, T., Kim, W., 2021. Nano-decolorization of methylene blue by Phyllanthus reticulatus iron nanoparticles: an eco-friendly synthesis and its antimicrobial, phytotoxicity study. Appl. Nanosci. 1–11.
Diebold, U., 2003. The surface science of titanium dioxide. Surf. Sci. Rep. 48 (5–8), 53–229.
Duraisamy, P., 2018. Green synthesis of aluminium oxide nanoparticles by using Aerva lanta and Terminalia chebula extracts. IJRASET 6 (1), 428–433.
N. El Messaoudi, Z. Ciğeroğlu, Z. Şenol, A. Bouich, E. Kazan-Kaya, L. Noureen and J. Américo-Pinheiro, "Green synthesis of nanoparticles for remediation organic pollutants in wastewater by adsorption," Advances in Chemical Pollution, Environmental Management and Protection, 2023.
El-Kassas, H., Aly-Eldeen, M., Gharib, S., 2016. Green synthesis of iron oxide (Fe_3O_4) nanoparticles using two selected brown seaweeds: characterization and application for lead bioremediation. Acta Oceanol. Sin. 35, 89–98.
El-Nemr, M., Aigbe, U., Hassaan, M., Ukhurebor, K., Ragab, S., Onyancha, R., Osibote, O., El Nemr, A., 2022. The use of biochar-NH 2 produced from watermelon peels as a natural adsorbent for the removal of Cu (II) ion from water. Biomass Convers. Biorefin. 1–17.
El-Seedi, H., El-Shabasy, R., Khalifa, S., Saeed, A., Shah, A., Shah, R., Iftikhar, F., Abdel-Daim, M., Omri, A., Hajrahand, N., Sabir, J., 2019. Metal nanoparticles fabricated by green chemistry using natural extracts: biosynthesis, mechanisms, and applications. RSC Adv. 9 (24), 24539–24559.
Faisal, S., Jan, H., Shah, S., Shah, S., Khan, A., Akbar, M., Rizwan, M., Jan, F., Wajidullah, A.N., Khattak, A., 2021. Green synthesis of zinc oxide (ZnO) nanoparticles using aqueous fruit extracts of Myristica fragrans: their characterizations and biological and environmental applications. ACS Omega 6 (14), 9709–9722.
Farré, M., Barceló, D., 2012. Analysis and Risk of Nanomaterials in Environmental and Food Samples: Comprehensive Analytical Chemistry. Elsevier.
Fouda, A., Eid, A., Abdelkareem, A., Said, H., El-Belely, E., Alkhalifah, D., Alshallash, K., Hassan, S., 2022. Phyco-synthesized zinc oxide nanoparticles using marine macroalgae, Ulva fasciata Delile, characterization, antibacterial activity, photocatalysis, and tanning wastewater treatment. Catalysts 12 (7), 756.
Fuku, X., Matinise, N., Masikini, M., Kasinathan, K., Maaza, M., 2018. An electrochemically active green synthesized polycrystalline NiO/MgO catalyst: use in photo-catalytic applications. Mater. Res. Bull. 97, 457–465.
Gaber, S., Hashem, A., El-Sayyad, G., Attia, M., 2023. Antifungal activity of myco-synthesized bimetallic ZnO-CuO nanoparticles against fungal plant pathogen Fusarium oxysporum. Biomass Convers. Biorefinery 1–15.
Gakis, G., Aviziotis, I., Charitidis, C., 2023. Metal and metal oxide nanoparticle toxicity: moving towards a more holistic structure–activity approach. Environ. Sci. Nano 10 (3), 761–780.
Gamedze, N., Mthiyane, D., Babalola, O., Singh, M., Onwudiwe, D., 2022. Physico-chemical characteristics and cytotoxicity evaluation of CuO and TiO_2 nanoparticles biosynthesized using extracts of Mucuna pruriens utilis seeds. Heliyon 8 (8).
Gangwar, J., Gupta, B., Srivastava, A., 2016. Prospects of emerging engineered oxide nanomaterials and their applications. Def. Sci. J. 66 (4).
Gareev, K., 2023. Diversity of iron oxides: mechanisms of formation, physical properties and applications. Magnetochemistry 9 (5), 1199.
Gebre, S., Sendeku, M., 2019. New frontiers in the biosynthesis of metal oxide nanoparticles and their environmental applications: an overview. SN Appl. Sci. 1, 1–28.
Gebre, S., 2023. Bio-inspired synthesis of metal and metal oxide nanoparticles: the key role of phytochemicals. J. Clust. Sci. 34 (2), 665–704.
Geldasa, F., Kebede, M., Shura, M., Hone, F., 2023. Experimental and computational study of metal oxide nanoparticles for the photocatalytic degradation of organic pollutants: a review. RSC Adv. 13 (27), 18404–18442.
George, J., Antony, A., Mathew, B., 2018. Metal oxide nanoparticles in electrochemical sensing and biosensing: a review. Microchim. Acta 185, 1–26.
Gershon, T., 2011. Metal oxide applications in organic-based photovoltaics. Mater. Sci. Technol. 27 (9), 1357–1371.
Gharpure, S., Yadwade, R., Ankamwar, B., 2022. Non-antimicrobial and non-anticancer properties of ZnO nanoparticles biosynthesized using different plant parts of Bixa Orellana. ACS Omega 7 (2), 1914–1933.
Gopinath, K., Karthika, V., Sundaravadivelan, C., Gowri, S., Arumugam, A., 2015. Mycogenesis of cerium oxide nanoparticles using Aspergillus niger culture filtrate and their applications for antibacterial and larvicidal activities. J. Nanostruct. Chem. 5, 295–303.
Gudkov, S., Burmistrov, D., Smirnova, V., Semenova, A., Lisitsyn, A., 2022. A mini review of antibacterial properties of Al_2O_3 nanoparticles. Nanomaterials 12 (15), 2635.
Guleria, A., Sachdeva, H., Saini, K., Gupta, K., Mathur, J., 2022. Recent trends and advancements in synthesis and applications of plant-based green metal nanoparticles: a critical review. Appl. Organomet. Chem. 36 (9), e6778.
Haider, F., Nabi, G., Shah, K., Khan, K., Khan, H., 2023. Green synthesis and electrochemical study of undoped and doped Al_2O_3 nanoparticles using Hibiscus rosa-sinensis leaves extract. Indones. J. Chem.
Hajiali, S., Daneshjou, S., Daneshjoo, S., 2022. Biomimetic synthesis of iron oxide nanoparticles from Bacillus megaterium to be used in hyperthermia therapy. AMB Express 12 (1), 145.
Hameed, H., Waheed, A., Sharif, M., Saleem, M., Afreen, A., Tariq, M., Kamal, A., Al-Onazi, W., Al Farraj, D., Ahmad, S., Mahmoud, R., 2023. Green synthesis of zinc oxide (ZnO) nanoparticles from green algae and their assessment in various biological applications. Micromachines 14 (5), 928 (Basel).
Hamida, R., Ali, M., Abdelmeguid, N., Al-Zaban, M., Baz, L., Bin-Meferij, M., 2021. Lichens—a potential source for nanoparticles fabrication: a review on nanoparticles biosynthesis and their prospective applications. J. Fungi 7 (4), 291.
Hay Allah, M.Albo, Alshamsi, H., 2023. Facile green synthesis of ZnO/AC nanocomposites using Pontederia crassipes leaf extract and their photocatalytic properties based on visible light activation. J. Mater. Sci. Mater. Electron. 34 (16), 1263.
He, Q., Yu, B., Li, Z., Zhao, Y., 2019. Density functional theory for battery materials. Energy Environ. Mater. 2 (4), 264–279.
Idris, N., Yusoff, H., Idris, N., Badar, N., Elong, K., Muhamad, S., Yusoff, N., Wai, C., 2023. Green synthesis of zinc oxide nanoparticles using leaves extract of Mariposa Christia vespertilionis and its potential as anode materials in sodium-ion batteries (SIBs. Arab. J. Sci. Eng. 1–13.
Ijaz, R., Hassan, S., Panhwar, S., Talpur, M., Uddin, S., Ahmed, Z., 2022. Fabrication of disposable electrodes based on green synthesized iron oxide nanoparticles for enumeration of bacteria in water. J. Electrochem. Soc. 169 (12), 127502.
Irshad, M., Nawaz, R., ur Rehman, M., Adrees, M., Rizwan, M., Ali, S., Ahmad, S., Tasleem, S., 2021. Synthesis, characterization and advanced sustainable applications of titanium dioxide nanoparticles: a review. Ecotoxicol. Environ. Saf. 212, 111978.
Ishwarya, R., Vaseeharan, B., Kalyani, S., Banumathi, B., Govindarajan, M., Alharbi, N., Kadaikunnan, S., Al-Anbr, M., Khaled, J., Benelli, G., 2018. Facile green synthesis of zinc oxide nanoparticles using Ulva lactuca seaweed extract and evaluation of their photocatalytic, antibiofilm and insecticidal activity. J. Photochem. Photobiol. B Biol. 178, 249–258.
Islam, M., Khatun, M., Rahman, M., Alam, M., 2021. Green synthesis of copper oxide nanoparticles using Justicia adhatoda leaf extract and its application in cotton fibers as antibacterial coatings. AIP Adv. 11 (12).

Jain, R., Mendiratta, S., Kumar, L., Srivastava, A., 2021. Green synthesis of iron nanoparticles using Artocarpus heterophyllus peel extract and their application as a heterogeneous Fenton-like catalyst for the degradation of Fuchsin Basic dye. Curr. Res. Green Sustain. Chem. 4, 100086.
Jamzad, M., Kamari Bidkorpeh, M., 2020. Green synthesis of iron oxide nanoparticles by the aqueous extract of Laurus nobilis L. leaves and evaluation of the antimicrobial activity. J. Nanostruct. Chem. 10, 193–201.
Jassal, P., Kaur, D., Prasad, R., Singh, J., 2022. Green synthesis of titanium dioxide nanoparticles: development and applications. J. Agric. Food Res., 100361
Jeevanandam, J., Kiew, S., Boakye-Ansah, S., Lau, S., Barhoum, A., Danquah, M., Rodrigues, J., 2022. Green approaches for the synthesis of metal and metal oxide nanoparticles using microbial and plant extracts. Nanoscale 14 (7), 2534–2571.
Jha, S., Rani, R., Singh, S., 2023. Biogenic zinc oxide nanoparticles and their biomedical applications: a review. J. Inorg. Organomet. Polym. Mater. 1–16.
Jia, Y., Alva, G., Fang, G., 2019. Development and applications of photovoltaic–thermal systems: a review. Renew. Sustain. Energy Rev. 102, 249–265.
Kadhem, A., Alshamsi, H., 2023. Biosynthesis of Ag-ZnO/rGO nanocomposites mediated Ceratophyllum demersum L. leaf extract for photocatalytic degradation of Rhodamine B under visible light. Biomass Convers. Biorefin. 1–15.
Kalaiarasi, J., Pragathiswaran, C., Subramani, P., 2021. Green chemistry approach for the functionalization of reduced graphene and ZnO as efficient supercapacitor application. J. Mol. Struct. 1242, 130704.
Kanagasubbulakshmi, S., Kadirvelu, K., 2017. Green synthesis of iron oxide nanoparticles using Lagenaria siceraria and evaluation of its antimicrobial activity. Defence Life Sci. J. 2 (4), 422–427.
Kannan, S., Sundrarajan, M., 2014. A green approach for the synthesis of a cerium oxide nanoparticle: characterization and antibacterial activity. Int. J. Nanosci. 13 (03), 1450018.
Karaduman, I., Güngör, A., Nadaroğlu, H., Altundaş, A., Acar, S., 2017. Green synthesis of γ-Fe_2O_3 nanoparticles for methane gas sensing. J. Mater. Sci. Mater. Electron. 20, 16094–16105.
Karlsson, H., Toprak, M., Fadeel, B., 2022. Toxicity of metal and metal oxide nanoparticles. Handbook on the Toxicology of Metals. Academic Press, pp. 87–126.
Kashale, A., Gattu, K., Ghule, K., Ingole, V., Dhanayat, S., Sharma, R., Chang, J., Ghule, A., 2016. Biomediated green synthesis of TiO_2 nanoparticles for lithium ion battery application. Compos. B Eng. 99, 297–304.
Kashale, A., Rasal, A., Kamble, G., Ingole, V., Dwivedi, P., Rajoba, S., Jadhav, L., Ling, Y., Chang, J., Ghule, A., 2019. Biosynthesized Co-doped TiO_2 nanoparticles based anode for lithium-ion battery application and investigating the influence of dopant concentrations on its performance. Compos. B Eng. 167, 44–50.
Keabadile, O., Aremu, A., Elugoke, S., Fayemi, O., 2020. Green and traditional synthesis of copper oxide nanoparticles—comparative study. Nanomaterials 10 (12), 2502.
Khan, M., Mohammad, A., Ali, W., Sharwani, A., 2022a. Recent developments in properties and applications of metal oxides. Inorganic Anticorrosive Materials. Elsevier, pp. 95–111.
Khan, M., Mashwani, Z., Ikram, M., Raja, N., Mohamed, A., Ren, G., Omar, A., 2022b. Efficacy of green cerium oxide nanoparticles for potential therapeutic applications: circumstantial insight on mechanistic aspects. Nanomaterials 12 (12), 2117.
Khan, A., Malik, N., Singh, B., Ansari, N., Rehman, M., Yadav, A., 2023a. Biosynthesis, and characterization of Zinc oxide nanoparticles (ZnONPs) obtained from the extract of waste of strawberry. J. Umm Al Qura Univ. Appl. Sci. 1–8.
Khan, M., Siddique, M., Sajid, M., Karim, S., Ali, M., Abid, R., Bokhari, S., 2023b. A comparative study of green and chemical cerium oxide nanoparticles (CeO_2-NPs): from synthesis, characterization, and electrochemical analysis to multifaceted biomedical applications. Bionanoscience 1–19.
Khayoon, H., Ismael, M., Al-nayili, A., Alshamsi, H., 2023. Fabrication of $LaFeO_3$-nitrogen deficient g-C_3N_4 composite for enhanced the photocatalytic degradation of RhB under sunlight irradiation. Inorg. Chem. Commun. 157, 111356.
Kiwumulo, H., Muwonge, H., Ibingira, C., Lubwama, M., Kirabira, J., Ssekitoleko, R., 2022. Green synthesis and characterization of iron-oxide nanoparticles using Moringa oleifera: a potential protocol for use in low and middle income countries. BMC Res. Notes 15 (1), 1–8.
Kovačec, E., Regvar, M., van Elteren, J., Arčon, I., Papp, T., Makovec, D., Vogel-Mikuš, K., 2017. Biotransformation of copper oxide nanoparticles by the pathogenic fungus Botrytis cinerea. Chemosphere 180, 178–185.
Krishnan, A., Swarnalal, A., Das, D., Krishnan, M., Saji, V., Shibli, S., 2023. A review on transition metal oxides based photocatalysts for degradation of synthetic organic pollutants. J. Environ. Sci.
Kulkarni, D., Malode, S., Prabhu, K., Ayachit, N., Kulkarni, R., Shetti, N., 2020. Development of a novel nanosensor using Ca-doped ZnO for antihistamine drug. Mater. Chem. Phys. 246, 122791.
Kumar, J., Krithiga, T., Manigandan, S., Sathish, S., Renita, A., Prakash, P., Prasad, B., Kumar, T., Rajasimman, M., Hosseini-Bandegharaei, A., Prabu, D., 2021a. A focus to green synthesis of metal/metal based oxide nanoparticles: various mechanisms and applications towards ecological approach. J. Clean. Prod. 324, 129198.
Kumar, S., Ahmed, F., Shaalan, N., Saber, O., 2021b. Biosynthesis of ceo2 nanoparticles using egg white and their antibacterial and antibiofilm properties on clinical isolates. Crystals 11 (6), 584.
Kumar, R., Pulikanti, G., Shankar, K., Rambabu, D., Mangili, V., Kumbam, L., Sagara, P., Nakka, N., Yogesh, M., 2022. Surface coating and functionalization of metal and metal oxide nanoparticles for biomedical applications. Metal Oxides for Biomedical and Biosensor Applications. Elsevier, pp. 205–231.
Kumbhakar, P., Gowda, C., Mahapatra, P., Mukherjee, M., Malviya, K., Chaker, M., Chandra, A., Lahiri, B., Ajayan, P., Jariwala, D., Singh, A., 2021. Emerging 2D metal oxides and their applications. Mater. Today 45, 142–168.
Kurhade, P., Kodape, S., Choudhury, R., 2021. Overview on green synthesis of metallic nanoparticles. Chem. Pap. 75 (10), 5187–5222.
Lane, M., Zimmerman, J., 2019. Controlling metal oxide nanoparticle size and shape with supercritical fluid synthesis. Green Chem. 21 (14), 3769–3781.
Laurent, S., Boutry, S., Muller, R., 2018. Metal oxide particles and their prospects for applications. Iron Oxide Nanoparticles for Biomedical Applications. Elsevier.
Lu, H., Wan, L., Li, X., Zhang, M., Shakoor, A., Li, W., Zhang, X., 2022. Combined synthesis of cerium oxide particles for effective anti-bacterial and anti-cancer nanotherapeutics. Int. J. Nanomed. 5733–5746.
Ma, R., Mao, S., Wang, C., Shao, Y., Wang, Z., Wang, Y., Qu, S., Peng, D., 2020. Luminescence in manganese (II)-Doped $SrZn_2S_2O$ crystals from multiple energy conversion. Front. Chem. 8, 752.
Madima, N., Kefeni, K., Mishra, S., Mishra, A., 2022. TiO_2-modified g-C_3N_4 nanocomposite for photocatalytic degradation of organic dyes in aqueous solution. Heliyon 8 (9).
Madivoli, E., Kareru, P., Maina, E., Nyabola, A., Wanakai, S., Nyang'au, J., 2019. Biosynthesis of iron nanoparticles using Ageratum conyzoides extracts, their antimicrobial and photocatalytic activity. SN Appl. Sci. 1, 1–11.
Mahanty, S., Bakshi, M., Ghosh, S., Gaine, T., Chatterjee, S., Bhattacharyya, S., Das, S., Das, P., Chaudhuri, P., 2019. Mycosynthesis of iron oxide nanoparticles using manglicolous fungi isolated from Indian Sundarbans and its application for the treatment of chromium containing solution: synthesis, adsorption isotherm, kinetics and thermodynamics study. Environ. Nanotechnol. Monit. Manag. 12, 100276.
Maheshna, N., Roopa, D., Karthick, R., Anandaram, H., Antony, J., Sangeetha, R., Anusuya, M., 2022. Green synthesis of titanium dioxide nanoparticles and their multifaceted applications. Int. J. Health Sci. 6, 5665–5680.
Mahmood, R., Kadhim, A., Ibraheem, S., Albukhaty, S., Mohammed-Salih, H., Abbas, R., Jabir, M., Mohammed, M., Nayef, U., AlMalki, F., Sulaiman, G., 2022. Biosynthesis of copper oxide nanoparticles mediated Annona muricata as cytotoxic and apoptosis inducer factor in breast cancer cell lines. Sci. Rep. 12 (1), 16165.
Mahmoud, A., Al-Qahtani, K., Alflaij, S., Al-Qahtani, S., Alsamhan, F., 2021. Green copper oxide nanoparticles for lead, nickel, and cadmium removal from contaminated water. Sci. Rep. 11 (1), 12547.
Majeed, S., Norshah, N., Danish, M., Ibrahim, M., Nanda, A., 2022. Biosynthesis of zinc oxide nanoparticles from Allium sativum extract: characterization and application. Bionanoscience 12 (3), 795–803.
Malleshappa, J., Nagabhushana, H., Prashantha, S., Sharma, S., Dhananjaya, N., Shivakumara, C., Nagabhushana, B., 2014. Eco-friendly green synthesis, structural and photoluminescent studies of CeO_2: Eu^{3+} nanophosphors using E. tirucalli plant latex. J. Alloy. Compd. 612, 425–434.
Malleshappa, J., Nagabhushana, H., Sharma, S., Vidya, Y., Anantharaju, K., Prashantha, S., Prasad, B., Naika, H., Lingaraju, K., Surendra, B., 2015. Leucas aspera mediated multifunctional CeO_2 nanoparticles: structural, photoluminescent, photocatalytic and antibacterial properties. Spectrochim. Acta A Mol. Biomol. Spectrosc. 149, 452–462.
Malode, S., Shetti, N., Reddy, K., 2021. Highly sensitive electrochemical assay for selective detection of Aminotriazole based on TiO_2/poly (CTAB) modified sensor. Environ. Technol. Innov. 21, 101222.
Manikandan, V., Jayanthi, P., Priyadharsan, A., Vijayaprathap, E., Anbarasan, P., Velmurugan, P., 2019. Green synthesis of pH-responsive Al_2O_3 nanoparticles: application to rapid removal of nitrate ions with enhanced antibacterial activity. J. Photochem. Photobiol. A Chem. 371, 205–215.
Manimaran, R., 2023. Optimization of Azadirachta indica leaf extract mediated cerium oxide nanoparticles synthesis, characterization, and its applications. Ind. Crops Prod. 204, 117304.
Manuja, A., Kumar, B., Kumar, R., Chhabra, D., Ghosh, M., Manuja, M., Brar, B., Pal, Y., Tripathi, B., Prasad, M., 2021. Metal/metal oxide nanoparticles: toxicity concerns associated with their physical state and remediation for biomedical applications. Toxicol. Rep. 8, 1970–1978.
Masroor, S., 2022. Basics of metal oxides: properties and applications. Inorg. Anticorros. Mater. 85–94.
Matinise, N., Kaviyarasu, K., Mongwaketsi, N., Khamlich, S., Kotsedi, L., Mayedwa, N., Maaza, M., 2018. Green synthesis of novel zinc iron oxide ($ZnFe_2O_4$) nanocomposite via Moringa Oleifera natural extract for electrochemical applications. Appl. Surf. Sci. 446, 66–73.
Mbenga, Y., Adeyemi, J., Mthiyane, D., Singh, M., Onwudiwe, D., 2023. Green synthesis, antioxidant and anticancer activities of TiO_2 nanoparticles using aqueous extract of Tulbhagia violacea. Results Chem., 101007
Melnikova, N., Malygina, D., Korokin, V., Al-Azzawi, H., Zdorova, D., Mokshin, E., Liyaskina, E., Kurgaeva, I., Revin, V., 2023. Synthesis of cerium oxide nanoparticles in a bacterial nanocellulose matrix and the study of their oxidizing and reducing properties. Molecules 28 (6), 2604.
Michael, A., Singh, A., Roy, A., Islam, M., 2022. Fungal-and algal-derived synthesis of various nanoparticles and their applications. Bioinorg. Chem. Appl.
Miri, A., Sarani, M., 2018. Biosynthesis, characterization and cytotoxic activity of CeO_2 nanoparticles. Ceram. Int. 44 (11), 12642–12647.
Miri, A., Darroudi, M., Sarani, M., 2020. Biosynthesis of cerium oxide nanoparticles and its cytotoxicity survey against colon cancer cell line. Appl. Organomet. Chem. 34 (1), e5308.
Mishra, D., Chitara, M., Negi, S., Kumar, R., Chaturvedi, P., 2023. Biosynthesis of zinc oxide nanoparticles via leaf extracts of catharanthus roseus (L.) G. Don and their application in improving seed germination potential and seedling vigor of Eleusine coracana (L.) Gaertn. Adv. Agric. 2023.
Miu, B., Dinischiotu, A., 2022. New green approaches in nanoparticles synthesis: an overview. Molecules 27 (19), 6472.

Mohamed, R., Fawzy, E., Shehab, R.A.D., Salah El Din, R., Abd El Fatah, H., 2021. Green biosynthesis, structural characterization and anticancer activity of copper oxide nanoparticles from the brown alga Cystoseira myrica. Egypt. J. Aquat. Biol. Fish. 25 (4).
Mohamed, A., Atta, R., Kotp, A., Abo El-Ela, F., Abd El-Raheem, H., Farghali, A., Alkhalifah, D., Hozzein, W., Mahmoud, R., 2023. Green synthesis and characterization of iron oxide nanoparticles for the removal of heavy metals (Cd^{2+} and Ni^{2+}) from aqueous solutions with antimicrobial investigation. Sci. Rep. 13 (1), 7227.
Mohammed, Y., Alghamdi, S., Jabbar, B., Marghani, D., Beigh, S., Abouzied, A., Khalifa, N., Khojali, W., Huwaimel, B., Alkhalifah, D., Hozzein, W., 2023. Green synthesis of zinc oxide nanoparticles using Cymbopogon citratus extract and its antibacterial activity. ACS Omega 8 (35), 32027–32042.
Monica Ahmad, N., Hasan, A., 2023. Synthesis of green cerium oxide nanoparticles using plant waste from Colocasia Esculenta for seed germination of Mung Bean (Vigna radiata). J. Nanotechnol. 2023.
Montemore, M., van Spronsen, M., Madix, R., Friend, C., 2017. O_2 activation by metal surfaces: implications for bonding and reactivity on heterogeneous catalysts. Chem. Rev. 118 (5), 2816–2862.
Mostakim, K., Hasanuzzaman, M., 2022. Solar photovoltaic thermal systems. Technologies for Solar Thermal Energy. Academic Press, pp. 123–150.
Murphin Kumar, P., Kyaw, H., Myint, M., Al-Haj, L., Al-Muhtaseb, A., Al-Abri, M., Thanigaivel, V., Ponnusamy, V., 2020. Green route synthesis of nanoporous copper oxide for efficient supercapacitor and capacitive deionization performances. Int. J. Energy Res. 44 (13), 10682–10694.
Muthuvel, A., Jothibas, M., Mohana, V., Manoharan, C., 2020. Green synthesis of cerium oxide nanoparticles using Calotropis procera flower extract and their photocatalytic degradation and antibacterial activity. Inorg. Chem. Commun. 119, 108086.
Muzafar, W., Kanwal, T., Rehman, K., Perveen, S., Jabri, T., Qamar, F., Faizi, S., Shah, M., 2022. Green synthesis of iron oxide nanoparticles using Melia azedarach flowers extract and evaluation of their antimicrobial and antioxidant activities. J. Mol. Struct. 1269, 133824.
Nadeem, M., Khan, R., Afridi, K., Nadhman, A., Ullah, S., Faisal, S., Mabood, Z., Hano, C., Abbasi, B., 2020. Green synthesis of cerium oxide nanoparticles (CeO2 NPs) and their antimicrobial applications: a review. Int. J. Nanomed. 5951–5961.
Narayanan, M., Rakesh, S., 2018. Synthesis of colloidal alumina nanoparticles using green method. IOP Conf. Ser. Mater. Sci. Eng.
Naseem, T., Durrani, T., 2021. The role of some important metal oxide nanoparticles for wastewater and antibacterial applications: a review. Environ. Chem. Ecotoxicol. 3, 59–75.
Naseer, M., Aslam, U., Khalid, B., Chen, B., 2020. Green route to synthesize zinc oxide nanoparticles using leaf extracts of Cassia fistula and Melia azadarach and their antibacterial potential. Sci. Rep. 10 (1), 9055.
Nassar, A., Atta, H., Abdel-Rahman, M., El Naghy, W., Fouda, A., 2023. Myco-synthesized copper oxide nanoparticles using harnessing metabolites of endophytic fungal strain Aspergillus terreus: an insight into antibacterial, anti-Candida, biocompatibility, anticancer, and antioxidant activities. BMC Complement. Med. Ther. 23 (1), 261.
Ndou, N., Rakgotho, T., Nkuna, M., Doumbia, I., Mulaudzi, T., Ajayi, R., 2023. Green synthesis of iron oxide (Hematite) nanoparticles and their influence on Sorghum bicolor growth under drought stress. Plants 12 (7), 1425.
Negrescu, A., Killian, M., Raghu, S., Schmuki, P., Mazare, A., Cimpean, A., 2022. Metal oxide nanoparticles: review of synthesis, characterization and biological effects. J. Funct. Biomater. 13 (4), 274.
Nehru, L., Kandasamy, G., Sekar, V., Alshehri, M., Panneerselvam, C., Alasmari, A., Kathirvel, P., 2023. Green synthesis of ZnO-NPs using endophytic fungal extract of Xylaria arbuscula from Blumea axillaris and its biological applications. Artif. Cells Nanomed. Biotechnol. 51 (1), 318–333.
Nichelson, A., Madhavan, B., Veerasubramani, G., Tanveer, W., Theerthagiri, J., Ramu, A., Vikraman, D., Karuppasamy, K., Yi, S., 2022. Metal oxides-free anodes for lithium-ion batteries. Oxide Free Nanomaterials for Energy Storage and Conversion Applications. Elsevier, pp. 149–176.
Noxpanco, M., Wilkins, J., Riffat, S., 2020. A review of the recent development of photovoltaic/thermal (Pv/t) systems and their applications. Futur. Cities Environ. 6, 9-9.
Nwachukwu, I., Nwanya, A., Alshoaibi, A., Awada, C., Ekwealor, A., Ezema, F., 2023. Recent progress in green synthesized transition metal-based oxides in lithium-ion batteries as energy storage devices. Curr. Opin. Electrochem. 39.
Nwanya, A., Botha, S., Ezema, F., Maaza, M., 2021. Functional metal oxides synthesized using natural extracts from waste maize materials. Curr. Res. Green Sustain. Chem. 4, 100054.
Nyoka, M., Choonara, Y., Kumar, P., Kondiah, P., Pillay, V., 2020. Synthesis of cerium oxide nanoparticles using various methods: implications for biomedical applications. Nanomaterials 10 (2), 242.
Nzilu, D., Madivoli, E., Makhanu, D., Wanakai, S., Kiprono, G., Kareru, P., 2023. Green synthesis of copper oxide nanoparticles and its efficiency in degradation of rifampicin antibiotic. Sci. Rep. 13 (1), 14030.
Ogunyemi, S., Abdallah, Y., Zhang, M., Fouad, H., Hong, X., Ibrahim, E., Masum, M., Hossain, A., Mo, J., Li, B., 2019. Green synthesis of zinc oxide nanoparticles using different plant extracts and their antibacterial activity against Xanthomonas oryzae pv. oryzae. Artif. Cells Nanomed. Biotechnol. 47 (1), 341–352.
Ogunyemi, S., Zhang, M., Abdallah, Y., Ahmed, T., Qiu, W., Ali, M., Yan, C., Yang, Y., Chen, J., Li, B., 2020. The bio-synthesis of three metal oxide nanoparticles (ZnO, MnO_2, and MgO) and their antibacterial activity against the bacterial leaf blight pathogen. Front. Microbiol. 11, 588326.
Onyancha, R., Aigbe, U., Ukhurebor, K., Kusuma, H., Darmokoesoemo, H., Osibote, O., Pal, K., 2022. Influence of magnetism-mediated potentialities of recyclable adsorbents for heavy metal ions removal from aqueous solutions–an organized review. Results Chem. 4, 100452.
Ouerghi, O., Geesi, M., Riadi, Y., Ibnouf, E., Kaiba, A., 2023. Phytosynthesis of anatase TiO_2 nanostructures using grapefruit extract for antimicrobial and catalytic applications. J. Solgel Sci. Technol. 1–10.
Pal, G., Rai, P., Pandey, A., 2019. Green synthesis of nanoparticles: a greener approach for a cleaner future. Green Synthesis, Characterization and Applications of Nanoparticles. Elsevier, pp. 1–26.
Pan, S., Goudoulas, T., Jeevanandam, J., Tan, K., Chowdhury, S., Danquah, M., 2021. Therapeutic applications of metal and metal-oxide nanoparticles: dermato-cosmetic perspectives. Front. Bioeng. Biotechnol. 9, 724499.
Pandit, C., Roy, A., Ghotekar, S., Khusro, A., Islam, M., Emran, T., Lam, S., Khandaker, M., Bradley, D., 2022. Biological agents for synthesis of nanoparticles and their applications. J. King Saud Univ. Sci. 34 (3), 101869.
Parvathy, S., Manjula, G., Balachandar, R., Subbaiya, R., 2022. Green synthesis and characterization of cerium oxide nanoparticles from Artabotrys hexapetalus leaf extract and its antibacterial and anticancer properties. Mater. Lett. 13181.
N. Patel and S. Munjal, "Metal oxide nanoparticles and their applications: a report," arXiv preprint arXiv, p. 2201.04938, 2021.
Patel, A., Enman, J., Gulkova, A., Guntoro, P., Dutkiewicz, A., Ghorbani, Y., Rova, U., Christakopoulos, P., Matsakas, L., 2021. Integrating biometallurgical recovery of metals with biogenic synthesis of nanoparticles. Chemosphere 263, 128306.
Pattnaik, A., Sahu, J., Poonia, A., Ghosh, P., 2023. Current perspective of nano-engineered metal oxide based photocatalysts in advanced oxidation processes for degradation of organic pollutants in wastewater. Chem. Eng. Res. Des.
Pavithra, S., Bessy, T., Bindhu, M., Venkatesan, R., Parimaladevi, R., Alam, M., Mayandi, J., Umadevi, M., 2023. Photocatalytic and photovoltaic applications of green synthesized titanium oxide (TiO_2) nanoparticles by Calotropis gigantea extract. J. Alloy. Compd. 960, 170638.
Periakaruppan, R., Palanimuthu, V., Abed, S., Danaraj, J., 2023. New perception about the use of nanofungicides in sustainable agriculture practices. Arch. Microbiol. 205 (1), 4.
Perumal, P., Sivaraj, P., Abhilash, K., Soundarya, G., Balraju, P., Selvin, P., 2020. Green synthesized spinel lithium titanate nano anode material using Aloe Vera extract for potential application to lithium ion batteries. J. Sci. Adv. Mater. Devices 5 (3), 346–353.
Phang, Y., Aminuzzaman, M., Akhtaruzzaman, M., Muhammad, G., Ogawa, S., Watanabe, A., Tey, L., 2021. Green synthesis and characterization of CuO nanoparticles derived from papaya peel extract for the photocatalytic degradation of palm oil mill effluent (POME). Sustainability 13 (2), 796.
Poolakkandy, R., Menamparambath, M., 2020. Soft-template-assisted synthesis: a promising approach for the fabrication of transition metal oxides. Nanoscale Adv. 2 (11), 5015–5045.
Pratt, A., 2014. Environmental applications of magnetic nanoparticles. Frontiers of Nanoscience. Elsevier, pp. 259–307 vol. 6.
Priya, N.K.K., Sidhu, A., 2021. Green synthesis: an eco-friendly route for the synthesis of iron oxide nanoparticles. Front. Nanotechnol. 3, 655062.
Puthalapattu, R., Punyasamudram, S., Bathinapatla, A., Venkata, N., Kanchi, S., 2023. Electrochemical non-enzymatic strategy with green synthesized Fe_2O_3CuO nanocomposite for detection of amiprofos-methyl herbicide in industrial effluents and soils. Chem. Phys. Impact 6, 100195.
Putri, G., Rilda, Y., Syukri, S., Labanni, A., Arief, S., 2021. Highly antimicrobial activity of cerium oxide nanoparticles synthesized using Moringa oleifera leaf extract by a rapid green precipitation method. J. Mater. Res. Technol. 15, 2355–2364.
Qamar, H., Rehman, S., Chauhan, D., Tiwari, A., Upmanyu, V., 2020. Green synthesis, characterization and antimicrobial activity of copper oxide nanomaterial derived from Momordica charantia. Int. J. Nanomed. 2541–2553.
Rahayu, E., Wonoputri, V., Samadhi, T., 2020. Plant extract-assisted biosynthesis of zinc oxide nanoparticles and their antibacterial application. IOP Conf. Ser. Mater. Sci. Eng.
Raja, V., Selvan, G., Anbarasu, R., Baskar, S., 2019. Green synthesis of zinc oxide nanoparticles using hyptis leaf extract and activated carbon based zinc oxide composite of supercapacitor applications. Indian J. Sci. Technol 12, 107–108.
Rajiv, P., Manikandan, R., Sangeetha, S., Vanathi, P., Dhanasekaran, S., 2022. Fabrication of biogenic iron oxide and their efficiency to detect carbofuran in vegetable samples. Inorg. Chem. Commun. 142, 109649.
Rajput, P., Dasgupta, S., Chakraborty, M., Nandwani, S., Hajoori, M., 2018. Green synthesis of titanium dioxide nanoparticles (TiO_2 nps) using leaf extract of datura innoxia. Int. J. Pharm. Biol. Sci. 8, 1086–1092.
Ramanarayanan, R., Bhabhina, N., Dharsana, M., Nivedita, C., Sindhu, S., 2018. Green synthesis of zinc oxide nanoparticles using extract of Averrhoa bilimbi (L) and their photoelectrode applications. Mater. Today Proc. 5 (8), 16472–16477.
Ramasubbu, K., Padmanabhan, S., Al-Ghanim, K., Nicoletti, M., Govindarajan, M., Sachivkina, N., Rajeswari, V., 2023. Green synthesis of copper oxide nanoparticles using Sesbania grandiflora leaf extract and their evaluation of anti-diabetic, cytotoxic, anti-microbial, and anti-inflammatory properties in an *in-vitro* approach. Fermentation 9 (4), 332.
Ramos, C., Alcaso, A., Cardoso, A., 2019. Photovoltaic-thermal (PVT) technology: review and case study. Earth Environ. Sci.
Rasheed, A., Li, H., Tahir, M., Mahmood, A., Nawaz, M., Shah, A., Aslam, M., Negm, S., Moustafa, M., Hassan, M., Wu, Z., 2022. The role of nanoparticles in plant biochemical, physiological, and molecular responses under drought stress: a review. Front. Plant Sci. 13, 976179.

Razack, S., Suresh, A., Sriram, S., Ramakrishnan, G., Sadanandham, S., Veerasamy, M., Nagalamadaka, R., Sahadevan, R., 2020. Green synthesis of iron oxide nanoparticles using Hibiscus rosa-sinensis for fortifying wheat biscuits. SN Appl. Sci. 2, 1–9.
Reddy, P., Shaik, D., Ganesh, V., Nagamalleswari, D., Thyagarajan, K., Prasanth, P., 2019. Structural, optical and electrochemical properties of TiO2 nanoparticles synthesized using medicinal plant leaf extract. Ceram. Int. 45 (13), 16251–16260.
Reddy, P., Shaik, D., Ganesh, V., Nagamalleswari, D., Thyagarajan, K., Prasanth, P., 2021a. High electrochemical activity of 3D flower like nanostructured TiO_2 obtained by green synthesis. Appl. Surf. Sci. 561, 150092.
Reddy, P., Shaik, D., Nagamalleswari, D., Thyagarajan, K., Prasanth, P., 2021b. Electrochemical activity of TiO_2 nanoparticles in NaOH electrolyte via green synthesis using Calotropis gigantea plant leaf extract. Indian J. Sci. Technol 14, 2766–2772.
Saka, A., Shifera, Y., Jule, L., Badassa, B., Nagaprasad, N., Shanmugam, R., Priyanka Dwarampudi, L., Seenivasan, V., Ramaswamy, K., 2022. Biosynthesis of TiO2 nanoparticles by Caricaceae (Papaya) shell extracts for antifungal application. Sci. Rep. 12 (1), 15960.
Salih, A., Al-Qurainy, F., Khan, S., Tarroum, M., Nadeem, M., Shaikhaldein, H., Gaafar, A., Alfarraj, N., 2021. Biosynthesis of zinc oxide nanoparticles using Phoenix dactylifera and their effect on biomass and phytochemical compounds in Juniperus procera. Sci. Rep. 11 (1), 19136.
Sanko, V., Kuralay, F., 2023. Label-free electrochemical biosensor platforms for cancer diagnosis: recent achievements and challenges. Biosensors 13 (3), 333.
Santhoshkumar, T., Rahuman, A., Jayaseelan, C., Rajakumar, G., Marimuthu, S., Kirthi, A., Velayutham, K., Thomas, J., Venkatesan, J., Kim, S., 2014. Green synthesis of titanium dioxide nanoparticles using Psidium guajava extract and its antibacterial and antioxidant properties. Asian Pac. J. Trop. Med. 7 (12), 968–976.
Santhoshkumar, J., Kumar, S., Rajeshkumar, S., 2017. Synthesis of zinc oxide nanoparticles using plant leaf extract against urinary tract infection pathogen. Resour. Effic. Technol. 3 (4), 459–465.
Santiago, M., Rivera, D., Torres, A., 2023. Green synthesis of titanium oxide nanoparticles using natural extracts. J. Mater. Sci. Chem. Eng. 11 (2), 29–40.
Sari, I., Yulizar, Y., 2017. Green synthesis of magnetite (Fe_3O_4) nanoparticles using Graptophyllum pictum leaf aqueous extract. IOP Conf. Ser. Mater. Sci. Eng.
Sathiyavimal, S., Durán-Lara, E., Vasantharaj, S., Saravanan, M., Sabour, A., Alshiekheid, M., Chi, N., Brindhadevi, K., Pugazhendhi, A., 2022. Green synthesis of copper oxide nanoparticles using Abutilon indicum leaves extract and their evaluation of antibacterial, anticancer in human A549 lung and MDA-MB-231 breast cancer cells. Food Chem. Toxicol. 168, 113330.
Selvaraj, R., Pai, S., Vinayagam, R., Varadavenkatesan, T., Kumar, P., Duc, P., Rangasamy, G., 2022. A recent update on green synthesized iron and iron oxide nanoparticles for environmental applications. Chemosphere, 136331.
Şerban, I., Enesca, A., 2020. Metal oxides-based semiconductors for biosensors applications. Front. Chem. 8, 354.
Sethy, N., Arif, Z., Mishra, P., Kumar, P., 2020. Green synthesis of TiO_2 nanoparticles from Syzygium cumini extract for photo-catalytic removal of lead (Pb) in explosive industrial wastewater. Green Process. Synth. 9 (1), 171–181.
Shafey, A., 2020. Green synthesis of metal and metal oxide nanoparticles from plant leaf extracts and their applications: a review. Green Process. Synth. 9 (1), 304–339.
Shaheen, I., Ahmad, K., Zequine, C., Gupta, R., Thomas, A., Malik, M., 2021. Facile ZnO-based nanomaterial and its fabrication as a supercapacitor electrode: synthesis, characterization and electrochemical studies. RSC Adv. 11 (38), 23374–23384.
Shaheen, I., Hussain, I., Zahra, T., Javed, M., Shah, S., Khan, K., Hanif, M., Assiri, M., Said, Z., Arifeen, W., Akkinepally, B., 2023. Recent advancements in metal oxides for energy storage materials: design, classification, and electrodes configuration of supercapacitor. J. Energy Storage 72, 108719.
Sharma, V., Singh, I., Chandra, A., 2018. Hollow nanostructures of metal oxides as next generation electrode materials for supercapacitors. Sci. Rep. 8 (1), 1307.
Sharma, S., Shrivastava, N., Rossi, F., Thanh, N., 2019. Nanoparticles-based magnetic and photo induced hyperthermia for cancer treatment. Nano Today 29, 100795.
M. Sharon, "Nanotechnology to aid biological and chemical warfare defense," in Nanotechnology in the Defense Industry: Advances, Innovation, and Practical Applications, 2019, pp. 165–234.
Shetti, N., Malode, S., Nayak, D., Bagihalli, G., Kalanur, S., Malladi, R., Reddy, C., Aminabhavi, T., Reddy, K., 2019. Fabrication of ZnO nanoparticles modified sensor for electrochemical oxidation of methdilazine. Appl. Surf. Sci. 496, 143656.
Shetti, N., Malode, S., Nayak, D., Naik, R., Kuchinad, G., Reddy, K., Shukla, S., Aminabhavi, T., 2020. Hetero-nanostructured iron oxide and bentonite clay composite assembly for the determination of an antiviral drug acyclovir. Microchem. J. 155, 104727.
Shkir, M., 2022. Green method for synthesis and characterization of copper oxide nanoparticles using Mulberry plant extract and their antibacterial, antioxidant and photocatalytic activity. Phys. Scr. 97 (10), 105001.
Shobana, M., 2019. Metal oxide coated cathode materials for Li ion batteries–a review. J. Alloy. Compd. 802, 477–487.
Sieugaing Tamwa, M., Njimou, J., Nguelo, B., Nanseu-Njiki, C., Vunain, E., Tripathy, B., Ngameni, E., 2023. Electrochemical sensor based on green-synthesized iron oxide nanomaterial modified carbon paste electrode for Congo red electroanalysis and capacitance performance. Mater. Res. Innov. 27 (4), 243–252.
Singh, J., Dutta, T., Kim, K., Rawat, M., Samddar, P., Kumar, P., 2018. Green'synthesis of metals and their oxide nanoparticles: applications for environmental remediation. J Nanobiotechnology 16 (1), 1–24.
Singh, D., Jain, D., Rajpurohit, D., Jat, G., Kushwaha, H., Singh, A., Mohanty, S., Al-Sadoon, M., Zaman, W., Upadhyay, S., 2023. Bacteria assisted green synthesis of copper oxide nanoparticles and their potential applications as antimicrobial agents and plant growth stimulants. Front. Chem. 11, 1154128 p.., vol. 11, p.
Slavin, Y., Asnis, J., Hńfeli, U., Bach, H., 2017. Metal nanoparticles: understanding the mechanisms behind antibacterial activity. J. Nanobiotechnol. 15, 1–20.
Smita, S., Gupta, S., Bartonova, A., Dusinska, M., Gutleb, A., Rahman, Q., 2012. Nanoparticles in the environment: assessment using the causal diagram approach. Environ. Health 11, 1–11.
Soltys, L., Olkhovyy, O., Tatarchuk, T., Naushad, M., 2021. Green synthesis of metal and metal oxide nanoparticles: principles of green chemistry and raw materials. Magnetochemistry 7 (11), 145.
Sriramulu, M., Sumathi, B., Sumathi, S., 2021. Photo catalytic, antimicrobial and antifungal activity of biogenic iron oxide nanoparticles synthesised using aegle marmelos extracts. J. Inorg. Organomet. Polym. Mater. 31, 1738.
Stefaniuk, I., Cieniek, B., Rogalska, I., Virt, I., Kościak, A., 2018. Magnetic properties of ZnO: co layers obtained by pulsed laser deposition method. Mater. Sci. 36 (3), 439–444. Poland.
Subhapriya, S., Gomathipriya, P., 2018. Green synthesis of titanium dioxide (TiO_2) nanoparticles by Trigonella foenum-graecum extract and its antimicrobial properties. Microb. Pathog. 116, 215–220.
Sukumar, S., Rudrasenan, A., Padmanabhan Nambiar, D., 2020. Green-synthesized rice-shaped copper oxide nanoparticles using Caesalpinia bonducella seed extract and their applications. ACS Omega 5 (2), 1040–1051.
Sumesh, K., Kanthavel, K., 2019. Green synthesis of aluminium oxide nanoparticles and its applications in mechanical and thermal stability of hybrid natural composites. J. Polym. Environ. 27, 2189–2200.
Sunny, N., Mathew, S., Chandel, N., Saravanan, P., Rajeshkannan, R., Rajasimman, M., Vasseghian, Y., Rajamohan, N., Kumar, S., 2022. Green synthesis of titanium dioxide nanoparticles using plant biomass and their applications-a review. Chemosphere 300, 134612.
Surendra, T., Roopan, S., 2016. Photocatalytic and antibacterial properties of phytosynthesized CeO_2 NPs using Moringa oleifera peel extract. J. Photochem. Photobiol. B Biol. 161, 122–128.
Sutradhar, P., Saha, M., 2016. Green synthesis of zinc oxide nanoparticles using tomato (Lycopersicon esculentum) extract and its photovoltaic application. J. Exp. Nanosci. 11 (5), 314–327.
Szczyglewska, P., Feliczak-Guzik, A., Nowak, I., 2023. Nanotechnology–general aspects: a chemical reduction approach to the synthesis of nanoparticles. Molecules 28 (13), 4932.
Tabrez, S., Khan, A., Mirza, A., Suhail, M., Jabir, N., Zughaibi, T., Alam, M., 2022. Biosynthesis of copper oxide nanoparticles and its therapeutic efficacy against colon cancer. Nanotechnol. Rev. 11 (1), 1322–1331.
Taha, T., Barzinjy, A., Hussain, F., Nurtayeva, T., 2022. Nanotechnology and computer science: trends and advances. Mem. Mater. Devices Circuits Syst. 2, 100011.
Tan, H., Lim, Y., Ng, L., Lim, Y., 2023. Plant-mediated synthesis of iron nanoparticles for environmental application: mini review. Mater. Today Proc.
Tarrahi, R., Mahjouri, S., Khataee, A., 2021. A review on *in vivo* and *in vitro* nanotoxicological studies in plants: a headlight for future targets. Ecotoxicol. Environ. Saf. 208, 111697.
Thu, C., Ehrenreich, P., Wong, K., Zimmermann, E., Dorman, J., Wang, W., Fakharuddin, A., Putnik, M., Drivas, C., Koutsoubelitis, A., Vasilopoulou, M., 2018. Role of the metal-oxide work function on photocurrent generation in hybrid solar cells. Sci. Rep. 8 (1), 3559.
Tunkara, E., DeJarnette, D., Saunders, A., Baldwin, M., Otanicar, T., Roberts, K., 2019. Indium tin oxide and gold nanoparticle solar filters for concentrating photovoltaic thermal systems. Appl. Energy 252, 113459.
Umamaheswari, A., Prabu, S., John, S., Puratchikody, A., 2021. Green synthesis of zinc oxide nanoparticles using leaf extracts of Raphanus sativus var. Longipinnatus and evaluation of their anticancer property in A549 cell lines. Biotechnol. Rep. 29, e00595.
Üstün, E., Önbaş, S., Çelik, S., Ayvaz, M., Şahin, N., 2022. Green synthesis of iron oxide nanoparticles by using Ficus carica leaf extract and its antioxidant activity. Biointerface Res. Appl. Chem. 12, 2108–2116.
Varghese, R., Zikalala, N., Oluwafemi, O., 2020. Green synthesis protocol on metal oxide nanoparticles using plant extracts. Colloidal Metal Oxide Nanoparticles. Elsevier.
Vijayaram, S., Razafindralambo, H., Sun, Y., Vasantharaj, S., Ghafarifarsani, H., Hoseinifar, S., Raeeszadeh, M., 2023. Applications of green synthesized metal nanoparticles—a review. Biol. Trace Elem. Res. 1–27.
Vinardell, M., Mitjans, M., 2015. Antitumor activities of metal oxide nanoparticles. Nanomaterials 5 (2), 1004–1021.
Wang, P., Jiang, L., Han, R., 2020. Biosynthesis of zinc oxide nanoparticles and their application for antimicrobial treatment of burn wound infections. Mater. Res. Express 7 (9), 095010.
Wang, S., Chen, D., Hong, Q., Gui, Y., Cao, Y., Ren, G., Liang, Z., 2023. Surface functionalization of metal and metal oxide nanoparticles for dispersion and tribological applications-a review. J. Mol. Liq., 122821
Wani, N., Khanday, W., Tirumale, S., 2020. Biosynthesis of iron oxide nanoparticles using ethyl acetate extract of Chaetomium cupreum and their anticancer activity. Matrix Sci. Pharma 4 (2), 23–30.
Win, T., Khan, S., Bo, B., Zada, S., Fu, P., 2021. Green synthesis and characterization of Fe_3O_4 nanoparticles using Chlorella-K01 extract for potential enhancement of plant growth stimulating and antifungal activity. Sci. Rep. 11 (1), 21990.
Xu, J., Zhang, W., Guo, Y., Chen, X., Zhang, Y., 2022. Metal nanoparticles as a promising technology in targeted cancer treatment. Drug Deliv. 29 (1), 664–678.
Yadav, S., Rani, N., Saini, K., 2022. Green synthesis of ZnO and CuO NPs using Ficus benghalensis leaf extract and their comparative study for electrode materials for high performance supercapacitor application. Mater. Today Proc. 49, 2124–2130.
Yoon, Y., Truong, P., Lee, D., Ko, S., 2021. Metal-oxide nanomaterials synthesis and applications in flexible and wearable sensors. ACS Nanosci. Au 2 (2), 64–92.

Yu, L., Sun, L., Zhang, Q., Zhou, Y., Zhang, J., Yang, B., Xu, B., Xu, Q., 2022. Nanomaterials-based ion-imprinted electrochemical sensors for heavy metal ions detection: a review. Biosensors 12 (12), 1096.

Zakariya, N., Jusof, W., Majeed, S., 2022. Green approach for iron oxide nanoparticles synthesis: application in antimicrobial and anticancer-an updated review. Karbala Int. J. Mod. Sci. 8 (3), 421–437.

Zhang, N., Xiong, G., Liu, Z., 2022. Toxicity of metal-based nanoparticles: challenges in the nano era. Front. Bioeng. Biotechnol. 10, 1001572.